Multivariate Analysis to Assess Hydromorphic Response of Groundwater and Surface Water Systems

A dissertation submitted by

Brian Frank Thomas

In partial fulfillment of the requirements
for the degree of

Doctor of Philosophy

in

Civil and Environmental Engineering

TUFTS UNIVERSITY

August 2012

© 2012, Brian F. Thomas

Advisor:
Dr. Richard M. Vogel
Civil and Environmental Engineering

Preface

This dissertation consists of three chapters under the unifying theme of understanding human impacts to groundwater-surface water systems. The overall objective of this research was to illustrate how human impacts including urban storm water regulation and groundwater withdrawals have altered groundwater and surface water interaction. In Chapter 1, the behavior of groundwater elevations in Boston is investigated to address the impact of storm water recharge best management practices. Results illustrate that recharge practices in Boston have resulted in a very small yet statistically significant increase in groundwater elevations in Back Bay. Further, hybrid multivariate regression model developed for the study are used to illustrate future storm water planning scenarios. Chapters 2 and 3 explore the effect of human withdrawals in the characterization of groundwater-surface water (gw-sw) behaviors using baseflow recession analysis. Baseflow recession analysis generally falls into two categories: 1) a nonlinear ($n \neq 1$) or 2) a linear ($n=1$) relationship between baseflow (Q) and groundwater storage (S) assuming a power low relationship given by $Q=\alpha S^n$. In Chapter 2, the difficulty in baseflow recession analysis is investigated using traditional estimation procedures which require no *a priori* assumption of the linearity of the gw-sw behaviors. Multiple factors including a rigorous approach to fitting the lower envelope within the recession plot, estimation of the time derivative of streamflow and including human water use into baseflow recession are presented. Results illustrate highly variable estimates of the baseflow recession parameters due to the estimation scheme employed; further, hypothesis

testing to test the ability to assess if watersheds do, in fact, behave linearly found that few sites which exhibited linear behavior across all seasonal experiments performed. In Chapter 3, linear behaviors are assumed to illustrate the effect of including human withdrawals in estimation of baseflow parameters, which for the linear assumption is termed the baseflow recession constant. The performance of traditional estimators is compared to newly derived estimators; our results suggest that traditional semi-log estimation approaches adapted to include withdrawal terms are preferred. Further, analysis of variance methods are developed to identify factors which give rise to variability in estimates of the baseflow recession constant. Among the factors considered, both drainage density and human withdrawals were found to have significant and similar explanatory power for the baseflow recession constant. Thus, results document the importance of incorporating human withdrawals into models of the baseflow response of a watershed.

Chapter 1 has been published in the Journal of Hydrologic Engineering (Thomas, B.F. and R.M. Vogel, Impact of storm water recharge practices on Boston groundwater elevations, Journal of Hydrologic Engineering, 17(8), DOI: 10.1061/(ASCE)HE.1943-5584.0000534).

Acknowledgements

Many years ago, I began my college educational journey in poetry with a goal of hearing the whisper of words. The poem by A.R. Ammons (Corson's Inlet) that traced the first steps in my journey is one of a man walking along the shore; his movement mimicking that of the ocean. "In nature there are few sharp lines." Who knew that such words would be so fitting for the journey?

This dissertation represents the end of that journey and the beginning of another. There have been many friends, family and colleagues that have supported my journey, and to them I say "Thank You". From my 4th grade teacher who forced a kid to focus to my freshman poetry professor who used literature to express the loss of his wife during the semester to my Ph.D. advisor who pushed expectations to levels I never thought I could reach. I dedicate this dissertation to those that inspire, antagonize, reject, accept and, most importantly, dream.

Table of Contents

List of Tables ..... **viii**
List of Figures ..... **ix**

Chapter 1: The Impact of Storm Water Recharge Practices on Boston Groundwater Elevations

Abstract **1**
1.0 Introduction **2**
2.0 Study Goals **5**
3.0 Previous work **8**
4.0 Methodology **9**
4.1 Data 11
5.0 Multivariate Statistical Analyses **14**
5.1 Model Development 14
5.2 Screening Model 17
5.3 Goodness of fit 19
5.4 Discussion 20
5.5 Model validation 22
5.6 Blind-sample validation 23
6.0 Application of Regional Groundwater Model **24**
6.1 Impact of an Individual Recharge BMP 24
6.2 The Impact of a System of Recharge BMPs 27
7.0 Conclusions **29**
8.0 Acknowledgements **31**

Chapter 2: Baseflow Recession Analysis: Testing the Nonlinear Hypothesis

Abstract **32**
1.0 Introduction **33**
2.0 Experimental Methodology **39**
2.1 Data 39
2.2 Study Area Hydrology/Geology 42
2.3 Hydrograph Separation 43
3.0 Experiments **43**
3.1 Quantile Regression 44
3.2 Numerical Derivatives 47
3.3 Seasonality 53
3.4 Degree of withdrawal 56
4.0 Discussion **60**
4.1 Numerical Derivative 62
4.2 Seasonality 62
4.3 Degree of withdrawal 63
4.4 Physical Interpretation of a 63
5.0 Conclusions **66**
6.0 Acknowledgments **67**

Chapter 3: Estimation of the baseflow recession constant under human interference

Abstract **68**
1.0 Introduction **69**
2.0 Model Development **74**
2.1 Case 1: No Withdrawals, W(t)=0, Traditional Approach 76
2.2 Case 2: W(t)≠0, Traditional Approach 77
2.3 Case 3: Recession Envelope Methods, W(t)=0 79
2.4 Case 4: Recession Envelope (W(t)≠0) 80
3.0 Data: K_b estimation **80**
4.0 Experimental Design **84**
4.1 Results: K_b Estimation 85
5.0 Multivariate Hypothesis Tests **91**
5.1 Multivariate Regression Data 92
5.2 Model Development 96
5.3 Goodness of fit 98
5.4 Model Validation 100
6.0 Conclusions **103**
7.0 Acknowledgments **105**

Bibliography **106**
Chapter 1 References 106
Chapter 2 References 110
Chapter 3 References 118
Appendix 2.A **129**
Appendix 3.A **130**
Appendix 3.B **132**

List of Tables

TABLE 1-1: POTENTIAL EXPLANATORY VARIABLES 17
TABLE 1-2: SUMMARY OF REGIONAL GROUNDWATER MODEL RESULTS 19
TABLE 2-1: SUMMARY OF U.S. GEOLOGICAL SURVEY STREAMGAGES 41
TABLE 2-2: FINITE-DIFFERENCE ESTIMATORS USED TO ESTIMATE STREAMFLOW TIME DERIVATIVE (CHAPRA AND CANALE, 2006). 50
TABLE 2-3: CORRELATION OF a^* TO LOW FLOW STATISTICS (7Q10) FOR WATERSHEDS BASED ON ESTIMATION SCHEMES. 64
TABLE 3-1: SUMMARY OF 15 U.S. GEOLOGICAL SURVEY GAGES IN NORTHERN NEW JERSEY 82
TABLE 3-2: SUMMARY OF EQUATIONS USED FOR CASES DERIVED. 85
TABLE 3-3: POTENTIAL EXPLANATORY VARIABLES. 93
TABLE 3-4: SUMMARY OF CASE-SPECIFIC REGRESSION MODELS. 98

List of Figures

FIGURE 1-1: BOSTON BACK BAY MODEL DOMAIN. 11
FIGURE 1-2: COMPARISON OF PREDICTED VERSUS OBSERVED GROUNDWATER ELEVATION; DATA SET INCLUDES OBSERVED GROUNDWATER ELEVATIONS FROM JUNE 1999 TO SEPTEMBER 2009. 20
FIGURE 1-3: GROUNDWATER MODEL COEFFICIENT CROSS VALIDATION RESULTS: (A) $\sum$BMP COEFFICIENT; (B) CALIBRATION AND VALIDATION NSE. 22
FIGURE 1-4: BLIND SAMPLE VALIDATION; DATA SET INCLUDES OBSERVED GROUNDWATER ELEVATIONS FROM OCTOBER 2009 TO JUNE 2010. 24
FIGURE 1-5: RELATIONSHIP BETWEEN AVERAGE RISE IN GROUNDWATER ELEVATIONS AND DISTANCE FROM BMP TO LOCATION OF INTEREST. 25
FIGURE 1-6: AVERAGE RISE IN GROUNDWATER ELEVATION IN METERS RESULTING FROM RECHARGE BMP OF PARTICULAR CAPACITY LOCATED A DISTANCE FROM A PARTICULAR LOCATION OF INTEREST. 26
FIGURE 1-7: RESULTS FROM SCENARIO 1 (A, TOP) AND SCENARIO 2 (B, BOTTOM) DOCUMENTING AVERAGE EFFECT OF RECHARGE BMPS TO GROUNDWATER ELEVATIONS WITHIN BACK BAY. 28
FIGURE 2-1: LOCATION OF 45 U.S. GEOLOGICAL SURVEY GAGES AND NATIONAL CLIMATIC DATA SITES (NCDC) IN NEW JERSEY, USA. 40
FIGURE 2-2: GRAPHICAL ILLUSTRATION OF SLOPE ANALYSIS BETWEEN THE Q=0.05 AND Q=0.10 (5% AND 10%) QUANTILES. (A) SITE 1 (USGS 01379000). (B) SITE 41 (USGS 01466500). 47
FIGURE 2-3: PARAMETER ESTIMATION VARIABILITY CAUSED BY CALCULATION OF STREAMFLOW TIME DERIVATIVE IN (3B). THIS GRAPH ILLUSTRATES THE VARIABILITY ENCOUNTERED ACROSS ALL SITES BASED ON METHODS SUMMARIZED IN TABLE 2-2 IN ADDITION TO THE GCV SPLINE. 51
FIGURE 2-4: PERCENT DIFFERENCE AS CALCULATED BY (6) WHICH COMPARES BASEFLOW PARAMETERS ESTIMATED USING FINITE DIFFERENCE EQUATIONS IN TABLE 2-2 TO GCV SPLINE PROCEDURES. 52
FIGURE 2-5: BOX PLOTS ILLUSTRATING VARIABILITY IN SEASONAL ESTIMATES OF B USING GCV SPLINES TO ESTIMATE STREAMFLOW TIME DERIVATIVES. 55
FIGURE 2-6: RECESSION PLOT ILLUSTRATING VARIABILITY IN SLOPE (B) DEPENDING ON SEASON. IN THIS EXAMPLE, ONE MAY ASSUME LINEAR BEHAVIOR BASED ON WINTER ESTIMATES WHILE SUMMER ESTIMATES DOCUMENT NONLINEAR BEHAVIOR. 56
FIGURE 2-7: SCATTERPLOTS ILLUSTRATING THE VARIABILITY IN ESTIMATES OF BASEFLOW RECESSION PARAMETERS FROM (3B) AS A FUNCTION OF SEASON AND GROUNDWATER IMPACTS. TRENDS ILLUSTRATE THE DECREASE IN B AS Γ INCREASES BASED ON ESTIMATION FROM (3B). THE P-VALUE IN PARENTHESIS ILLUSTRATES THE SIGNIFICANCE OF THE TREND. 58
FIGURE 2-8: RECESSION PLOTS ILLUSTRATING IMPACT OF GROUNDWATER WITHDRAWALS. FIGURE 2-8(A) ILLUSTRATES A SITE WITH LOW GROUNDWATER AFFECTS RESULTING IN NEARLY IDENTICAL RESULTS BETWEEN THE BRUTSAERT METHOD (3B) AND WANG-CAI METHOD (9). FIGURE 2-8(B) DOCUMENTS THE IMPACT OF GROUNDWATER WITHDRAWALS, ESPECIALLY AT LOW FLOWS, WHICH ALTER THE SLOPE OF THE QUANTILE LOWER ENVELOPE FIT. 60
FIGURE 2-9: SCATTERPLOTS ILLUSTRATING THE VARIABILITY IN ESTIMATES OF BASEFLOW RECESSION PARAMETERS FROM (9) AS A FUNCTION OF SEASON AND GROUNDWATER IMPACTS. TRENDS ILLUSTRATE THE INCREASE IN B AS Γ INCREASES BASED ON ESTIMATION FROM (9) WHICH IS THE TREND PREDICTED IN PREVIOUS STUDIES. THE P-VALUE IN PARENTHESIS ILLUSTRATES THE SIGNIFICANCE OF THE TREND. 60
FIGURE 2-10: SUMMARY FIGURE OF HYPOTHESIS TESTS PERFORMED. DERIVATIVE RESULTS ARE BASED ON GCV SPLINE FITTING TO ESTIMATE DQ/DT; SEASONALITY INCLUDES GCV SPLINE FITTING AND SEASONALLY DEPENDENT RECESSION PERIODS; WITHDRAWAL IMPACTS INCLUDE GCV SPLINE FITTING AND SEASONALITY. ALL RESULTS ESTIMATED PARAMETERS USING A 0.05 QUANTILE REGRESSION PROCEDURE. 65
FIGURE 3-1: LOCATIONS OF 15 WATERSHEDS, NATIONAL CLIMATIC DATA SITES (NCDC) AND UTAH CLIMATE CENTER SITES IN NEW JERSEY. 83

FIGURE 3-2: ESTIMATES OF K_B FOR INDIVIDUAL HYDROGRAPHS AT SITE 0139700 USING (A) CASE 1, (B) CASE 2, (C) CASE 3 AND (D) CASE 4 AS COMPARED TO THE HORIZONTAL LINE REPRESENTING THE RECESSION WEIGHTED AVERAGE SHOWN IN (19).....87
FIGURE 3-3: COMPARISON OF VARIABILITY IN SEASONAL RECESSION WEIGHTED AVERAGES OF THE BASEFLOW RECESSION CONSTANT FOR CASE 1 (A), CASE 2 (B), CASE 3 (C) AND CASE 4 (D) SUMMARIZED IN TABLE 3-2.....89
FIGURE 3-4: COMPARISON BETWEEN ESTIMATES OF K_B OBTAINED FROM CASE 1 AND CASE 2 (A) AND CASE 3 AND CASE 4 (B).....90
FIGURE 3-5: COMPARISON OF PREDICTED VERSUS OBSERVED BASEFLOW RECESSION CONSTANTS AFTER BIAS CORRECTION PROCEDURES FOR CASE 1 (MODEL 4) (A), CASE 2 (MODEL 4) (B), CASE 3 (MODEL 2) (C) AND CASE 4 (MODEL 3) (D).....99
FIGURE 3-6: COEFFICIENT CROSS-VALIDATION RESULTS FOR CASE 2 MODEL SUMMARIZED IN TABLE 3-4. THE RESULTS ILLUSTRATE THAT SELECTION OF WATERSHEDS RESULTS IN MEDIAN ESTIMATES OF COEFFICIENTS SIMILAR TO THOSE SUMMARIZED IN TABLE 3-4.....101
FIGURE 3-7: COMPARISON OF ELASTICITIES OBTAINED FROM CASE 1, CASE 2, CASE 3 AND CASE 4 SUMMARIZED IN TABLE 3-4.....103

Chapter 1

The Impact of Storm Water Recharge Practices on Boston Groundwater Elevations

Abstract

Over the past century, the City of Boston, Massachusetts, has periodically experienced a decline in groundwater elevations and the associated deterioration of untreated wood piles which support building foundations. To combat declining water tables, Boston enacted a groundwater conservation overlay district enforced by City zoning boards to require storm water recharge practices for any activity that triggers the zoning bylaw. In Boston, recharge to the water table results from the infiltration of rainfall and snowmelt, leakage from water mains, and recharge from man-made systems. Increased mitigation activities to reduce unaccounted-for water have reduced leakage from water mains in the city. Given the high percentage of impervious cover in Boston, the remaining sources of recharge are primarily man-made systems, including pump and infiltrate systems and storm water recharge BMPs. The primary objective of this research was to exploit existing information on groundwater elevations and recharge practices to quantify the impact of the required recharge best management practices (BMPs) on the behavior of groundwater elevations in the Back Bay region of Boston. Regional multivariate regression models were developed to determine the potential effects of recharge BMPs on observed groundwater elevations. Our literature review revealed several analogous multivariate linear regression studies, but none which focused on behavior of storm water BMPs. Our model reveals that the installation

of recharge BMPs has a small but highly statistically significant positive impact on groundwater elevations in the Back Bay with the effect being proportional to their capacity and inversely proportional to their distance from the location of interest. The resulting model can be used to predict the impact on average groundwater elevations at a particular location resulting from the installation of a recharge BMP (or a set of such BMPs) of a particular capacity at a particular distance from the location of interest.

1.0 Introduction

Anthropogenic alterations associated with urban development can have a profound hydrologic impact on both surface and ground water systems. In Boston, Massachusetts, the urban hydrologic system has been impacted by the man-made filling of estuaries and wetlands, increased impervious cover which has reduced natural groundwater recharge, and installation of urban infrastructure that impacts the natural flow direction and velocity in groundwater systems.

The impact of urbanization on the urban groundwater system includes: decreased infiltration which results in reduced groundwater elevations (Gilroy and McCuen 2009; Horner et al. 1994) and increased groundwater elevations due to leakage from water and sewer systems (Foster et al. 1999; Lerner 1990). Changes in urban groundwater elevations which result from anthropogenic alterations can result in expensive consequences. For instance, declining groundwater elevations can cause land subsidence, building damage, and ecological habitat deterioration in groundwater-fed streams and wetlands. Likewise, rising groundwater elevations can cause increased infiltration into sewer and storm water

infrastructure, increased flooding in basements, and augmented building costs associated with dewatering activities for new development.

In Boston and other urban environments, alteration of the landscape limits recharge to the water table by restricting infiltration of rainfall and snowmelt, leakage from water mains, and recharge from man-made systems (Aldrich and Lambrechts 1986). American Rivers (2002) estimates lost groundwater infiltration within Boston of 166.2 to 388 million cubic meters annually due to increased impervious areas. Overall, the Back Bay region of Boston has experienced periodic declines in groundwater elevations potentially caused by a combination of decreased infiltration due to increased impervious area and active mitigation management for both water and sewer leaks. In the Back Bay region of Boston (Figure 1-1), the decline in groundwater elevations has resulted in multiple adverse effects. As described by Aldrich and Lambrechts (1986), the Back Bay was filled and untreated wood piles were used for structural supports of building foundations. Exposure of the wood piles by periodic declines in groundwater elevations creates favorable conditions for degradation of the piles by fungus, insects and bacteria. Degradation of the piles affects the stability of foundations throughout Back Bay. Such conditions have been commonplace, resulting in cracking of walls, and has required structural underpinning of the wood piles to support foundations.

In an effort to mitigate the anthropogenic impacts of urbanization on groundwater elevations in the city, Boston enacted a zoning code, Article 32, which created the Groundwater Conservation Overlay District (GCOD). Article

32 requires installation of a storm water collection and recharge system, also termed a recharge best management practice (BMP), for any specified activity that triggers the zoning requirement. Regulations require the capture, storage and infiltration of the volume of rainfall up to the first 25.4 cm of precipitation depth from the portion of the project triggering the zoning article. Excess rainfall overflows from the recharge systems are directed to the city storm water system. From 2006 to 2010, a total of 79 recharge BMPs had been installed throughout Boston. This potential recharge capacity of the installed recharge BMPs totaled 1,188 m^3 of recharge. Of these, 24 recharge BMPs have been installed within the study area in the Back Bay region of Boston (Figure 1-1) totaling an estimated potential recharge of 256 m^3, which averages to 0.25 mm of precipitation being directly recharged to the subsurface over the Back Bay area for each storm event.

Storm water management using infiltration strategies has been shown to reduce storm water runoff, increase groundwater recharge and urban baseflow, reduce erosion and stream scour, and potentially improve surface water quality (Holman-Dodds et al. 2003, Prince George Country 1999, U.S. EPA 2002). To date, few studies have investigated the temporal and spatial impacts of such storm water management practices. Recently, studies have investigated changes to peak-flow discharges in urban environments using infiltration-based strategies (Holman-Dodds et al. 2003; Perez-Pedini et al. 2005) which indicated sensitivity of mitigation benefits due to the location of infiltration sites. Similarly, Gilroy and McCuen (2009) found that reported storm water benefits would be minimal if detention basins were not placed properly to mitigate storm water runoff. Spatial

storm water management strategies have been evaluated for their ability to impact groundwater elevations. For example, Gobel et al. (2004) found that decentralized infiltration systems have limited influence on the groundwater surface. Endreny and Collins (2009) found that groundwater mounding could result due to spatial arrangements of bioretention basins. Likewise, Machusick et al. (2011) found that BMP design mitigated groundwater mounding and the effectiveness of groundwater observations in design of recharge systems. Understanding the impact of storm water mitigation strategies such as recharge BMPs on urban groundwater systems is difficult due to the transient nature of the system (Foster et al. 1999) in addition to continued land-use modifications in urban environments. Lerner (2002) recommended piezometric methods to identify signatures of point recharge in urban systems similar to the water table fluctuation method described by Scanlon et al. (2002). Boston, Massachusetts, is a unique urban environment because groundwater elevations have been recorded regularly at observation wells to monitor the potential impact of changes in groundwater elevations on wood piles which support the buildings. Therefore, a large spatial and temporal dataset of urban groundwater elevations is available that predates efforts to install recharge BMPs and these elevations continue to be collected as newly permitted recharge BMPs are installed in the Back Bay region of Boston.

2.0 Study Goals

The primary goal of this project is to determine the impact of recently introduced storm water recharge best management practices (BMPs) on the behavior of groundwater elevations in Boston. A mathematical model is needed which is able to sort out the complex interactions among all the factors which

control groundwater elevations in an urban environment. We were unable to find any previous studies which developed modeling methods which could be readily applied to evaluate the impact of BMPs on average groundwater elevations on a regional basis. Groundwater elevations are impacted by the heterogeneous subsurface environment as well as by leaks in the storm water, water and sewer systems, climatic controls, vegetation, land-use, BMPs and a variety of other minor factors including pumping and dewatering activities. It would be extremely difficult to develop a physically based mathematical model which accounts for all of these factors. For example, Carneiro and Carvalho (2010) report the difficulty in groundwater model implementation in an urban environment at a similar scale (~1 km^2). The authors report that the greatest difficulty in model calibration was spatial recharge and argued for the need of future research; this paper presents an alternative method employing multivariate linear regression to detect the effect of recharge BMPs to groundwater elevations.

Previous investigations which have attempted to model groundwater elevation changes due to storm water management (Endreny and Collins 2009; Gobel et al. 2004) have used site-specific groundwater flow models to determine groundwater impacts from infiltration. The difficulty in creating a model of an urban groundwater environment arises from the heterogeneity of the system due to both variability in hydrogeologic conditions and urban infrastructure (Carneiro and Carvalho 2010). A transient groundwater model becomes even more difficult to calibrate, validate, and simulate scenarios due to continued and variable disturbance of the hydrologic system (Lemonsu et al. 2007). Furthermore, even if

one could develop a physically based modeling system, without statistical methods, one is unable to determine whether observed changes due to recharge practices are statistically significant. Other methods may be available for evaluating such changes, for example perturbation modeling or stochastic groundwater modeling approaches (Li et al. 2003; Yi and Lee 2004), however such approaches are far more complex to apply than the approach described here.

Since a very large database of groundwater elevations is available from 234 observation wells throughout the study area over the period 1999-2010, we took a hybrid multivariate statistical/physical modeling approach which is able to exploit all available well data combined with climatic and land use data as well as BMP location and capacity data. Our approach was to develop a spatial multivariate statistical model which accounts for the primary determinants of changes in groundwater elevations in an urban environment. Such a regional statistical approach is useful because it enables us to make quantitative and rigorous statements regarding the significance of the various factors which govern groundwater elevations in an urban environment including recently introduced recharge BMPs.

A second goal of the study was to identify the regional average impact of all the currently installed recharge BMPs on groundwater elevations under historical conditions as well as a variety of future storm water recharge BMP planning scenarios. Although the model described here was developed for the case study of Boston, Massachusetts, the modeling approach taken and its application for evaluating future storm water BMP policies could be applied to

any urban environment with necessary adaptations where appropriate such as groundwater extractions, leaking water mains and groundwater gradients. Our results document the impact of the transient recharge caused by the installation of recharge BMPs to average long-term groundwater elevations throughout the Back Bay region of Boston.

3.0 Previous work

Early investigations into the use of multivariate linear regression (MLR) for groundwater elevations studies (Hodgson 1978) identified that groundwater elevations could be expressed using

$$GW_t = GW_{t-1} + SR + UR - UD - P - T \qquad (1)$$

where, in (1), GW_t is the observed groundwater elevation at time t, GW_{t-1} is the previously observed groundwater elevation, SR is the surface recharge term, UR is the recharge from underground storage, UD is the underground discharge/leakage term, P is pumpage, and T is transpiration. Hodgson (1978) used a multivariate regression method along with a monthly version of (1) with data on pumpage and monthly rainfall in addition to a lagged groundwater elevation to simulate groundwater elevations. Similarly, Azmon (1989) documented an MLR relationship between groundwater elevation, pumpage and rainfall in Israel, with high correlation found across multiple well fields between these variables. Adamowski et al. (1986) used an MLR approach with a water balance model for the Castor River watershed in Ontario, Canada, which incorporated hydrogeologic characteristics such as specific yield. This study uses MLR, but takes a different approach by using only observable physical

characteristics such as evapotranspiration and precipitation in the model while adhering to the physical groundwater balance equation in (1).

In summary, several previous studies used MLR to estimate groundwater elevations based on physical explanatory variables including pumpage, precipitation, and lagged groundwater elevations in addition to physical hydrogeologic characteristics of the aquifer. The results of these previous studies identify the physical influences on groundwater systems that could be used to predict groundwater elevations. Our study extends these previous studies to include the impact of storm water recharge BMPs on groundwater elevations.

4.0 Methodology

This section describes the development of a regional multivariate statistical model to estimate groundwater elevations within Back Bay. Aldrich and Lambrechts (1986) reported groundwater recharge within Back Bay as being limited to infiltration of rainfall and snowmelt, leakage from water mains, and recharge from man-made systems. Although pumping activities are known to exist near the study area due to dewatering for public transit tunnels, pumping records were not available and therefore were not included in the model. Installed recharge BMPs vary in terms of their location and storage capacity in addition to the timing of their installation, requiring additional model terms than those included in (1) to account for their potential impact on groundwater elevations. For example, the distance between a recharge BMP and an observation well as well as the capacity of the BMP should impact observed groundwater elevations. Here we attempt to fit multivariate statistical models which predict the groundwater elevation at a particular location and time period as a function of

numerous potential explanatory variables including previous groundwater elevation, precipitation and potential evapotranspiration, and the distance and capacity of recharge BMPs as well as several other explanatory variables described below.

The study area shown in Figure 1-1 is the Back Bay region of Boston; an area of the city created by the filling of the Charles River estuary beginning in the 1840s. The study area is underlain by an unconfined aquifer system comprised of a mixture of sand and gravel and urban fill deposited upon silt and clay. The eastern and southern boundary of the study area represents the extent of filled land. The northern boundary, running along Beacon Street, represents a no-flow condition due to the presence of the Old Mill Dam, constructed in 1829, which remains under the street. To the west, the boundary represents a variable head boundary, Muddy Brook, which flows into the Charles River. A total of 24 recharge BMPs and 234 observation wells are located within the study area with 8,014 groundwater elevation observations. Since the study area is made up of several hundred individual well locations, we refer to the model as a "regional" model.

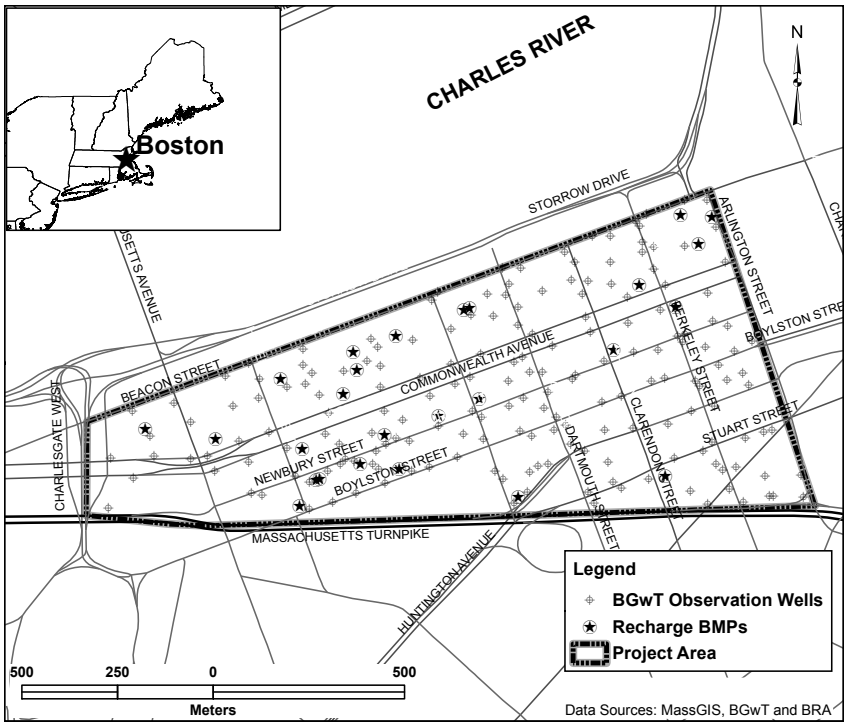

Figure 1-1: Boston Back Bay model domain.

4.1 Data

The data necessary for the proposed models include time series of daily precipitation, climatic effects and historic groundwater elevations, as well as capacity and locations of all recharge BMPs and observation wells within the model domain. A summary of potential explanatory variables is shown in Table 1-1.

4.1.1 Groundwater elevations

Groundwater elevations have been collected by the Boston Groundwater Trust (BGwT) since 1999 throughout the study area at geospatially-referenced observation wells. In addition, new observation wells are installed annually resulting in varying record lengths of groundwater observations. Since groundwater elevations were collected spatially on a predefined grid within the study area, there did not exist a particular day at which all groundwater elevation

readings were completed. Hence resulting groundwater elevation data is unequally spaced. Given the urban location of the observation wells, it was sometimes difficult to locate and measure groundwater elevations during winter months due to snow and ice cover. This variability in data collection resulted in an average time between groundwater measurements of 56 days with a standard deviation of 23 days, indicating high variability in the timing of groundwater observations. Given that the largest spatial dataset of groundwater elevations are manually collected observations, a time-lag, k, (in days between observations at each individual well site) was used to account for the irregular time intervals between observations.

4.1.2 Climate

Daily weather observation data was collected from the National Oceanic and Atmospheric Administration (NOAA) National Climatic Data Center for the Boston Logan International Airport (KBOS) weather station to serve as a proxy for precipitation inputs to the model. Due to the variability in the elapsed time between observations (k), various precipitation terms were tested as explanatory variables. The following precipitation variables (in meters) were considered: precipitation that occurred the day of the well observation (P_{day}), the precipitation on the previous day (P_1), the cumulative precipitation a week prior (P_7), and the cumulative precipitation between well observations (P_k).

4.1.3 Potential Evapotranspiration

Hodgson (1978) suggested that transpiration can affect an observed groundwater elevation at time t (see (1)). To mimic the impact of variations in

transpiration, daily potential evapotranspiration (PET) was estimated using the Hargreaves method (Shuttleworth 1993) given by

$$PET = 0.0023 S_o (T + 17.8)\sqrt{\delta_t} \quad \text{(mm/day)} \qquad (2)$$

where PET is the daily potential evapotranspiration in mm/day, S_O is the extraterrestrial radiation measured in water equivalent in mm/day, T is the average daily temperature in degrees Celsius, and δ_T is the difference between daily maximum and daily minimum temperatures in degrees Celsius. PET variables were adjusted to meters per day for inclusion in the model. The Hargreaves method was the highest ranked temperature based method for computing PET in comparisons reported in the ASCE Manual 70 (Jensen et al. 1990). Allen (1993) showed that the Hargreaves method performs well in a wide range of latitudes and climates for periods of five days or longer, without significant error. Among all temperature-based methods, the Hargreaves method is the only one recommended by Shuttleworth (1993).

PET is the maximum rate at which evapotranspiration would occur with access to an unlimited supply of water. Therefore, the estimated PET represents the maximum actual evapotranspiration (ET) that could possibly occur and was used as a proxy for actual evapotranspiration. Here PET represents the transient relationship between the groundwater elevations and both vegetative and atmospheric interactions. Initial evaluations considered use of individual tree locations mapped as part of the Greater Boston Urban Forest Inventory as input to the model. Experiments showed that inclusion of PET produced models with better goodness of fit measures than those which used individual tree locations.

Future studies should consider regional calibration of any temperature-based estimates of PET using the more advanced and accurate Penman-Monteith approach (see Fennessey and Vogel 1996).

4.1.4 BMP Recharge Capacity

A total of 79 recharge BMPs have been installed and were operational in Boston with 24 recharge BMPs installed within the study area. The total storage capacity of installed recharge systems within the study area is 256 m^3. Boston Redevelopment Authority (BRA) completes site reviews for requirements under Article 80 of the Boston code for any proposed new development or redevelopment within the city. Site plans submitted to BRA document recharge BMP designs to meet city requirements under both Article 80 and Article 32 in addition to State regulations for storm water (310 CMR 10.00 and 314 CMR 9.00). The BRA maintains a database of impervious areas that contribute storm water flow to onsite recharge BMPs, thereby reducing directly-connected impervious area within the study area. The location, capacity and date of installation of all operational recharge BMPs were obtained from the BGwT. From this data, distances between each observation well and recharge BMP were obtained using a geographic information systems (GIS).

5.0 Multivariate Statistical Analyses

5.1 Model Development

Ordinary least squares (OLS) multivariate regression procedures were used to estimate the model parameters of the following hybrid physical/statistical regional model:

$$GW_t = \beta_0 + \beta_1 X_1 + \beta_2 X_2 + \cdots + \beta_n X_n + \varepsilon_t \quad (3)$$

where GW_t represents groundwater elevation at time t, $X_1,\ldots,X_n$ are observable physical explanatory variables, $\beta_0,\ldots,\beta_n$ are model coefficients, and ε_t are normally distributed model errors with zero mean and constant variance σ^2_ε. We expect a variety of explanatory variables to produce changes in water table elevations including recharge BMP capacity (Endreny and Collins, 2009): proximity of recharge BMPs to wells and other recharge BMPs; rainfall events and previous groundwater elevations.

To evaluate the influence of a single recharge BMP on groundwater elevations at a nearby well, the following explanatory variable is employed

$$BMP_i = \frac{Y_{i,t} * CAP_i}{D^q_{i,j}} \quad (4)$$

where $Y_{i,t}$ is an indicator variable which takes the value of 1 if the BMP is installed at site i at time t, and zero otherwise. The variable CAP_i is simply the capacity of the BMP at site i in cubic meters and the variable $D_{i,j}$ is the distance in meters from the BMP_i to the well of interest, j. The variable q, the power on the variable $D_{i,j}$, was tested at q=1 and q=2 as shown in Table 1-1.

The cumulative effect of recharge BMPs was computed for the entire Back Bay region as follows. The model assumes that the impact of recharge BMPs are additive so that the cumulative impact of BMPs could be defined as

$$\sum BMP = \sum_{i=1}^{n} BMP_i = \sum_{i=1}^{n} \frac{Y_{i,t} * CAP_i}{D^q_{i,j}} \quad (5)$$

where i refers to a specific recharge BMP and $D_{i,j}$ refers to the distance between BMP i and observation well j and n is the total number of BMPs in the region.

The assumption inherent in (5) is the principle of superposition. In general, superposition assumes that two differential equations, in this case two-dimensional groundwater flow and a recharge BMP, are linear and additive (for a full description of superposition, the reader is referred to Bear (1972) and Strack (1989)). As described by Strack (1989), the solution considering unconfined groundwater flow with rainfall and radial flow toward a well can be solved assuming superposition. For this evaluation, the well represents the recharge BMP with a negative discharge, and hence we must assume radial flow away from the well. Explicit assumptions for the principle of superposition to solve radial flow from a well are that the lower aquifer boundary is impermeable, flow in the aquifer is horizontal, and that the hydraulic conductivity is uniform. As documented in historic reports (Seasholes 2003), fill material was deposited on estuarine clays which can be considered impermeable. Horizontal flow within the groundwater system can be assumed as suggested by Freeze and Witherspoon (1967) since the groundwater system has little variability in topographic elevation in addition to being identified as a local system without deep recharge of a regional groundwater system. Local variability in hydraulic conductivity is likely given the urban infrastructure and historic documentation of filling of the study area (Seasholes 2003; Newman and Holton 2006). Such variability leads to violation of the assumption of uniform hydraulic conductivity. However, for the purpose of this study, we have assumed that (5) represents a superposition approach to physically describe the impact of the recharge BMPs on observed groundwater elevations.

Table 1-1 summarizes the explanatory variables considered for inclusion in the final multivariate statistical model.

Table 1-1: Potential Explanatory Variables

Variable Name	Description	Units	Data Source
k	Time elapsed (in days) between observed groundwater elevations	Days	BGwT
Groundwater Observations			
GW_t	Observed groundwater elevation at time t; 234 wells	m	BGwT
GW_{t-k}	Previous recorded groundwater elevation k days prior to GW_t	m	BGwT
Climate Variables			
P_{day}, P_1, P_7, P_k	Precipitation obtained from KBOS	m	NCDC
PET_{day}, PET_1, PET_7, PET	Potential evapotranspiration (Eqn 2)	m/day	BGwT/NCDC
Stormwater Recharge BMPs			
∑BMP with q=1 or 2	Recharge BMP terms (Eqn 5)	m^3/m^q	BGwT/GIS
∑BMP*P with q=1 or 2	Recharge BMP Interaction terms with precipitation interaction	m^3/m^q*m	BGwT/NCDC

5.2 Screening Model

To decide which of the explanatory variables in Table 1-1 to include in the model, various multivariate model selection methods were employed using Minitab® (Release 15) including stepwise regression analyses and best subsets regression. Backward elimination and forward selection stepwise regression methods were used to identify explanatory variables to predict groundwater elevations using potential explanatory variables summarized in Table 1-1.

Goodness of fit of resulting models was evaluated by comparing Mallows Cp, prediction sum of squares (PRESS), Nash-Sutcliff Efficiency (NSE) and prediction R^2 (Helsel and Hirsch, 2002). Mallows Cp represents the expected number of explanatory variables to be included in a model and was kept close to

the number of model parameters to reduce bias in resulting predictions. PRESS, the prediction sum of squares represents the regression residual computed by deleting the ith observation. In practice, PRESS is termed a delete-one residual and provides a validation estimate of regression error. To improve model prediction, influence and leverage statistics were also calculated to isolate observations that exhibited unrealistic influence on regression model parameter estimates. Another attractive metric of the overall goodness-of-fit is the Nash-Sutcliffe efficiency criterion termed NSE (Nash and Sutcliffe 1970). Perfect agreement between observed and simulated groundwater elevations is obtained if NSE is equal to 1. An advantage of NSE over other goodness fit metrics is that it is impacted by both cross correlation and bias between the observations and predictions.

After evaluating dozens of alternative models using the above model screening, diagnostic and goodness-of-fit procedures, the following general model form was chosen:

$$GW_t = \beta_0 + \beta_1 GW_{t-k} + \beta_2 P_k + \beta_3 k + \beta_4 PET_1 + \beta_5 \sum BMP + \varepsilon_t \quad (6)$$

A summary of the model coefficients for the multivariate model given in (6) is provided in row 5 of Table 1-2. Table 1-2 reports numerous models each with improved goodness-of-fit as significant explanatory variables are introduced. The final model shown in the fifth row of Table 1-2 is recommended for use in practice because it exhibits the lowest PRESS and the highest Prediction R^2, both validation type statistics which are likely the best overall measures of goodness of fit. The values shown in parentheses in Table 1-2 are the t-ratios of each model

coefficient defined as the ratio of the model coefficient divided by its standard deviation. The t-ratios reported in Table 1-2 are uniformly large, which indicates that the estimated model coefficients are extremely stable.

Table 1-2: Summary of Regional Groundwater Model Results

	Constant	GW_{t-1}	P_k	K	PET_1	$\sum$BMP					
Model	β_0	β_1	β_2	β_3	β_4	β_5	Adj-R^2	Pred-R^2	NSE	SE	PRESS
1	-0.11 (16.6)	0.93 (234.3)					87.5%	87.5%	0.88	0.16	2151
2	-0.05 (-7.33)	0.94 (273.5)	0.83 (48.4)				90.6%	90.6%	0.91	0.14	1683
3	0.04 (5.23)	0.94 (281.8)	1.19 (52.9)	-0.002 (-25.4)			91.2%	91.2%	0.92	0.14	1591
4	0.09 (11.9)	0.95 (303.6)	1.24 (59.5)	-0.003 (-31.1)	-9.87 (-21.7)		92.4%	92.4%	0.92	0.13	1345
5	**0.07** (10.5)	**0.95** (324.5)	**1.25** (64.0)	**-0.003** (-31.7)	**-10.19** (-24.0)	**0.052** (5.85)	93.4%	93.4%	0.92	0.13	1091

Note. The table reports model coefficients (β's in) along with their t-ratios (in parentheses), adjusted and prediction R^2, Nash-Sutcliffe Efficiency (NSE), the average prediction error (SE. in meters) for each model, and PRESS. All coefficients were significant at the 1% level

5.3 Goodness of fit

Table 1-2 documents that for the recommended model, the prediction R^2 value was 93.4%, indicating that the model accounts for approximately 93% of the variability in groundwater observations within Back Bay. Since the prediction R^2 is a validation type statistic, we expect similar goodness of fit when the model is employed in prediction mode. The NSE value is 0.92, with average prediction error (SE) of 0.11 meters and root mean square of the residuals (r.m.s.) of 0.13 meters. Figure 1-2 illustrates the model goodness of fit by comparing the calibration results with actual observed values. The calibration data included observations collected from June, 1999, to September, 2009. Results in Figure 1-2 indicate that the regional groundwater model reproduces the observed groundwater elevations with a relatively high level of confidence and little or no bias.

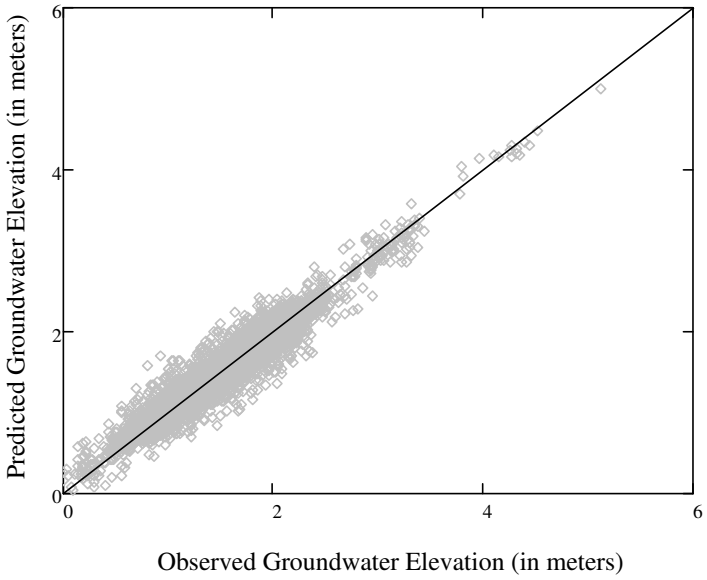

Figure 1-2: Comparison of predicted versus observed groundwater elevation; data set includes observed groundwater elevations from June 1999 to September 2009.

5.4 Discussion

It is important to emphasize that regression methods yield an estimate of the conditional mean value of the variable of interest, in this case the groundwater elevation at a particular well location, conditioned on the various values of the explanatory variables. Thus the regression model provides an estimate of the conditional mean groundwater elevation as a function of previous groundwater elevations, time lag since that observation, precipitation and potential evapotranspiration, and the impacts of the location and capacity of various installed BMPs. The final regional model given as model 5 in Table 1-2 can be summarized as

$$GW_t = 0.07 + 0.95GW_{t-k} + 1.25P_k - 0.003k - 10.19PET_1 + 0.052\sum BMP \quad (7)$$

The regional regression model documents that the recharge BMPs have a statistically significant positive impact on average groundwater elevations. The model coefficient for the ∑BMP term was found to be 0.052 with a t-ratio of 5.85. This implies that the model coefficient has a standard deviation of only 0.009; thus, we are extremely confident of the value of this coefficient. The ∑BMP coefficient 0.052 represents the positive change in predicted groundwater elevation, on average, that would occur by holding all other explanatory variables constant. For example, a 1 m^3 recharge BMP installed 1 meter from an observation well would, on average, increase the observed groundwater elevation by 0.052 meters. Likewise, a 10 m^3 recharge BMP installed 100 m from an observation well would increase the average observed groundwater elevation by only 0.0052 meters. This result illustrates the small yet statistically significant impact of the recharge BMPs on groundwater elevations. It would be very difficult to isolate this observed impact using advanced groundwater modeling methods (Yao et al. 2010; Li et al. 2003) given the very slight influence which each BMP has on local groundwater elevations.

It is important to note that the coefficient β_5=0.052 represents the conditional average increase in groundwater elevations to be expected across the region; this assumption is important given that conditions at specific well locations will display either more or less of an increase in groundwater elevations. For example, groundwater gradients and local groundwater flow directions may greatly affect observed changes in groundwater elevations as a result of recharge BMPs. Overall, across the Back Bay region of Boston, the

coefficient provides an average impact that is likely to occur at any specific location.

5.5 Model validation

Cross validation methods were conducted to evaluate the application of the model to situations not considered when fitting the model summarized in Table 1-2. Cross validation was conducted using a standard method of blind testing, or validating the model with data not used during model calibration. Additionally, repeated random sub-sampling was employed where the calibration data was randomly split into validation and training data sets. Model split-sample validations were conducted by using 50% of the calibration data (4,007 observations) as the training data set, with the remaining 50% of the data used for cross validation. The random sub-sampling procedure was repeated 100,000 times to increase the probability that observations were selected for both the calibration and validation data sets during the validation procedure.

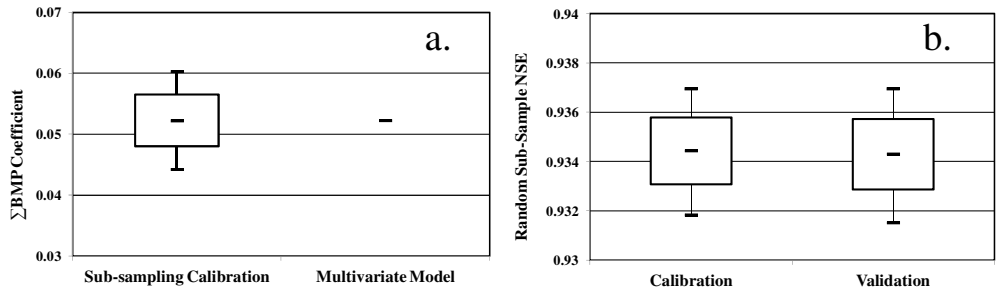

Figure 1-3: Groundwater model coefficient cross validation results: (a) ∑BMP coefficient; (b) calibration and validation NSE.

Figure 1-3.a illustrates box plots for estimates of the model coefficient associated with the variable ∑BMP obtained in the random sub-sampling

validation compared to the multivariate model results included in Table 1-2. Figure 1-3.a illustrates that the variability in the ∑BMP term coefficient is small and averages to the value summarized in Table 1-2. These results indicate that it is highly likely that a similar model coefficient would be obtained, regardless of the particular observations used in the development of the model. The results also indicate that the model predicts the impact of recharge BMPs on observed groundwater elevations with a relatively high degree of precision. Also reported in Figure 1-3.b is the variability in the NSE for the validation and training sets. The variability in NSE values was quite similar for both the calibration and validation datasets.

5.6 Blind-sample validation

A second data set of observed groundwater elevations from October, 2009, to June, 2010, was obtained from BGwT and used to conduct a blind-sample validation. These observations were not used in the development of the regression model reported above. The blind sample validation dataset included two additional recharge BMP installations that were approved and activated after October, 2009. Model performance was tested by comparing observed data to predicted groundwater elevations as illustrated in Figure 1-4. Results indicate, once again, that the model in (7) was able to accurately reproduce groundwater elevations with a NSE of 0.87 and a r.m.s. of 0.17 meters.

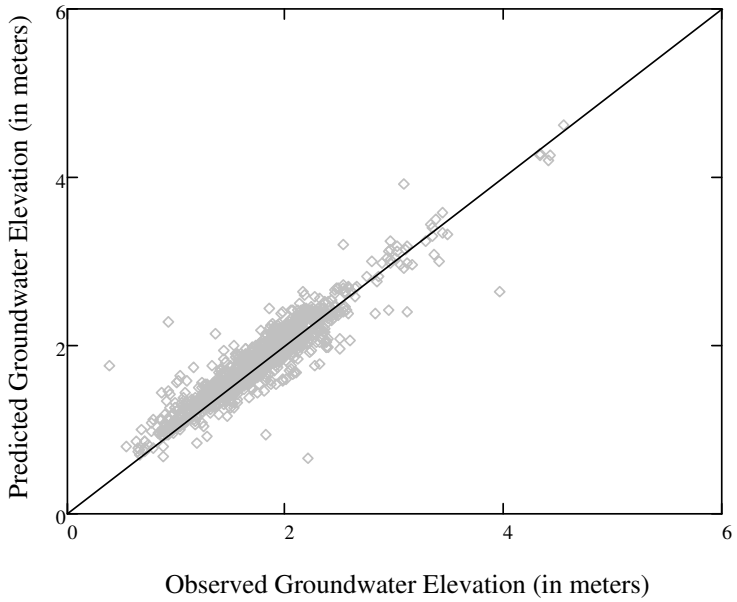

Figure 1-4: Blind sample validation; data set includes observed groundwater elevations from October 2009 to June 2010.

Overall, our validation results indicate a high degree of stability in model parameter estimates and model performance. These results indicate that the model coefficients are stable and within a reliable range to conduct additional analyses which explore the impact of future storm water BMP recharge facilities in the Back Bay on groundwater elevations. The r.m.s. is reported to be 0.13 m for the calibration dataset and 0.17 m for the validation dataset; which are both better fits than reported for similar scale (~1 km^2) urban groundwater models (Carneiro and Carvalho 2010).

6.0 Application of Regional Groundwater Model

6.1 Impact of an Individual Recharge BMP

The model coefficient for the ∑BMP term given in Table 1-2 can be used to predict the average increase in groundwater elevations at a particular location which will result from a recharge BMP of known capacity located a specific

distance from the location of interest. Given the resulting model coefficient for the ∑BMP term, the impact of a particular recharge BMP can be represented graphically as illustrated in Figure 1-5. Figure 1-5 documents the expected average rise in groundwater elevation given a specific recharge BMP capacity located a particular distance from a location of interest. For example, Figure 1-5 illustrates that a recharge BMP of 50 m^3 capacity placed 500 meters from an observation well would, on average, increase groundwater elevations by 0.0052 meters.

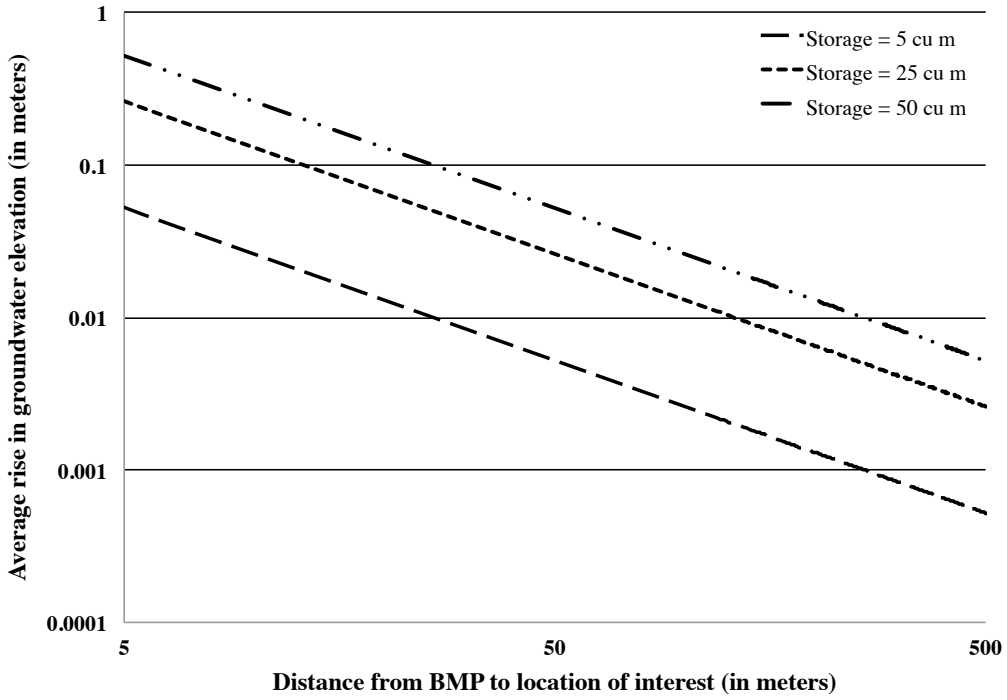

Figure 1-5: Relationship between average rise in groundwater elevations and distance from BMP to location of interest.

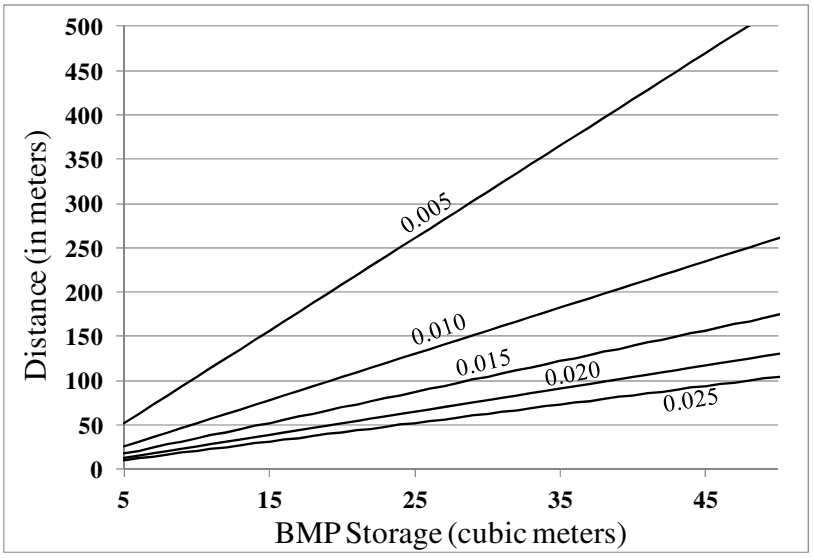

Figure 1-6: Average rise in groundwater elevation in meters resulting from recharge BMP of particular capacity located a distance from a particular location of interest.

Figure 1-6 also illustrates how the ∑BMP model coefficient can be used for urban storm water planning. For example, if an increase in groundwater elevation of 0.01 meters was desired, with a recharge BMP storage capacity of 20 cubic meters, the recharge BMP should be placed approximately 105 meters from the groundwater observation well.

The two graphical summaries shown in Figures 1-5 and 1-6 illustrate the predictive power of the model in (7). Figures 1-5 and 1-6 provide guidance on how to interpret the implications of the model for use in future storm water recharge BMP planning or urban streamflow restoration which may benefit from additional groundwater discharge to surface flows

We emphasize that the results in Figures 1-5 and 1-6 are based on the model summarized in (7) and Table 1-2 which was developed using all the

existing recharge BMPs installed as of September 2009. As future BMPs are added to the Back Bay region, the results shown in Figures 1-5 and 1-6 may change and may need to be updated. However, our validation experiments reported earlier indicate rather robust results, regardless of the number of well observations considered in the development of the model.

6.2 The Impact of a System of Recharge BMPs

The BMP groundwater model given in (7) can also be used to evaluate the impact of an installed system of future recharge BMPs. For illustrative purposes, three recharge BMP scenarios were developed to illustrate the application of (7) for storm water planning. The following three scenarios are considered:

Scenario 1: Single recharge BMP per block; located centrally; 7.93 m^3 capacity

Scenario 2: BMPs placed at approximately every 10th building; approximately 6 BMPs per block; 7.93 m^3 capacity

Scenario 3: Remove all existing BMPs

For each of the above scenarios, the $\sum$BMP term given in (7) is estimated using assumed location and average regional BMP capacities for each scenario and the results of the analysis are illustrated in Figure 1-7. Scenario 1 resulted in an average groundwater elevation increase of 0.037 meters, with local areas experiencing an increase of up to 0.08 meters (Figure 1-7.a). Scenario 2 increased average groundwater elevations by 0.226 meters, with areas installing multiple recharge BMPs experiencing up to a 0.29 meter increase in groundwater elevations (Figure 1-7.b).

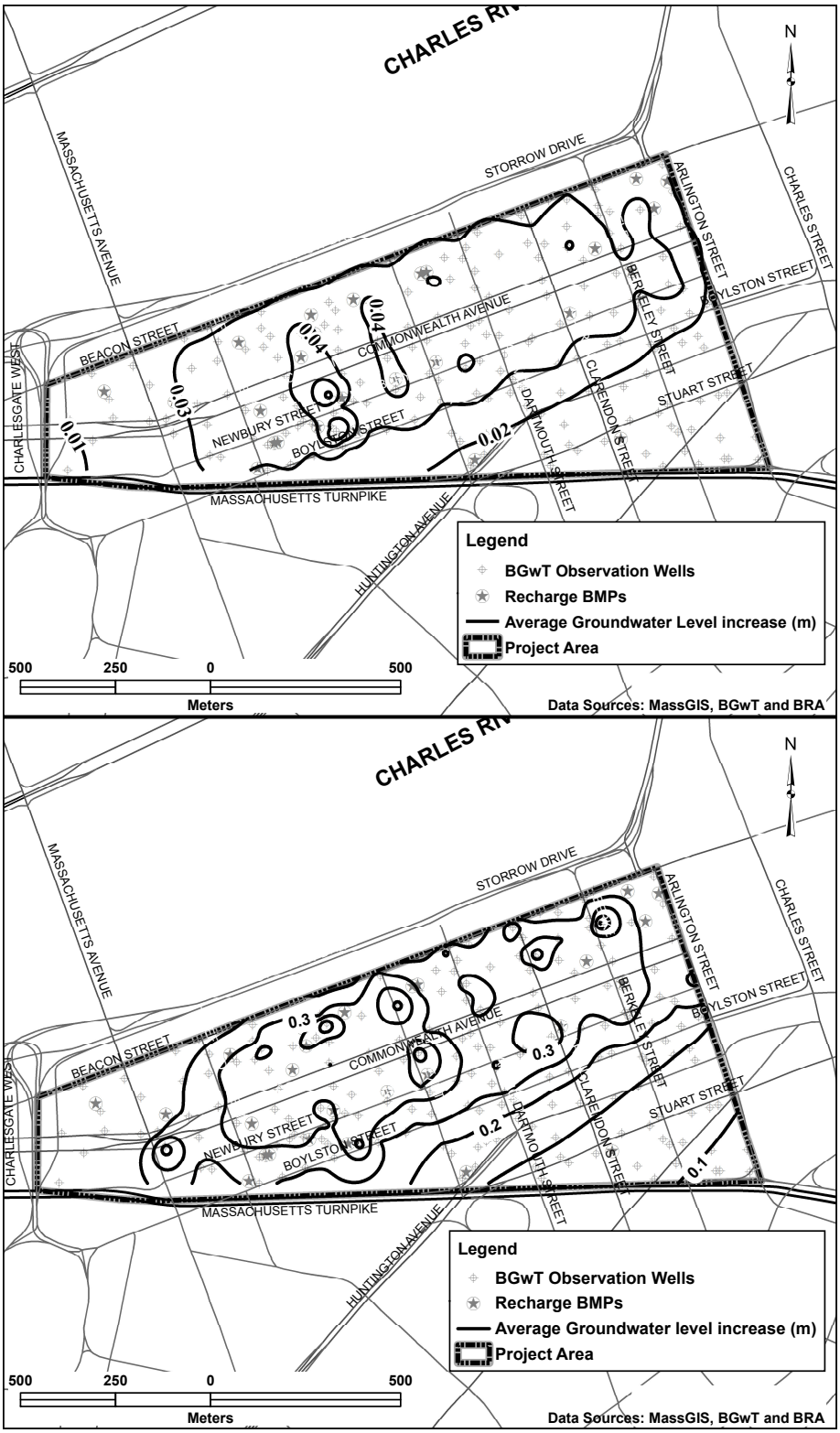

Figure 1-7: Results from Scenario 1 (a, top) and Scenario 2 (b, bottom) documenting average effect of recharge BMPs to groundwater elevations within Back Bay.

In addition Scenario 3 considered the removal of all existing recharge BMPs from the Back Bay region. This was accomplished by simply setting the ∑BMP term in the model to zero and reapplying the model at each of the well locations. This resulted in decreases in the average groundwater levels for all regions across the site. The average reduction in groundwater elevation was -0.03 meters, however, reductions ranged from -0.012 to -0.10 meters when the existing recharge BMPs were artificially removed from the Back Bay region. These results indicate that the regional BMP groundwater model can be used to assess the potential average groundwater increase across Back Bay resulting from various installed BMP recharge facilities.

7.0 Conclusions

Multivariate statistical methods were employed to develop a relationship between groundwater elevations in the Back Bay region of Boston and various explanatory variables, including rainfall, potential evapotranspiration, previous groundwater elevations and the location and capacity of installed storm water recharge BMPs. Our results document that the inclusion of recharge BMP variables into the regression equations leads, on average, to very small but positive and significant increases on groundwater elevations across the Back Bay region of Boston. Our regional model indicates that well elevations are most impacted by previous well elevations and the recharge which results from the precipitation which occurred since those previous well elevations were observed. We also show how the resulting models can be useful for determining the influence of future BMP installations on groundwater elevations in the Back Bay region of Boston.

Although our approach is based primarily on the theory of statistics, it is also based on the physical water balance given by Hodgson (1978) which is similar to Scanlon et al. (2002). The regression constant and the time lag between well observations, k, represents a combination of natural aquifer drainage in addition to reduced groundwater storage as a result of anthropogenic influences such as municipal infrastructure and conduits of groundwater flow. The inclusion of previous groundwater elevations indicates that the relationship between current and previous groundwater elevations reflects the physical geohydrologic structure of the aquifer in the vicinity of each well which is known to be quite heterogeneous.

We examined the ability of a regional multivariate groundwater model to predict groundwater elevations within the Back Bay region of Boston using observable and easily measured explanatory variables. The model validations illustrated in Figure 1-4 document the performance of the regional models to predict observed groundwater elevations within Back Bay with well data not included in the calibration of the regional model. Goodness of fit statistics including the Nash-Sutcliffe efficiency criterion and prediction R^2 indicate excellent goodness of fit. Additional model split-sample, cross-validation and blind-validation analyses were performed to ensure that model coefficients exhibited the type of stability needed to ensure that model applications would be meaningful.

Perhaps the most important result of this study is that the regional models described here can be used to predict the impact of future BMP installations on

groundwater elevations, because the model relates the average increase in groundwater elevations at a particular location to the capacity, time of installation and location of a particular recharge BMP or a set of such BMPs. The results of the various case studies documents that groundwater elevations generally are not drastically increased over the region until multiple recharge BMPs are placed throughout the study area given the small but significant effect of the recharge BMPs to observed groundwater elevations.

8.0 Acknowledgements

This research project was supported by the *Boston Groundwater Trust* and the *Tufts University Program in Water: Systems, Science and Society.* The authors are especially indebted to Elliott Laffer, Christian Simonelli and the technical advisory committee of the Boston Groundwater Trust. The authors also express their appreciation to the three anonymous reviewers whose comments contributed to substantial improvements to the original manuscript.

Chapter 2

Baseflow Recession Analysis: Testing the Nonlinear Hypothesis

Abstract

A streamflow recession curve has theoretically been shown to exhibit behavior attributed to the relationship between aquifer formations and groundwater outflow to a stream channel. The recession plot, the log-log plot of dQ/dt versus Q, is commonly used to estimate recession parameters corresponding to the slope and intercept of the recession slope curve. This study develops and tests a comprehensive approach to evaluate the degree to which watersheds act as linear reservoirs by employing new methodologies including quantile regression, efficient estimation of dQ/dt, inclusion of groundwater withdrawals, and seasonal effects. Our results illustrate highly variable estimates of baseflow recession parameters due to finite difference schemes and ignoring groundwater withdrawal impacts. A null hypothesis of linear watershed storage behaviors was tested using our recession parameter estimation methodology which illustrated that watersheds in our study area did not exhibit linear storage behaviors. Such results illustrate the importance of a clearly defined estimation procedure to compare behaviors across watersheds.

1.0 Introduction

A streamflow hydrograph can be separated into the rising limb reflecting increases in discharge generally ascribed to precipitation events or recession limbs which represent decreased streamflow maintained by watershed storage discharge. A streamflow recession curve exhibits behavior which is related to watershed aquifer formations and the associated groundwater outflow to the stream channel. *Tallaksen* (1995) and *Hall* (1968) review applications of streamflow recession analysis and its use in characterizing the bulk hydraulic and hydrologic properties of a watershed. The theory of recession analysis emerged from early studies of groundwater flow (*Dupuit*, 1863; *Boussinesq*, 1877; *Mailet*, 1905) and has since spurred multiple approaches to characterize groundwater/surface water interactions. Increased attention has focused on the quality and quantity of groundwater because groundwater outflow sustains surface water flow during drought periods and because it is recognized as a significant component of the global freshwater budget (Alley et al., 2002). Therefore, understanding the contribution of groundwater to streamflow, termed baseflow, is a fundamental focus of engineering, hydrogeologic and ecological studies.

Many investigations have studied streamflow recession behavior to further their understanding of watershed processes. *Szilagyi et al.* (2007) estimated basin evapotranspiration by analysis of baseflow recession behaviors. *Devito et al.* (1996) documented morphological controls which influenced the sustainability of baseflow to wetlands within the Canadian Shield. *Kirchner* (2009) characterized catchment behavior by deriving a sensitivity function related to nonlinear storage-

discharge relationships. *Clark et al.* (2011) suggested that it was necessary to understand baseflow processes in hydrologic models to accurately understand and predict groundwater/surface water interactions. *Lo et al.* (2010) developed a parametric model of baseflow behavior to enable estimation of water table depths within a land surface watershed model. In these previous studies, estimation of watershed storage characteristics were inconsistent relative to other baseflow studies or ignored the influence of anthropogenic impacts which have been shown to alter groundwater-surface water interaction (*Wang and Cai*, 2009).

Integrated management of groundwater and surface water has generally relied on baseflow characterization. The baseflow response of a river has been found to depend on both urban water quality management (*Shepard et al*., 2006) and land use management (*Wayland et al*., 2003). *Dow* (1999) and *Schilling and Libra* (2003) explored trends in baseflow and attributed significant changes over time to land-use/land cover alteration. Baseflow sustains aquatic ecosystems in dry summer months because groundwater discharge provides constant stabilizing temperatures to streams. Ecological studies suggest benthic organisms and macroinvertebrates rely on baseflow (*Robinson et al*., 2000) similarly to the reported relationship between stream fish assemblages and baseflow stability, an index defined by *Poff and Allan* (1995) as the average of annual ratios of lowest daily flow to the mean daily flow.

A fundamental assumption inherent in nearly all the previously cited studies is that watersheds exhibit a fixed time constant known as the 'baseflow recession constant'. There is considerable controversy over this issue as

emphasized by baseflow scale investigations ranging from slope-scale (*Harman and Sivapalan*, 2008) to large-scale watersheds (*Vogel and Kroll*, 1996; *Wittenberg*, 2003). Characterizing watershed behaviors is vital to understand the temporal variability in quality and quantity of watershed discharge to streamflow. To study discharge behaviors at the watershed scale, *Brutsaert and Nieber* (1977) introduced estimation of recession parameters obtained from the recession slope curve on the log-log plot of –dQ/dt versus Q (recession plot) where Q is streamflow. Even with the recession plot method, characterizing storage behaviors remains problematic (*Brutsaert*, 2008). The primary purpose of this study is to develop and test a comprehensive scientific approach in baseflow parameter estimation which allowed for hypothesis tests to determine whether or not watershed recessions can be characterized by a fixed time constant. The following sections provide an introduction to the theoretical derivation of baseflow recession characteristics and the motivation for this study.

To characterize relationships between groundwater and surface water systems, we conceptualize a simple basin model which assumes that the initial rapid inputs that contributed to the increase in streamflow (the rising limb of the hydrograph) have been fully depleted. This assumption implies that all observable streamflow is derived exclusively from long-term storage or groundwater discharge. *Hall* (1968) and *Dooge* (1983) and many others have suggested the use of a power law model to relate groundwater storage in an unconfined aquifer in direct hydraulic connection to a stream, S [mm d^{-1}], and the observed groundwater discharge to the stream, Q [mm d^{-1}], as

$$Q = \alpha S^n \quad (1)$$

where α and n are constants. Equation 1 can also be interpreted as an idealized solution to the Dupuit-Boussinesq equation under the assumption of horizontal groundwater flow to a fully penetrating river channel (*Bear*, 1972).

For an aquifer, ignoring potential capillary effects, continuity can be written as

$$\frac{dS}{dt} = I(t) - Q(t) \qquad (2)$$

where I(t) represents infiltration from the vadose zone to the water table. The analysis is conducted during stream recession periods (i.e. no precipitation events) with rapid initial percolation which ceases after precipitation; thus, I(t)=0.

Szilagyi et al. (2007) and *Wang and Cai* (2009) document potential seasonal effects on the baseflow response due to changes in evapotranspiration (ET). *Wang and Cai* (2010) employ similar equations to (2) which account for the impact of groundwater withdrawals on hydrograph recessions, which we consider in Section 3.4. Initially we assume groundwater withdrawals are negligible and ET is either constant or has a negligible impact on (1) and (2) during baseflow events. These assumptions are consistent with numerous previous studies (*Brutsaert*, 2008; *Szilagyi et al*., 1988, among many others).

Combining (1) and (2) leads to

$$\frac{dQ}{dt} = -n\alpha^{\frac{1}{n}} Q^{\frac{(2n-1)}{n}} \qquad (3a)$$

$$\frac{dQ}{dt} = -aQ^b \quad (3b)$$

where n and α are constants with $b = (2n-1)/n$ and $a = n\alpha^{1/n}$. Equation (3b) was presented by *Brutsaert and Nieber* (1977) to graphically illustrate that on a log-log plot of -dQ/dt vs Q, termed the recession plot, the log of parameter "a" is the intercept while "b" is the slope of the fitted envelope to the streamflow recession data. *Brutsaert and Nieber* (1977) recommended fitting a lower envelope to data points created by the recession plot when employing the graphical estimation method. The justification for the lower envelope arises from the assumption that, for any given streamflow Q, the lowest change in flow per time (dQ/dt) represents flow originating solely from groundwater storage.

Although the value of n in (3a) can take on any value in the range (0,∞), it is often assumed that n=b=1, or that the aquifer behaves as a linear reservoir (*Fetter*, 1994; *Domenico and Schwartz*, 1998). Note that Brutsaert and Nieber (1977) also derived solutions to the Boussinesq equation for b = 1.5 and 3. Given the assumption of a linear reservoir, the solution to (3a) is

$$Q = Q_o e^{-\alpha t} \quad (4a)$$

where Q_o is the observed streamflow at time t=0. Equation (4a) can also be written as

$$Q = Q_o K_b^t \quad (4b)$$

where K_b is the recession time constant, commonly referred to as the baseflow recession constant. *Brutsaert and Nieber* (1977) and *Vogel and Kroll* (1992) relate K_b to bulk hydrogeologic properties of the watershed. *Vogel and Kroll* (1996) assumed n=1 for watersheds in Massachusetts to study the statistical properties of recession estimators and their use in regional regression models.

Zecharias and Brutsaert (1988) assumed n=1 for basins within the Appalachian Plateau to illustrate dependence of baseflow behavior on watershed characteristics. *Eng and Milly* (2007) documented variability in n between 0.78 and 1.85 with a median value of 1.11 for 93 watersheds in southeastern US; they assumed that n=1 to characterize recession behaviors at partial-record stream gage sites. Additionally, many common hydrologic models, too numerous to list exhaustively, (HEC-HMS, HSPF and National Weather Service models, for example) use the baseflow recession constant, K_b, given the assumption that n=1.

Wittenberg and Sivapalan (1999) illustrate that nonlinear reservoir behaviors ($n \neq 1$) are more physically realistic since ranges of recession curves tend to increase with decreasing streamflow. *Tague and Grant* (2004) attribute flow regime control to the heterogeneity of natural groundwater systems. *Brutsaert and Nieber* (1977) documented results for watersheds in the Finger Lakes region of New York that supported the assumption that n=2. *Wittenberg* (1999) showed that $n \geq 2$ for 80 watersheds in Germany, while *Troch et al*. (1993) obtained n=2 for a watershed in Belgium. *Harman et al*. (2009) documented increasing nonlinear behavior due to increasing heterogeneities at hill slope scales. *Pulido-Velazquez et al.* (2005) illustrate the use of multi-reservoir models to reproduce observed nonlinear behaviors in surface water/groundwater interaction.

Brutsaert (2008) notes that, at the watershed scale, streamflow measurement error and inconsistent parameter estimation methods result in continued concerns over the meaning and relevance of estimated baseflow parameters. Given the recent findings that water withdrawals (*Wang and Cai*,

2009) and evapotranspiration (*Szilagyi et al*., 2007) can influence the baseflow recession response of watersheds, combined with the concerns raised by *Brutsaert* (2008), we conjecture that all of these issues could have an important influence on our ability to determine whether or not a watershed exhibits either linear (n=1) or nonlinear behavior. It is difficult to decipher the true relationship of (3a) since one never knows the true value of n. The purpose of this paper is to test the hypothesis that groundwater outflow responds as a linear reservoir (n=b=1) and thus is characterized by a fixed time constant, K_b. To evaluate our hypothesis, a new methodology is introduced and applied to evaluate the degree to which watersheds act as linear reservoirs. Our new methodology includes several innovations including: (1) a more rigorous quantile regression approach to fit the power law model to the lower envelope of the relationship between –dQ/dt vs. Q, (2) an efficient and reproducible approach for estimation of the numerical derivative in (3b), and evaluation of the influence of both (3) seasonality and (4) the degree of groundwater withdrawals in the watershed on recession characteristics. Our approach is based on the power law relationships shown in (1) described by *Brutsaert and Nieber* (1977) which does not presume an *a priori* value of n.

2.0 Experimental Methodology

2.1 Data

This study is conducted on watersheds within New Jersey since a large database of groundwater withdrawal information is readily available for the priod of 1990-2007. This study uses groundwater withdrawal, precipitation and streamflow data for that time period. Daily streamflow records at 45 U.S.

Geological Survey (USGS) stream gages were used to isolate suitable recession hydrographs for the analysis (Figure 2-1 and Table 2-1). USGS stream gage sites were selected based on continuous daily records for calendar years 1990-2007. For this study, it was necessary that the entire contributing watershed be within state boundaries.

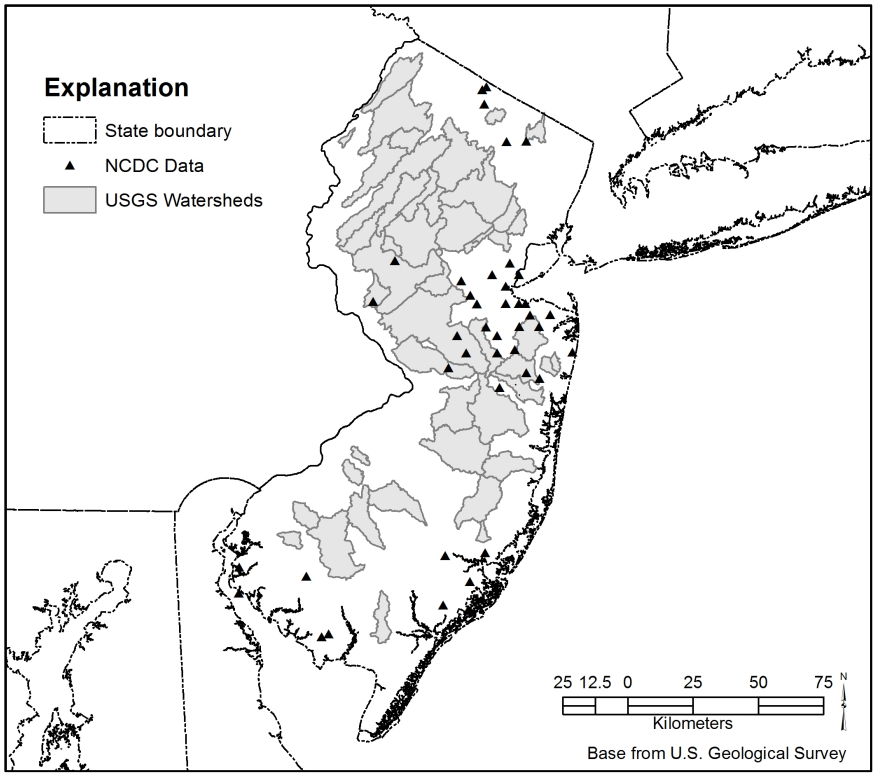

Figure 2-1: Location of 45 U.S. Geological Survey gages and National Climatic Data sites (NCDC) in New Jersey, USA.

Table 2-1: Summary of U.S. Geological Survey Streamgages

Site Number	USGS Streamgage Number	Streamgage Name (in NJ)	Drainage Area (km^2)
1	01379000	Passaic River, Millington	143.49
2	01379773	Green Pond Brook, Picatinny Arsenal	19.81
3	01379780	Green Pond Brook, Picatinny Lake	23.72
4	01380500	Rockaway River, Boonton	300.44
5	01381000	Rockaway River, Boonton	308.21
6	01381900	Passaic River, Pine Brook	903.91
7	01393450	Elizabeth River, Elizabeth	43.77
8	01394500	Rahway River, Springfield	66.04
9	01396500	South Branch Raritan River, High Bridge	169.13
10	01396660	Mulhockaway Creek, Van Syckel	30.56
11	01396800	Spruce Run, Clinton	106.97
12	01398000	Neshanic River at Reaville	66.56
13	01398500	North Branch Raritan River, Far Hills	67.86
14	01399500	Lamington River, Pottersville	84.95
15	01399670	Rockaway Creek, Whitehouse Station	29.27
16	01401000	Stony Brook, Princeton	115.25
17	01401650	Pike Run, Belle Mead	13.88
18	01402000	Millstone River, Blackwells Mills	668.22
19	01403150	West Branch Middle Brook, Martinsville	5.15
20	01403400	Green Brook, Seeley Mills	16.14
21	01403540	Stony Brook, Watchung	14.27
22	01405400	Manalapan Brook, Spotswood	105.41
23	01407705	Shark River, Neptune City	25.80
24	01407760	Jumping Brook, Neptune City	16.73
25	01408000	Manasquan River, Squankum	113.96
26	01408500	Toms River, Toms River	318.57
27	01409400	Mullica River, Batsto	120.95
28	01410000	Oswego River, Harrisville	187.77
29	01410150	East Branch Bass River, New Gretna	21.00
30	01411000	Great Egg Harbor River, Folsom	147.89
31	01411300	Tuckahoe River, Head of River	79.77
32	01411456	Little Ease Run, Clayton	25.30
33	01411500	Maurice River, Norma	290.08
34	01440000	Flat Brook, Flatbrookville	165.76
35	01443500	Paulins Kill, Blairstown	326.34
36	01443900	Yards Creek, Blairstown	13.83
37	01445500	Pequest River, Pequest	274.54
38	01457000	Musconetcong River, Bloomsbury	365.19
39	01464000	Assunpink Creek, Trenton	234.65
40	01464500	Crosswicks Creek, Extonville	211.08
41	01466500	McDonalds Branch, Byrne State Forest	6.09
42	01467000	North Branch Rancocas Creek, Pemberton	305.62
43	01467081	South Branch Pennsauken Creek, Cherry Hill	23.26
44	01467150	Cooper River, Haddonfield	44.03
45	01477120	Raccoon Creek, Swedesboro	69.67

Precipitation data was obtained from the National Climatic Data Center (NCDC) for sites with continuous daily precipitation records for the period 1990-2007. Selected sites are illustrated in Figure 2-1. For the purpose of this paper, precipitation totals reported as trace (T) were considered to be zero.

Groundwater withdrawals over the period 1990-2007 were obtained from the New Jersey Geological Survey (*NJGS*, 2011). The withdrawal database contains recorded municipal and estimated irrigation and industrial monthly withdrawals reported by HUC-14 regions across the state. Total watershed withdrawals were calculated by aggregating HUC-14 withdrawals within delineated watersheds shown in Figure 2-1. Total watershed monthly withdrawals were assumed to be uniformly distributed across the month for this study.

2.2 Study Area Hydrology/Geology

Watersheds of this study span the four physiographic provinces which characterize the geology of New Jersey. The Valley and Ridge province is underlain by sedimentary bedrock which have undergone geophysical stresses resulted in folding and faulted bedrock characteristicized as trending north east-south west ridges and valleys. Hilly regions characterize the Highland province with incised valleys as a result of erosion-resistant metamorphic bedrock. The Piedmont region is underlain by both metamorphic and sedimentary bedrock which have been folded and faulted resulting in gentle plains with few ridges. Finally, the Coastal Plain of southern New Jersey is comprised of unconsolidated sand and gravel deposits with gentle or flat topography. Thus, in general, small valley aquifers tend to occur in northern New Jersey characterized by the Valley

and Ridge, Highland and Piedmont provinces while expansive unconfined aquifer tend to occur in Coastal Plain.

2.3 Hydrograph Separation

Recession hydrograph separation from streamflow time series data followed criteria commonly used in recession analysis (*Brutsaert*, 2008; *Wang and Cai*, 2009, among many others). Hydrographs were filtered to 1) eliminate data points with positive and zero estimates of dQ/dt, 2) eliminate 4 data points after the last positive or zero estimate of dQ/dt, and 3) eliminate any data points from recession hydrographs during which streamflow was observed to decrease despite a concurrent precipitation event. For this study, a precipitation event was represented as a daily precipitation total greater than 0.25 mm observed at the nearest two NCDC sites to a stream gage location since most watersheds did not have precipitation records within watershed boundaries (Figure 2-1).

3.0 Experiments

Our null hypothesis is that watersheds behave as linear reservoirs under baseflow conditions (H_o: b=1; H_a:b≠1). Our methodology examines how our ability to reject this hypothesis may be complicated by the effects of numerous traditional approaches used to characterize the behavior of hydrograph recessions. Although such hypothesis tests can never be definitive because one never knows the true behavior of the system, we present how each of the effects under investigation can possibly deter us from 'seeing' the true recession behavior of a watershed.

3.1 Quantile Regression

Brutsaert and Nieber (1977) originally recommended fitting a lower envelope to the cloud of data created on a log-log recession plot of dQ/dt vs Q. *Wittenberg* (1994) recommended an iterative technique to fit the lower envelope. *Mendozza et al.* (2003) recommended the lower envelope be fit so that 10% of the data is below the regression line. In that study, data were filtered to isolate points around the estimated fit and ordinary least squares regression was use to fit the remaining data. *Vogel and Kroll* (1992) used OLS regression to fit the entire data set since they felt the sampling error in streamflow measurements as well as the error associated with the resolution in which USGS streamflow data is reported creates natural variability in dQ/dt at a specific Q. *Kroll et al.* (2004) used 3-day moving averages instead of daily flows in deriving baseflow recession constants from dQ/dt vs. Q plots to minimize the impact of sampling and resolution error.

Vogel and Kroll (1996) documented numerous methods to estimate parameters assuming a linear reservoir system including time series and regression estimators. *Wang and Cai* (2010) fit lower and upper envelopes by assuming specific values for parameter a. Likewise, *Wang* (2011) fit recession envelopes "by eye" to allow 5% of data points to lie below the fit given specific values for a.

Previous methods to fit envelopes to data on the recession plot are generally not reproducible due to their subjective nature. *Brutsaert* (2008) recommends a 5% lower envelope to allow for error associated with flow estimation during low flow and selection of baseflow conditions. Here, we propose the use of quantile regression which is a rigorous and reproducible

method for fitting the lower envelope in the recession plot that remains robust in the sense that it allows for the possible errors suggested by *Brutsaert* (2008).

Most commonly used methods of ordinary least squares (OLS) regression provide estimates of a conditional mean, or the mean value of some variable as a function of one or more explanatory variables. Interest often is on the statistics other than the mean, thus quantile regression was introduced by *Koenker and Bassett* (1978) to estimate any conditional quantile. Unlike OLS regression, quantile regression minimizes the sum of the errors of the conditional quantile function, typically by linear programming methods to minimize the sum of weighted absolute deviations of a percentile of interest given by τ (*Koenker*, 2005). Thus, we may find a function $Y(\tau|x_i)$ for a dependent variable Y and explanatory variable x_i where τ% of the data lies below the line for any quantile of interest. This property reduces the effect of outliers similar to the robust nature of rank based estimates of the median. A quantile regression approach for recession parameter estimation is attractive since we are interested in the lower envelope, or quantile, of extreme observations (5-10% percentiles) within the recession plot which could exhibit outlier behavior in ordinary least square regression approaches. Another attractive feature of quantile regression in hydrologic studies includes assumptions about the nature of the residuals. Least squares regression approaches used in hydrologic recession investigations have documented serial correlation in residuals (*Kirchner,* 2009), which is expected due to the time dependency of hydrologic data. Parameter estimates from least squares regression with correlated residuals are unbiased (*Johnston and DiNardo*,

1997); however, inference procedures are invalid since autocorrelated residuals render ordinary least square approaches inconsistent. Standard methods exist to correct serial correlation of residuals for ordinary least squares, for example the Cochrane-Orcutt procedure described in *Johnston and DiNardo* (1997). Quantile regression, however, does not strictly depend on independence of residuals. Further, *Hao and Naiman* (2007) document that estimated model coefficients based on quantile regression are often distribution free. To our knowledge, the use of quantile regression in hydrologic studies has been limited to model prediction uncertainty (*Weerts et al*., 2011) and sediment dynamics (*Francke et al*., 2008).

Quantile regression was implemented to estimate recession parameters by fitting a lower envelope so as to allow 5% and 10% of the data to lie below the envelope. Quantile regression allows for consistent, well-defined and rigorous procedures to fit the lower envelope of data. All parameter estimates obtained from quantile regression procedures reported in this paper are significantly different from zero with a p-value less than or equal to 0.10 ($p \leq 0.10$). To ensure that slope estimatores for "b", $\hat{b}$, for various lower quantiles cited in recession literature (q=0.05 and q=0.10) were equal, t-tests were conducted with the R-Project (R Development Team, 2012). Slopes were found to be statistically equal at a significance level of 0.05 (α=0.05) across all tested sites. Figure 2-2 illustrates fitted envelopes of q=0.05 and q=0.10, based on quantile regression, within the recession plot. In Figure 2-2(a), the general slope of the lower envelope fits appear to be consistent with the trends shown by the data. However, in Figure 2-2(b), subjective methods would lead to a wide variability in estimates

of the slope of the lower envelope. Thus, we recommend the use of linear quantile regression procedures to estimate baseflow recession parameters ($\hat{a}$ and $\hat{b}$) with q=0.05. This approach is used throughout the remainder of our manuscript.

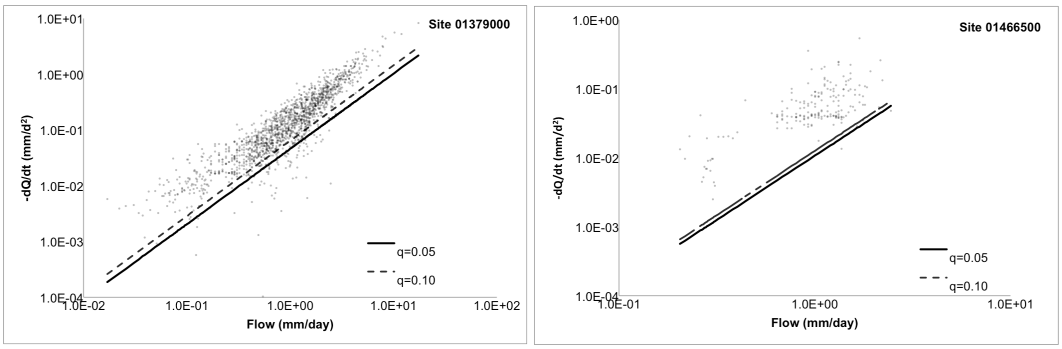

Figure 2-2: Graphical illustration of slope analysis between the q=0.05 and q=0.10 (5% and 10%) quantiles. (a) Site 1 (USGS 01379000). (b) Site 41 (USGS 01466500).

3.2 Numerical Derivatives

Fitting (3) to streamflow records requires estimation of numerical derivatives to evaluate the time derivative of streamflow. Numerical differentiation is "ill-posed" in a Hadamard sense (*D'Amigo and Ferrigino*, 1992) in that small measurement errors in a time series can result in large errors in derivative estimation. Streamflow derivative error can result from three potential sources: truncation error from the Taylor series approximations often used in practice, noise error (Liu et al., 2011) and systematic error in streamflow observations (*D'Amigo and Ferrigino*, 1992).

Brutsaert and Nieber (1977) provided an analytical approach to baseflow recession analysis by eliminating time t from the analysis and replacing it with a differential form, dt (3b). This approach required estimation of the time

derivative of streamflow (dQ/dt) for suitable Δt. *Brutsaert and Nieber* (1977) estimated the time derivative using the backward estimator

$$\frac{dQ}{dt} \approx \frac{Q_{i-\Delta t} - Q_i}{\Delta t} \quad (5)$$

It is well known that finite different methods to estimate gradients result in error based on step-size approximations (*Chapra and Canale*, 2006). Finite difference formulas derived from a Taylor series approximation are generally classified as centered, backward and forward difference. Center difference formulas are most often used in reported baseflow investigations (*Wang and Cai*, 2010; *Wang*, 2011). Although easy to use in practice, *James and Conyers* (1985) document limitations of finite difference methods given that difference values obtained from data at a sufficient Δt result in an inability to ascertain uncertainty in the estimate.

Various signal process methods are advocated for noisy time signals (for example, low pass finite impulse response filters described by *Bozzini and Rossini* (2003)). A literature review revealed that use of smoothing splines are optimal to fit smooth relationships to observed noisy data and are nearly optimal in estimating derivatives from such data. *Craven and Wahba* (1979) documented generalized cross-validation (GCV) methods to estimate nearly optimal derivatives from smoothing splines. *D'Amigo and Ferrigno* (1992) recommended GCV splines to smooth data with both systematic and random errors. *Ragozin* (1988) documented potential distortion in smoothing parameter selection due to noise in the data. However, *Ragozin* went on to prove that error in noisy data with optimal smoothing can result in nearly optimal derivative estimates. *Ritter* (1996) noted that errors in smoothing depend on the regularity of the function

implying that a smooth spline fit must be conducted on streamflow series that exhibit regular behavior.

Here, numerical derivative estimation using GCV splines were used on single recession hydrographs derived from the streamflow time series using an automated algorithm. Optimal cubic splines were fit to each individual recession hydrograph using the "pspline" package (*Ripley*, 2012) within the R-Project (*R Development Core Team*, 2012). We recognize previous studies that report methods to optimize spline fits to noisy data (*Craven and Wahba*, 1979; *Wahba*, 1973). For this study, however, we allowed automated kernel estimation procedures for optimal spline fitting to illustrate the methods we propose for estimating the time derivative of streamflow in (3b). Once splines were fit to individual recessions using automatic optimal curve fitting procedures, derivatives were estimated using the "sfsmisc" package (*Maechler et al*., 2012) within the R-Project to calculate the streamflow time derivative.

Table 2-2: Finite-difference Estimators used to estimate streamflow time derivative (Chapra and Canale, 2006).

Finite Difference Estimation	Equation	Equation Label
Backward	$f'(x_i) = \frac{f(x_i) - f(x_{i-1})}{h}$	B1
	$f'(x_i) = \frac{3f(x_i) - 4f(x_{i-1}) + f(x_{i-2})}{2h}$	B2
Forward	$f'(x_i) = \frac{f(x_{i+1}) - f(x_i)}{h}$	F1
	$f'(x_i) = \frac{-f(x_{i+2}) + 4f(x_{i+1}) - 3f(x_i)}{2h}$	F2
Centered	$f'(x_i) = \frac{f(x_{i+1}) - f(x_{i-1})}{2h}$	C2
	$f'(x_i) = \frac{-f(x_{i+2}) + 8f(x_{i+1}) - 8f(x_{i-1}) + f(x_{i+2})}{12h}$	C4

To explore the relation between the methods of estimation of the numerical derivative used in (3b), we tested various estimation formulas summarized in Table 2-2. Estimates of the numerical derivative using finite-difference methods summarized in Table 2-2 were computed from the entire daily streamflow time series for sites in Table 2-1 while GCV spline estimation was conducted using individual recession hydrographs. All estimates of dQ/dt for each method underwent hydrograph separation criteria to select data points for the analysis. Estimation of derivatives using finite difference formulas (see labels for each formula in Table 2-2) and from GCV spline fitting resulted in observable differences in data point locations as illustrated in Figure 2-3. At the site illustrated in Figure 2-3, estimates of $\hat{b}$ varied between 0.90 and 1.63 which corresponds to a range in values of n from 0.91 to 2.70. The results shown for this single site (Site 01399670), document that the method used to estimate the

numerical derivative dQ/dt can have a tremendous influence on both our estimate of a and $\hat{b}$ as well as our ability to discern whether or not reservoir behavior is linear (b=1). These results document that the method used for derivative estimation can dramatically alter our ability to understand whether or not watersheds act as linear reservoirs.

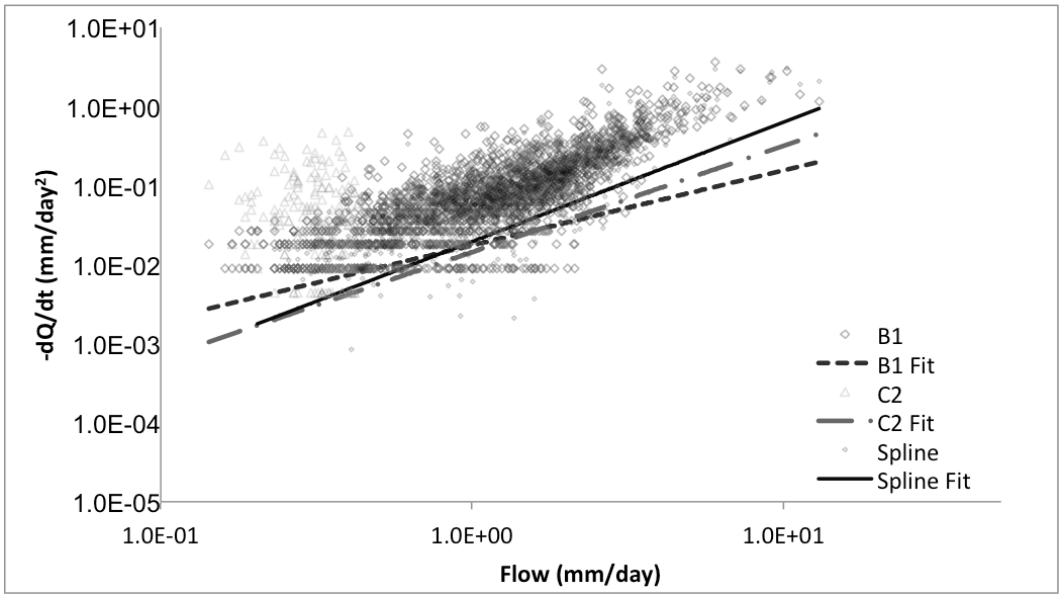

Figure 2-3: Parameter estimation variability caused by calculation of streamflow time derivative in (3b). This graph illustrates the variability encountered across all sites based on methods summarized in Table 2-2 in addition to the GCV spline.

Derivative estimation from GCV splines is nearly optimal (*Ragozin*, 1988) for noisy data, thus those estimates are used a reference here. We compare regression parameters obtained from finite difference schemes (see Table 2-2) to recession parameter estimates obtained from GCV splines by reporting percent difference defined as

$$\%Diff = 100 * \left[\frac{\hat{b}-b^*}{b^*}\right] \qquad (6)$$

where $\hat{b}$ is the estimate obtained from a finite difference method and b^* is the estimate obtained from the GCV spline derivative procedure. A graphical assessment of percent difference for each method is illustrated in Figure 2-4. The finite difference method most commonly employed in recent baseflow parameter research (*Brutsaert*, 2008; *Wang and Cai*, 2009; *Wang*, 2011; *Kirchner*, 2009) is the 2-point centered difference formula (C2, Table 2-2). Among all the finite difference methods considered, interestingly, the C2 method performs perhaps best in terms of percent difference, with differences generally within ±25% and a median percent difference very close to zero (-2%).

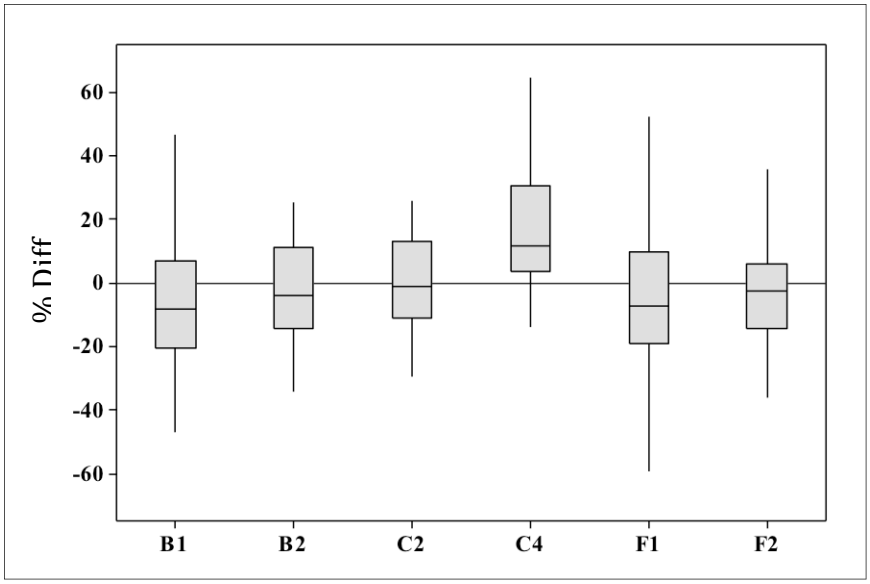

Figure 2-4: Percent difference as calculated by (6) which compares baseflow parameters estimated using finite difference equations in Table 2-2 to GCV spline procedures.

As one cannot know the true value of baseflow recession parameters in relating groundwater and surface water behaviors, it is impossible to characterize time derivative estimation scheme as being preferred over others. However, we recommend the spline method to estimate the time derivative of streamflow

dQ/dt. This recommendation is based on our inability to ascertain the uncertainty in finite difference estimation schemes due to both the natural variability in streamflow time series and the observation error in USGS gage readings. Secondly, our literature review identified GCV cubic splines as being nearly optimal in estimation of derivatives in noisy time series such as streamflow records.

3.3 Seasonality

Brutsaert and Nieber (1977) recommended a lower envelope fit to data points in the recession plot to characterize the power law relationship between $\left|dQ/dt\right|$ and Q. Their assumption is that the lower envelope represents the groundwater storage contribution to streamflow. Seasonal variability in streamflow can alter relationships between groundwater storage and streamflow due solely to groundwater recharge, groundwater withdrawal and possible ET effects (*Wittenberg*, 2003). Previous investigations to characterize the effect of seasonality in baseflow parameter estimation were performed by *Knisel* (1963) and *Federer* (1973). *Amit et al*. (2002) and *Birk and Hergarten* (2010) investigated spring hydrographs using recession approaches to interpret hydrologic characteristics. *Zecharias and Brutsaert* (1988) noted negligible effects from ET during recession analysis. *Wittenberg (2003)* and *Wang and Cai* (2009), however, documented seasonal variability in recession flows, which the authors attributed to ET effects.

Seasonal variability plays a dominant role in the hydrologic cycle and thus it plays a large role is determining the interaction between groundwater and

surface water systems. For example, *Xeflide and Ophori* (2009) documented the dependence of the lag-one serial correlation coefficient of seasonal streamflow observed in New Jersey streams as a result of previous seasonal precipitation totals. *Dow* (2007) documented the relationship between precipitation and stream hydrology, correlating baseflow index directly to precipitation in select watersheds in southern New Jersey. *Lins and Slack* (2005) report that, for the mid-Atlantic region, low flows tend to occur in September, median flows in January, and high flows in March. In general, groundwater elevations tend to be highest in the spring and lowest in the fall in this region. As described by *Van de Griend et al.* (2002), physical constraints of aquifer systems such as the decrease in hydraulic conductivity with depth in stratified drift aquifers due to compaction can greatly affect the seasonal storage-discharge behaviors. The variability in climate and hydrologic factors can, therefore, greatly influence groundwater and surface water behaviors.

To characterize seasonal effects to the linear reservoir hypothesis, recession data from each site was separated into 5 categories: winter (December - February), spring (March-May), summer (June-August), fall (September-November), and annual datasets which include all streamflow data for the period 1990-2007.

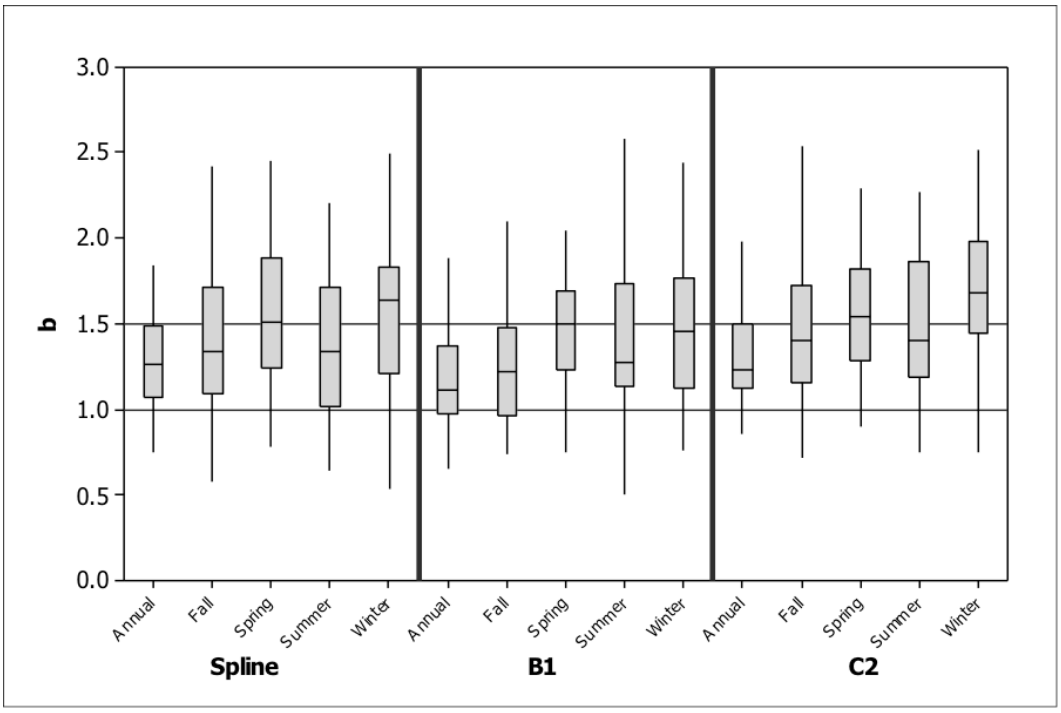

Figure 2-5: Box plots illustrating variability in seasonal estimates of b using GCV splines to estimate streamflow time derivatives.

Both seasonal variability and the method used to estimate streamflow time derivatives (dQ/dt) result in high variability in estimates of baseflow recession parameters as shown in Figure 2-5. Figure 2-5 illustrates boxplots of seasonal estimates of $\hat{b}$ based on the three methods: the GCV spline, backward difference (B1) and 2-point centered difference estimators (C2). Both the B1 and C2 estimation methods are commonly used in baseflow literature (for example, B1: *Kirchner*, 2009; C2: *Wang and Cai*, 2010). Generally, all 3 methods result in the lowest estimates of $\hat{b}$ when using an annual period of analysis. Generally estimates based on winter streamflow recession result in the highest estimates of $\hat{b}$. To illustrate the source of variability in $\hat{b}$ by season, Figure 2-6 illustrates,

for a single site, how the location of the data points varies by season which in turn influences estimation of the slope (b) using quantile regression.

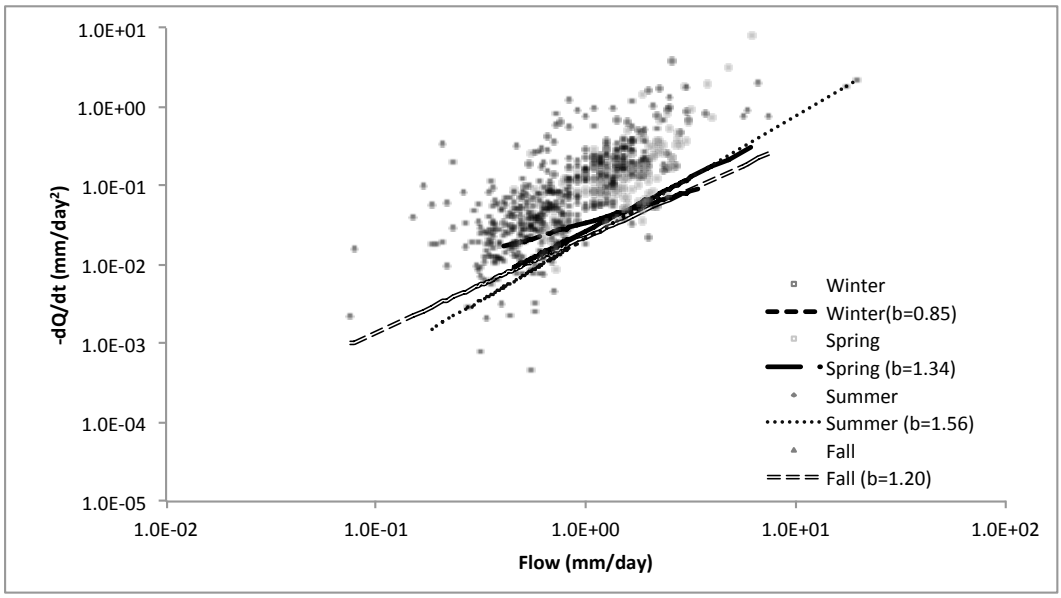

Figure 2-6: Recession plot illustrating variability in slope (b) depending on season. In this example, one may assume linear behavior based on winter estimates while summer estimates document nonlinear behavior.

3.4 Degree of withdrawal

Singh (1968) first introduced the impact of groundwater withdrawals on baseflow recessions. *Wittenberg* (1999) derived a groundwater recharge equation that incorporates the impacts of ET, groundwater withdrawals and baseflow contribution from storage. *Wang and Cai* (2010) introduced a groundwater withdrawal variable into the traditional formulation of baseflow recessions introduced earlier by *Brutsaert and Nieber* (1977). Here we explore the importance of including groundwater withdrawals in the analysis of baseflow recessions. For this purpose, we introduce a nondimensional withdrawal variable, γ, defined as the groundwater withdrawal as a ratio of overall streamflow during the recession:

$$\gamma_i = \frac{\sum_{j=1}^{n} \frac{W_j}{\overline{Q_{R_j}}}}{n_i} \qquad (7)$$

where W_j is the daily average withdrawal for hydrograph recession j, $\overline{Q_{R_j}}$ represents the average streamflow over the jth hydrograph recession, and n_i is the total number of observed hydrograph recessions available at site i.

Nonlinear behavior in groundwater response to a river is predicted by *Ahlfeld* (2004) who reported such behavior within a groundwater modeling framework (MODFLOW) using the Stream package. *Liu et al*. (2007) support such predictions given the documented nonlinear response between natural and human systems attributed to heterogeneous and transient activities which alter systems, such as groundwater withdrawals. Figure 2-7 illustrates findings of seasonal estimates of b by groundwater impacts (γ). In general, Figure 2-7 does not support conclusions of previous studies, which would predict increasing values of b due to increases in groundwater withdrawals. On the contrary, Figure 2-7 indicates either decreasing or constant trends in $\hat{b}$ as γ increases.. Results of the regression analysis document significant negative trends in the summer ($p=0.024$).

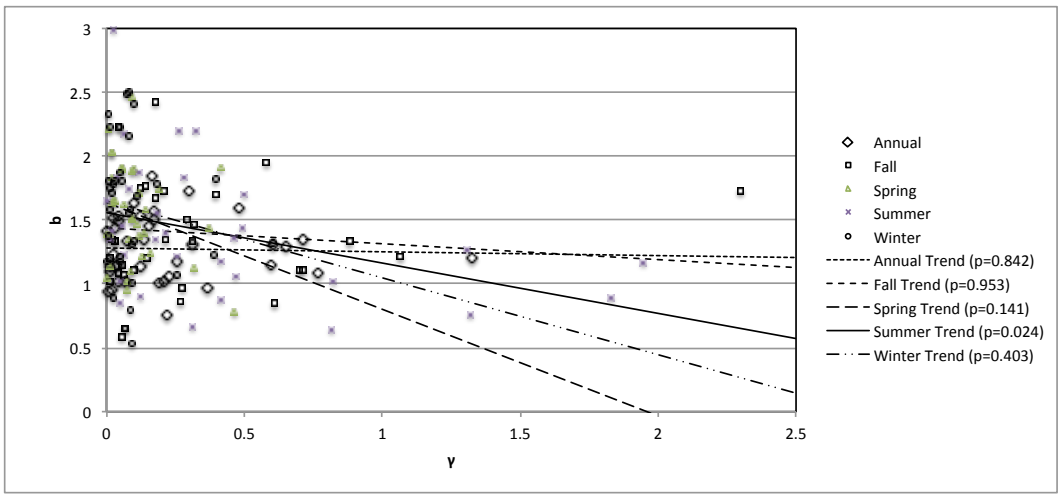

Figure 2-7: Scatterplots illustrating the variability in estimates of baseflow recession parameters from (3b) as a function of season and groundwater impacts. Trends illustrate the decrease in b as γ increases based on estimation from (3b). The p-value in parenthesis illustrates the significance of the trend.

From the above results, we hypothesize that inclusion of withdrawal terms into the analysis of baseflow recessions is needed to improve our understanding of the baseflow response of a river. To accomplish this, we incorporate the method proposed by *Wang and Cai* (2010) that includes withdrawal terms in (2). Continuity can then be expressed as

$$\frac{dS}{dt} = I(t) - Q(t) - W(t) \qquad (8)$$

where W(t) [mm d^{-1}] represents the average daily groundwater withdrawal. Combining (1) and (8) leads to

$$-\frac{dQ}{dt} = aQ^{b-1}\left(Q + W\right) \qquad (9)$$

Equation 9 is identical to equations by *Wang and Cai* (2010) and *Wang* (2011) and is derived by *Wang and Cai* (2010). The analysis summarized in Figure 2-7 was repeated using both the Brutsaert approach (3b) and the Wang-Cai Approach

(9). An example of the effect of (9) in estimating regression parameters is illustrated in Figure 2-8 where (9) is estimated by taking the logarithms and rearranging so that the left hand side of the equation becomes ln(-dQ/dt) – ln(Q+W). Figure 2-8(a) represents a site where withdrawal impacts are small (γ=0.0026) and, as a result, (9) can be approximated by (3b). Figure 2-8(b) illustrates results from a basin located near Princeton, NJ, that experiences large variability in groundwater withdrawals (γ=1.32) and natural variation in surface flows; Figure 2-8(b) illustrates the dramatic change in estimates of baseflow recession parameters using (9) compared to (3b) for a case with significant groundwater withdrawals. Summary results obtained while incorporating groundwater withdrawals are illustrated in Figure 2-9. Unlike earlier in Figure 2-7, estimates of $\hat{b}$ derived from (9) tend to increase as withdrawals increase, especially in fall and annual datasets. Such behavior indicates increasing nonlinear behavior ($\hat{b}$ increasing) with increasing degree of withdrawal. Regression results based on scatterplots of $\hat{b}$ versus γ resulted in significant positive trends in $\hat{b}$ with increasing withdrawal effects for annual and fall datasets (p=0.003 and p=0.031, respectively). These results support findings of *Ahlfeld* (2004) and *Liu et al* (2007). We conclude that it is necessary to include groundwater withdrawals into the analysis of baseflow recessions if one's goal is to understand the behavior of such recessions.

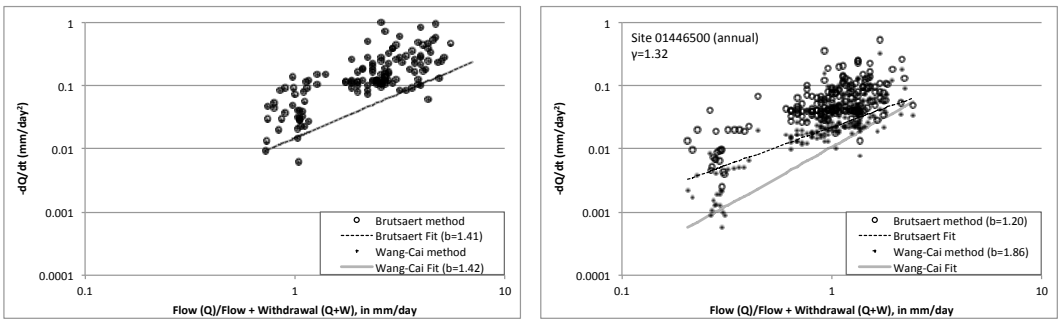

Figure 2-8: Recession plots illustrating impact of groundwater withdrawals. Figure 2-8(a) illustrates a site with low groundwater affects resulting in nearly identical results between the Brutsaert method (3b) and Wang-Cai method (9). Figure 2-8(b) documents the impact of groundwater withdrawals, especially at low flows, which alter the slope of the quantile lower envelope fit.

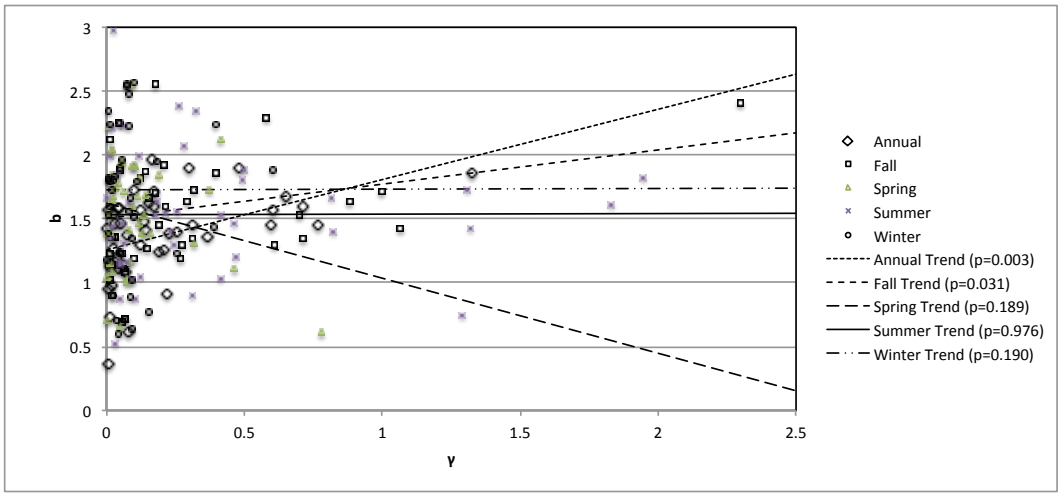

Figure 2-9: Scatterplots illustrating the variability in estimates of baseflow recession parameters from (9) as a function of season and groundwater impacts. Trends illustrate the increase in b as γ increases based on estimation from (9) which is the trend predicted in previous studies. The p-value in parenthesis illustrates the significance of the trend.

4.0 Discussion

We have shown that numerous factors involved in estimation of baseflow recession parameters using the recession plot may impact our ability to discern whether or not watersheds act as linear reservoirs. Here, we return to our hypothesis that groundwater outflow responds as a linear reservoir (n=b=1) and is

thus characterized by a fixed time constant, K_b. We conjecture that the physical relationship between streams and aquifers, at the watershed scale, provides insight to the storage behavior of a watershed. For this analysis, our null hypothesis of linear reservoir behavior (H_o: b=1) will be tested against the alternative hypothesis of nonlinear reservoir behavior (H_a: b≠1). Although we cannot know the true relationship of groundwater discharge to a stream, this analysis presents how such relationships can be misinterpreted due to approaches commonly employed to estimate recession parameters. For each experiment, we calculated the test statistic with the null hypothesis of b = 1 (linear reservoir hypothesis) as

$$T_{n-2} = \frac{\hat{b} - 1}{s_e} \qquad (10)$$

where s_e is the standard error of $\hat{b}$ estimated by bootstrapping methods. *Hao and Naiman* (2007) report that using this approach, asymptotically, our test statistic in (10) has a standard normal distribution. Unfortunately, asymptotic results are not relevant here thus T_{n-2} follows a Student's t distribution with 2 degrees of freedom. Hypothesis test for sites with significant estimations of baseflow recession constants results are summarized in Figure 2-10 which classifies the test results into categories, depending upon which factors were considered in performing the test. Results similar to those presented in Figure 2-10 are included in Appendix 2.A for null hypotheses of b=1.5 and b=3.0. Recall that we have shown the method of numerical differentiation, season, and impact of groundwater withdrawals can all have an impact on the analysis of groundwater

recessions. Figure 2-10 considers all of these factors and is discussed in the following sections.

4.1 Numerical Derivative

Hypothesis test results using annual datasets and numerical derivative estimates from Table 2-2 show that between 13-43% of sites failed to reject our null hypothesis, depending upon which numerical derivative is employed. The derivative procedure used by *Brutsaert and Nieber* (1977) resulted in 14 out of 38 sites failing to reject the null hypothesis while the 2-point centered difference formula (C2) employed in recent baseflow studies resulted in 12 out of 43 sites failing to reject the null hypothesis. Recall that our literature review recommended the nearly optimal estimation of the time derivative for noisy data such as streamflow, using a GCV spline fitting procedure to estimate the streamflow time derivative in (3b). Hypothesis testing using a GCV spline resulted in 15 out of 40 sites failing to reject the null hypothesis.

4.2 Seasonality

Previous baseflow studies have either selected seasons in which low flow typically occurs (summer and/or fall) or seasons with decreased ET (winter). Here we consider the GCV numerical derivative as above, but now consider the impact of season on the analyses. Results of hypothesis testing resulted in a failure to reject the null hypothesis at 61% (22/36) of the fall recessions compared to the spring where we could only fail to reject 30% (11/36) of the time. Summer periods found 40% (15/36) sites appearing linear. No sites were found where all seasons (and annual case) experiment failed to reject the null hypothesis. These

results suggest a high seasonal dependence in explaining groundwater reservoir behaviors based on recession plot analysis.

4.3 Degree of withdrawal

We conjecture that the degree of withdrawal, γ, affects the nonlinear response within a groundwater and surface water system due to complex nonlinear relationships documented in previous studies for aquifers that undergo withdrawals (*Alhfeld*, 2004). Recall that ignoring the effects of groundwater withdrawal terms (Figure 2-7) resulted in an apparent decrease in $\hat{b}$ with increasing withdrawals; however, accounting for withdrawals (Figure 2-9) supports previous studies that showed increasing nonlinear systems attributed to human impacts (*Liu et al*., 2007). In all seasons, introducing groundwater withdrawal terms into the analysis (9) resulted in increased estimates of $\hat{b}$. Figure 2-10 illustrates the decreased number of tests that failed to reject our null hypothesis after introducing withdrawal terms into the analysis as compared to seasonal results which did not include withdrawal terms. Similar to seasonal results, no site was found to exhibit linear behavior through all seasons and annual experiments performed for this study.

4.4 Physical Interpretation of a

The baseflow recession parameters a and b describe the behavior between streamflow and groundwater storage assuming the power law model in (1). Vogel and Kroll (1996) illustrate the correlation of the baseflow recession constant, K_b, to basin hydrogeologic properties for b=n=1. Further, Vogel and Kroll (1996) and Kroll et al. (2004) illustrate high correlation and increased prediction between

Kb and low flow statistics. For example, Vogel and Kroll (1996) illustrate improved regression estimates of $Q_{7,10}$ using estimators for K_b which assumed additive model errors in log-space. Thus, given different baseflow recession estimation schemes used for this study, one can assume a linear condition (n=1) and estimate a parameter to correlate to low flow statistics. Given that $K_b=\exp(-\alpha)$, one would expect a similar relationship to be apparent given that $a=(\alpha n)^{1/n}$.

For this initial study, we use the 7-day 10-year low flow ($Q_{7,10}$) reported by the USGS (USGS, 2005) to illustrate the physical interpretation of a as estimated by (3b) and (9). For the experiment, we relate a^* which is defined here as $a^*=\exp(-a)$ to $Q_{7,10}$for the watersheds used in this study. Results are summarized in Table 2-3.

Table 2-3: Correlation of a^* to low flow statistics ($Q_{7,10}$) for watersheds based on estimation schemes.

		a^* t-ratio	Adj-R^2	F-statistic
Time Derivative Estimation Scheme	B1	3.27	18.1	10.71
	B2	4.65	31.9	21.59
	C2	2.87	14.1	8.22
	C4	3.74	22.7	13.96
	F1	3.20	17.3	10.23
	F2	3.22	17.5	10.34
	Spline	6.78	50.6	45.98
Seasonality	**Annual**	**6.78**	**50.6**	**45.98**
	Spring	5.43	39.3	29.51
	Summer	4.67	32.1	21.81
	Fall	3.09	16.6	9.55
	Winter	2.55	11.1	6.51
Seasonality with Withdrawals	**Annual**	**8.48**	**62.8**	**71.93**
	Spring	6.03	45.7	36.34
	Summer	6.28	47.8	39.45
	Fall	5.13	37.6	26.31
	Winter	4.90	39.9	24.01

The results in Table 2-3 illustrate an increased ability of the baseflow recession parameter a to explain the observed variability in low flow statistics, specifically $Q_{7,10}$, across the sites using GCV cubic spline estimation for the time derivative of streamflow in (3b). Secondly, it is apparent that using all available data (the annual dataset) results in estimates of baseflow recession parameters that are most correlated to low flow statistics versus estimators obtained from seasonal recession hydrographs. One would expect that recession hydrographs from summer and fall would correlate to low flow statistics given that flow flows tend to occur between August and October for the study watersheds (USGS, 2005); however, it appears given results in Table 2-3 that using all available hydrographs may provide better estimates of average watershed behaviors. Finally, estimates which include groundwater withdrawals result in higher correlation to $Q_{7,10}$ as compared to all estimates which ignore withdrawals. Such results further illustrate the importance in estimation of baseflow recession parameters which include withdrawal information in the estimation methods.

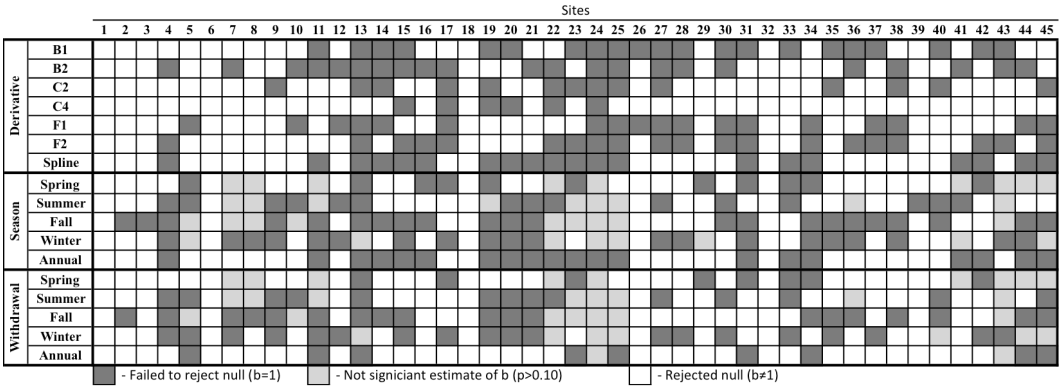

Figure 2-10: Summary figure of hypothesis tests performed. Derivative results are based on GCV spline fitting to estimate dQ/dt; seasonality includes GCV spline fitting and seasonally dependent recession periods; withdrawal impacts

include GCV spline fitting and seasonality. All results estimated parameters using a 0.05 quantile regression procedure.

5.0 Conclusions

Our primary goal was to assess the null hypothesis of linear watershed storage behaviors given multiple factors found to impact the baseflow response of a river. Experiments were performed to document impacts of these factors and the following conclusions were reached:

1. Quantile regression provides a rigorous and reproducible method to fit an envelope in baseflow recession plots.
2. We show that finite-difference estimators of the streamflow time derivative can yield different results depending on the form of the estimator (Table 2-2). Since optimal spline algorithms are now widely available and are nearly optimal for estimation of derivatives of noisy time series, we recommend them over finite difference schemes which are shown here to yield arbitrary results.
3. Future studies must clearly state objectives and reasoning for selecting seasonal data for analysis. Our results have documented statistically significant differences between baseflow recession parameters that depend on season.
4. We show that incorporating groundwater withdrawal terms into the analysis of baseflow recessions as shown in (9) reproduces the expected response of increasing nonlinear behavior (b increasing) as groundwater withdrawals increase. Given these results, we recommend procedures as described by *Wang and Cai* (2010) that incorporates groundwater

withdrawals and other anthropogenic impacts in estimation of baseflow recession parameters.

Finally, as evidenced in Figure 2-10, we found few sites to exhibit linear behaviors with no sites exhibiting consistent linearity through all seasonal experiments performed. Our results illustrate however, the inability of previous studies to compare baseflow recession parameters between sites obtained from different estimation schemes as evidenced by the high variability in apparent behavior illustrated in Figure 2-10; one would expect that consistent hypothesis results for a single site if estimation schemes were, in fact, comparable.

6.0 Acknowledgments

The authors would like to acknowledge partial support through the Summer Institute organized by Charles Vörösmarty at The City College of New York as part of the NSF-funded Hydrologic Synthesis project "Humans Transforming the Hydrologic Cycle (NSF Grant 0854957, C. Vörösmarty, PI). Additional project support was provided by a fellowship awarded to the first author by the Tufts Institute for the Environment (TIE).

Chapter 3

Estimation of the baseflow recession constant under human interference

Abstract

Baseflow recession parameters are used to characterize the interaction of groundwater and surface water systems. As such, estimation of the baseflow recession time constant is critical in many hydrologic problems including rainfall-runoff modeling, estimation of low flow statistics ($Q_{7,10}$) at ungaged locations and baseflow separation methods. We show that human withdrawals can have a important impact on baseflow recessions, even when withdrawals are relatively small. We compare the performance of various baseflow recession constant estimators including several traditional estimators as well as new approaches which account for the impact of human withdrawals. A traditional semi-log estimation approach adapted to incorporate the influence of human withdrawals was preferred over other estimators. Regional hydrologic regression models and analysis of variance methods were developed to identify factors which give rise to variability in the estimators of the baseflow recession constant including physical, climatic, and anthropogenic influences. Among the factors considered, both drainage density and human withdrawals were found to have very significant and similar explanatory power for the baseflow recession constant. This study documents the importance of incorporating human withdrawals into models of the baseflow recession response of a watershed.

1.0 Introduction

Numerous studies suggest that human impacts to ecosystem degradation, climate change, increased population and urbanization must be considered as part of the hydrologic cycle (Vorosmarty et al., 2004; Vorosmarty et al., 2010; Wagener et al., 2010). Hydrologic investigations that ignore the influence of humans have been shown to perform satisfactorily in relatively undisturbed watersheds (Mendoza et al., 2003); however, recent research indicates that even small disturbances in hydrologic systems, such as human withdrawals (Thomas, 2012) and land-use/land cover changes (Schilling and Libra, 2003), can be significant especially in studies which focus on the low flow response of a watershed (Wang and Cai, 2010; Schilling and Zhang, 2006; Brandes et al., 2005a, among many). During the 20th century, groundwater withdrawals intensified to meet increasing water demands in the United States, particularly in suburban areas experiencing population growth since the late 1940s as documented by the U.S. Geological Survey (USGS) National Water Use program (Barber, 2009). Theis (1940) states that any newly introduced groundwater withdrawal must be balanced by one or more of the following: 1) an increase in the recharge to an aquifer, 2) a decrease in the discharge from a groundwater system to either a surface water system or a deeper groundwater system or 3) a loss of storage to the aquifer. With the increase in water demand has come the need to characterize low flow behaviors for conjunctive water use management, maintenance of water quality and ability to maintain ecosystem services given the water balance component shifts predicted by Theis (1940).

Hall (1968) and Tallaksen (1995) review the historical and mathematical applications applied to characterize the low flow behavior of a river, referred to here as baseflow recession analysis. The theory of baseflow recession analysis emerged from early studies of groundwater flow (Dupuit, 1863; Boussinesq, 1877; Maillet, 1905) and has since led to multiple approaches to characterize the relation between groundwater and surface water during low flow periods. In general, the hydrologic characterization of the coupling between groundwater and surface water (gw-sw) systems can be grouped into two categories, (Dooge, 1983): (1) linear behavior in which the baseflow Q is a linear function of groundwater storage S and (2) nonlinear behavior in which baseflow Q is a function of groundwater storage S raised to a power other than 1.

Considerable controversy exists in the hydrologic literature over the issue of whether or not watersheds exhibit a fixed time constant associated with the linear assumption; this constant is often termed the baseflow recession constant. Despite the controversy over whether or not the system response is linear or nonlinear in the hydrologic literature (Wittenberg and Sivapalan, 1999, for example), the estimation of baseflow recession constants continues to be required for many common hydrologic models, too numerous to list exhaustively (HEC-HMS, HSPF, for example). Moreover, model dynamics of rainfall-runoff models (Ferket et al., 2010; Beven et al., 1995) are dependent on estimation and/or parameter fitting of baseflow recessions. Vogel and Kroll (1992), Kroll et al. (2004) and Eng and Milly (2007) advocate inclusion of the baseflow recession constant in estimation of low flow statistics at ungaged sites. Eckhardt (2008)

illustrates that partitioning of streamflow into baseflow and direct flow components generally relies on the assumption of linear storage behavior and further illustrates through sensitivity derivations how baseflow separation critically depends on estimation of the baseflow recession constant (Eckhardt, 2011). Estimation of the baseflow recession constant becomes important in calibration of hydrologic models which routinely employ baseflow separation to obtain runoff and groundwater discharges for model calibration and validation (for example, Lo et al., 2010). Given the ubiquitous use of the baseflow recession constant in so many hydrologic applications, it is important to accurately characterize groundwater/surface water (gw-sw) behavior and to characterize the sensitivity of gw-sw parameters as a result of physical and anthropogenic influences known to alter hydrologic systems.

Previous investigations have explored the behavior of the baseflow response as a function of watershed characteristics and climatic factors. Brandes et al. (2005b) found regression models incorporating drainage density and geologic indices could explain 70-80% of observed variability in the recession constant from 24 watersheds in Pennsylvania; such results support conclusions by Zecharias and Brutsaert (1998a) who found that drainage density along with basin slope and perennial stream length explained most of the variation in groundwater outflow behavior. Zecharais and Brutseart (1998b) noted that large-scale characteristics such as basin slope and drainage density explained greater variability in the baseflow recession constant as compared to small scale processes such as aquifer area percentages (α) and spatially heterogeneous

properties [for example, hydraulic conductivity (k) and aquifer porosity (f)]. Farvolden (1963) identified similar geologic and geomorphologic dependence to the baseflow recession constant which was found to vary with stream channel depth and drainage density while being inversely proportional to relief ratios. Farvolden (1963) also identified a weak correlation with a climate index, the aridity ratio, for arid environments. Likewise, van Dijk (2010) documented humidity index as being an important factor in the baseflow recession constant for dry catchments.

The Base Flow Index (BFI), defined as the steady-state ratio of baseflow to total streamflow, was developed in 1980 (Institute of Hydrology, 1980) and is now widely used (Smakhtin, 2001). BFI is related to low flow indices and, as such, is an important surrogate to characterize gw-sw behaviors during low flow and recession periods. Lacey and Grayson (1998) related dimensionless parameters to BFI including geology-vegetation parameters. Carlston (1965) suggested that baseflow discharge was a function of drainability and recharge while Biswal and Marani (2010) characterized baseflow discharge as being dominated by geomorphic properties of a watershed. Studies have investigated land-use/land cover (LULC) effects on BFI (Nie et al., 2011; Schilling, 2005) with results illustrating changes in groundwater recharge are a direct result of LULC changes. Regional regression studies of BFI have been performed for sites in Italy (Longobardi and Villani, 2008), UK (Bloomfield et al., 2009) and Tanzania (Mwakalia et al., 2002) to characterize dependent variables which explain variability in BFI.

Unlike previous approaches which have evaluated our ability to estimate and understand the baseflow recession relationship in either pristine watersheds or by ignoring human withdrawals, our study evaluates traditional approaches to estimate the baseflow recession constant and introduces new procedures that incorporate the impact of anthropogenic influences, namely groundwater withdrawals, on the recession constant. Such an approach is important to decipher the impact of human withdrawals in characterizing gw-sw behaviors via the baseflow recession constant and the linear reservoir assumption. We first consider traditional estimation methods (Barnes, 1939; Vogel and Kroll, 1992) which are given in most introductory hydrology textbooks (Dingman, 2002; Fetter, 1994; Domenico and Schwartz, 1998) and recession envelope plots introduced by Brutsaert and Nieber (1977). We then consider a recession envelope approach derived by Wang and Cai (2009) which includes groundwater withdrawals. A derivation is presented for a new estimator based on the traditional approach which also includes groundwater withdrawals. Analogous to Vogel and Kroll (1992), we then illustrate the physical and statistical significance of the various estimators. Finally, we employ multivariate regression procedures and the concept of elasticity to evaluate the relative impact and importance of geologic, geomorphic, climatic and anthropogenic effects on the baseflow recession constant. The goal of this study is to demonstrate the improved estimation of the baseflow recession constant by considering human withdrawals. In addition we want to quantify the influence of human withdrawals and other factors on observed variations in the baseflow recession constant.

2.0 Model Development

A streamflow hydrograph can be separated into two components: a rising limb reflecting increases in discharge resulting from precipitation events, and a falling limb during which discharge decreases. It is recognized that, at some time during the falling limb, observed streamflow is comprised entirely of discharge derived from watershed storage at which point the flow is termed baseflow and the hydrograph is termed the baseflow recession curve. A baseflow recession curve exhibits behavior attributed to the relationship between aquifer structure and the associated groundwater outflow to the stream channel.

To characterize the behavior of gw-sw systems, we follow the work of Barnes (1939), Hall (1968) and Brutsaert and Nieber (1977), all of whom have conceptualized a simplified fully penetrating stream with Dupuit assumptions which assumes that the initial rapid watershed input that contributed to the increase in streamflow, the rising limb of the hydrograph, have been fully depleted. This assumption implies that all observable streamflow is derived exclusively from long-term watershed storage, generally groundwater storage which Hall (1968) and others term baseflow. Hall (1968), Dooge (1983) and many others have suggested the use of a power law model to relate groundwater storage to an unconfined aquifer in direct hydraulic connection to a stream, S [mm d^{-1}], and the observed groundwater discharge to the stream, Q [mm d^{-1}], as

$$Q = \alpha S^n \quad (1)$$

where α and n are constants. Equation (1) can be also interpreted as an idealized solution to the Dupuit-Boussinesq equation under the assumption of horizontal groundwater flow to a fully penetrating river channel (Bear, 1972). For a linear

storage-discharge relationship, n in (1) is equal to 1 (n=1). Hall (1968), Vogel and Kroll (1992) and others relate α in (1) to the baseflow recession constant.

For an aquifer with no external transfers and ignoring capillary effects, continuity can be written as

$$\frac{dS}{dt} = I(t) - Q(t) - W(t) - ET(t) \quad (2)$$

where I(t) represents infiltration from the vadose zone to the water table, W(t) represents daily average groundwater withdrawals, and ET(t) represents evapotranspiration from the groundwater table and stream. To simplify (2), we make assumptions commonly employed in previous studies. First, we assume that the analysis is conducted during stream recession periods (i.e. no precipitation events) with rapid initial percolation which ceases after precipitation; thus, I(t)=0. Second, we assume that ET(t) has a negligible impact on (1) and (2) during baseflow events. Previous investigations (Szilagyi et al., 2007; Wang and Cai, 2009) document potential seasonal effects on the baseflow response due to changes in ET. To address this issue, we evaluate seasonal streamflow recessions to control for variations which we attribute to seasonal hydrologic characteristics including ET.

Combining (1) and (2), while ignoring groundwater withdrawals, leads to

$$\frac{dQ}{dt} = -n\alpha^{1/n}Q^{(2n-1)/n} \quad (3a)$$

$$\frac{dQ}{dt} = -aQ^{b} \quad (3b)$$

where b=(2n-1)/n and $a=n\alpha^{(1/n)}$. Under the linear reservoir hypothesis, n=b=1. Equation (3b) was presented by Brutsaert and Nieber (1977) to enable a graphical illustration that on a log-log plot of dQ/dt versus Q, the parameter "a" is the

intercept while "b" is the slope of the fitted line to the streamflow recession data. We term this the recession envelope method because Brutsaert and Nieber recommended fitting a curve to the lower envelope of the cluster of data to remove "unavoidable errors" (Brutsaert, 2008) generally attributed to streamflow measurement errors during low flow. More recently, Wang and Cai (2010) developed a model similar to (3b) which included the effects of the groundwater withdrawal term in (2) written as

$$\frac{dQ}{dt} = -aQ^{b-1}(Q + W) \qquad (4)$$

Combining equations (1), (3b) and (4), various estimators of the baseflow recession constant can be derived which include the effect of groundwater withdrawals. We illustrate the derivation of estimators of the recession constant including mathematical and physical assumptions. For all cases presented below, estimation of the baseflow recession constant was completed using linear regression methods. Linear regression assumptions for all cases must be met to enable statistical inference on resulting model parameter estimates. Those necessary assumptions include normally distributed model errors and homoscedastic residuals that are serially uncorrelated.

2.1 Case 1: No Withdrawals, W(t)=0, Traditional Approach

Case 1 represents the traditional hydrograph estimation method proposed by Barnes (1939) and included in most introductory hydrology textbooks. By ignoring withdrawals while adhering to previous simplification assumptions, (2) can be written as

$$\frac{dS}{dt} = -Q(t) \qquad (5)$$

Combining (1) and (5) while assuming that Δt=1 day yields

$$Q_{t+1} = e^{-\alpha} Q_t \text{ or } Q_{t+1} = K_b Q_t \quad (6)$$

where K_b=exp(-α). Barnes (1939) defined the term K_b as the dimensionless baseflow recession constant. Vogel and Kroll (1992) and others have shown that an equivalent version of (6) is

$$Q_t = Q_o K_b^t \quad (7)$$

where Q_o is the initial baseflow on day t=0, and Q_t is the streamflow at time t. Estimation of K_b can be viewed as a problem in regression by rewriting (7) as

$$Q_t = Q_o K_{b1}^t e^{\varepsilon_t} \quad (8)$$

where ε_t are independent model errors with zero mean and constant variance σ_ε^2 and K_{b1} is the estimate of the dimensionless baseflow recession constant for Case 1. Equation (8) can be rewritten in a linear form as

$$\ln(Q_t) = \ln(Q_o) + t\ln(K_{b1}) + \varepsilon_t \quad (9)$$

which can be solved graphically or mathematically by linear regression approaches where $\ln(Q_t)$ is the dependent variable and t is the independent variable with a fixed intercept of $\ln(Q_o)$ and a slope of $\ln(K_{b1})$. This model was investigated by *Vogel and Kroll* (1996) who showed that having log-space error terms (as opposed to real-space error) produced better behaving regression models and K_b estimates that better predicted low streamflow statistics.

2.2 Case 2: W(t)≠0, Traditional Approach

Here we introduce a new estimator of the dimensionless baseflow recession constant which includes the impact of human withdrawals. If we

include groundwater withdrawals which deplete aquifer storage, the continuity equation becomes

$$\frac{dS}{dt} = -Q(t) - W(t) \quad (10)$$

Combining (1) and (10) with k=1/α and subscripts representing time dependence, then

$$\frac{d[kQ_t]}{dt} = -Q_t - W \quad (11)$$

Here, we assume groundwater withdrawals are constant during each individual recession hydrograph and are therefore not a function of time during an individual hydrograph recession. This assumption is necessary given available withdrawal information at a monthly time scale. Thus we can multiply (11) by the integration factor exp(t/k) to obtain

$$ke^{t/k}\frac{dQ_t}{dt} + e^{t/k}Q_t = -e^{t/k}W \quad (12)$$

We then use the chain rule and integrate to obtain

$$Q_t = \frac{-Wk\left[e^{t/k}-1\right]+kQ_o}{ke^{t/k}} = -W\left(1-K_{b2}^t\right) + Q_oK_{b2}^t \quad (13)$$

where the integration constant is kQ_o and K_{b2}=exp(-1/k) or exp(-α); similar to Case 1, K_{b2} is a dimensionless baseflow recession constant. If we ignore withdrawals, (13) reverts to (9). Equation (13) can be solved by an algebraic expansion of the equation and taking logs to obtain

$$\ln(Q_t) = \ln(-W) + \ln(Q_o + W) + t \cdot \ln(K_{b2}) + \varepsilon_t \quad (14)$$

In (14), the intercept term is defined as ln(-W)+ln(Q_o+W) when solved graphically with ln(Q_t) as the dependent variable versus the independent variable of time t while the slope of the line equals ln(K_{b2}).

2.3 Case 3: Recession Envelope Methods, W(t)=0

Given (3b) from Brutsaert and Nieber (1977), Vogel and Kroll (1996) illustrate that the intercept parameter a is equal to $\ln(K_b)$ where K_b is the dimensionless baseflow recession constant. Therefore, taking the limit of (3b) as b approaches 1, we obtain the differential equation with independent model errors with zero mean and constant variance written as

$$\frac{dQ_t}{dt} = -\ln(K_{b3})\, Q_t e^{\varepsilon_t} \qquad (15)$$

which can be solved by taking logs to obtain

$$\ln\left(\frac{\mathrm{dQ_t}}{\mathrm{dt}}\right) = \ln(-\ln(\mathrm{K_{b3}})) + \ln(\mathrm{Q_t}) + \varepsilon_t \qquad (16)$$

Ordinary least squares regression procedures are used to solve for K_{b3} where ln(dQ/dt) is the dependent variable versus ln(Q) as the independent variable. Thomas (2012) addresses estimation of the time derivative of streamflow, dQ/dt, given that the streamflow time series exhibits noise due to flow estimation errors. In that study, generalized cross-validation (GCV) methods were found to estimate nearly optimal derivatives given noisy time series functions using smoothing splines based on results by Craven and Wahba (1979). To estimate dQ/dt for (16), optimal cubic splines were fit to each individual recession hydrograph using the "pspline" package (Ripley, 2012) within the R-project (R Development Core Team, 2012). Once GCV splines were fit to individual recessions using automatic optimal curve fitting procedures, derivatives were estimated at observed values of Q using the "sfsmisc" package (Maechler et al., 2012) within the R-project to calculate the streamflow time derivatives. The GCV spline derivatives were used for all estimates of the time derivative of streamflow for this study.

2.4 Case 4: Recession Envelope (W(t)≠0)

Given (4) as derived by Wang and Cai (2010) and applying the limit as b approaches 1, we find that

$$\frac{dQ_t}{dt} = -\ln(K_b)(Q_t + W)e^{\varepsilon_t} \quad (17)$$

which can be solved by taking logs to obtain

$$\ln\left(\frac{dQ_t}{dt}\right) = \ln\left(-\ln(K_{b4})\right) + \ln(Q_t + W) + \varepsilon_t \quad (18)$$

Wang and Cai (2009, 2010) did not estimate recession parameters assuming linear behavior as shown in (18); thus, the estimation of K_{b4} presents a new estimator procedure for the dimensionless baseflow recession constant. Equation (18) can be solved by ordinary least squares (OLS) the independent variable ln(dQ/dt) versus the dependent variable ln(Q+W). As described above, the time derivative of streamflow (dQ/dt) was estimated using GCV spline derivatives. Estimation of the baseflow recession constant from (18) deviates from the method proposed by Brutsaert and Nieber (1977) in that the dependent variable has changed from ln(Q) to ln(Q+W). Taylor series expansion or log-linearization methods can be used to approximate ln(Q+W) to allow for estimation the baseflow recession constant graphically as ln(dQ/dt) versus ln(Q). For this study, however, estimation of the baseflow recession constant K_{b4} was conducted using (18).

3.0 Data: K_b estimation

This study uses groundwater withdrawal, precipitation, and streamflow data for 15 sites within New Jersey, USA. Daily streamflow records at U.S. Geological Survey (USGS) stream gages were used to isolate suitable recession hydrographs for analysis (Figure 3-1) using hydrograph selection algorithms as

described by Vogel and Kroll (1996). USGS stream gage sites were selected based on continuous daily records for the calendar years 1990-2007. Selected contributing watersheds were delineated using the USGS Streamstats Package (Watson and Schoop, 2009). Available geographical information databases obtained from the New Jersey Department of Environmental Protection Bureau of Geographic Information Systems (GIS) were also used to isolate selected watersheds; for the purpose of this study, we selected watersheds with documented surficial aquifers which did not intersect multiple watershed boundaries and which exhibited possible hydraulic connection to streams based on visual intersection of aquifer and hydrography layers. Watersheds selected for this study are located in northern New Jersey within the Valley and Ridge, Highlands and Piedmont geologic provinces characterized as having valley fill aquifers (Kummel, 1940). A summary of physical watershed characteristics for the selected watersheds illustrated in Figure 3-1 is included in Table 3-1. Throughout this study, streamflow was normalized by contributing watershed area ($Q[mm\ d^{-1}]$).

Table 3-1: Summary of 15 U.S. Geological Survey gages in Northern New Jersey.

USGS Gage Number	Site Name	Area (km^2)	Length (km)	f	k (km^2/d)	alpha
01379000	Passaic River, Millington NJ	140.38	168.98	0.3	4041.3	0.35
01379773	Green Pond Brook, Picatinny Arsenal NJ	19.87	21.56	0.3	603.9*	0.06
01379780	Green Pond Brookk, Picatinny Arenal NJ	23.80	23.657	0.3	603.9*	0.05
01380500	Rockaway River, Boonton NJ	303.03	336.35	0.3	802.2	0.09
01381000	Rockaway River, Boonton NJ	313.39	341.18	0.3	802.2	0.09
01381900	Passaic River, Pine Brook NJ	906.50	1004.23	0.3	1028.8	0.20
01394500	Rahway River, Springfield NJ	67.08	47.80	0.1	46.5	0.12
01396500	South Branch Raritan River, High Bridge NJ	171.72	121.83	0.2	254.5	0.02
01399500	Lamington River, Pottersville NJ	83.40	76.44	0.3	524.7	0.16
01403400	Green Brook, Seeley Mills NJ	16.16	14.79	0.3	802.2*	0.02
01440000	Flat Brook, Flatbrookville NJ	168.352	191.51	0.3	603.9	0.07
01443500	Paulins Kill, Blairstown NJ	326.34	315.43	0.1	29.8	0.06
01443900	Yards Creek, Blairstown NJ	13.83	14.21	0.2	371.6	0.22
01445500	Pequest River, Pequest NJ	274.54	259.10	0.1	37.4	0.11
01457000	Musconetcong River, Bloomsbury NJ	360.0	313.82	0.2	380.6	0.01

*Watershed physical attributes were estimated based on geologic characterization of other watersheds using relational comparisons.

Precipitation data was obtained from the National Climatic Data Center (NCDC) and the Utah Climate Center database for sites with nearly continuous daily precipitation records for the period 1990-2007. Selected sites are illustrated in Figure 3-1. For the purpose of this study, precipitation totals reported as trace (T) are considered to be zero. Precipitation data was used to eliminate any recession hydrograph during which streamflow was observed to decrease despite a concurrent precipitation event totaling greater than 0.10 mm measured at the two nearest precipitation gage sites to the streamflow gage.

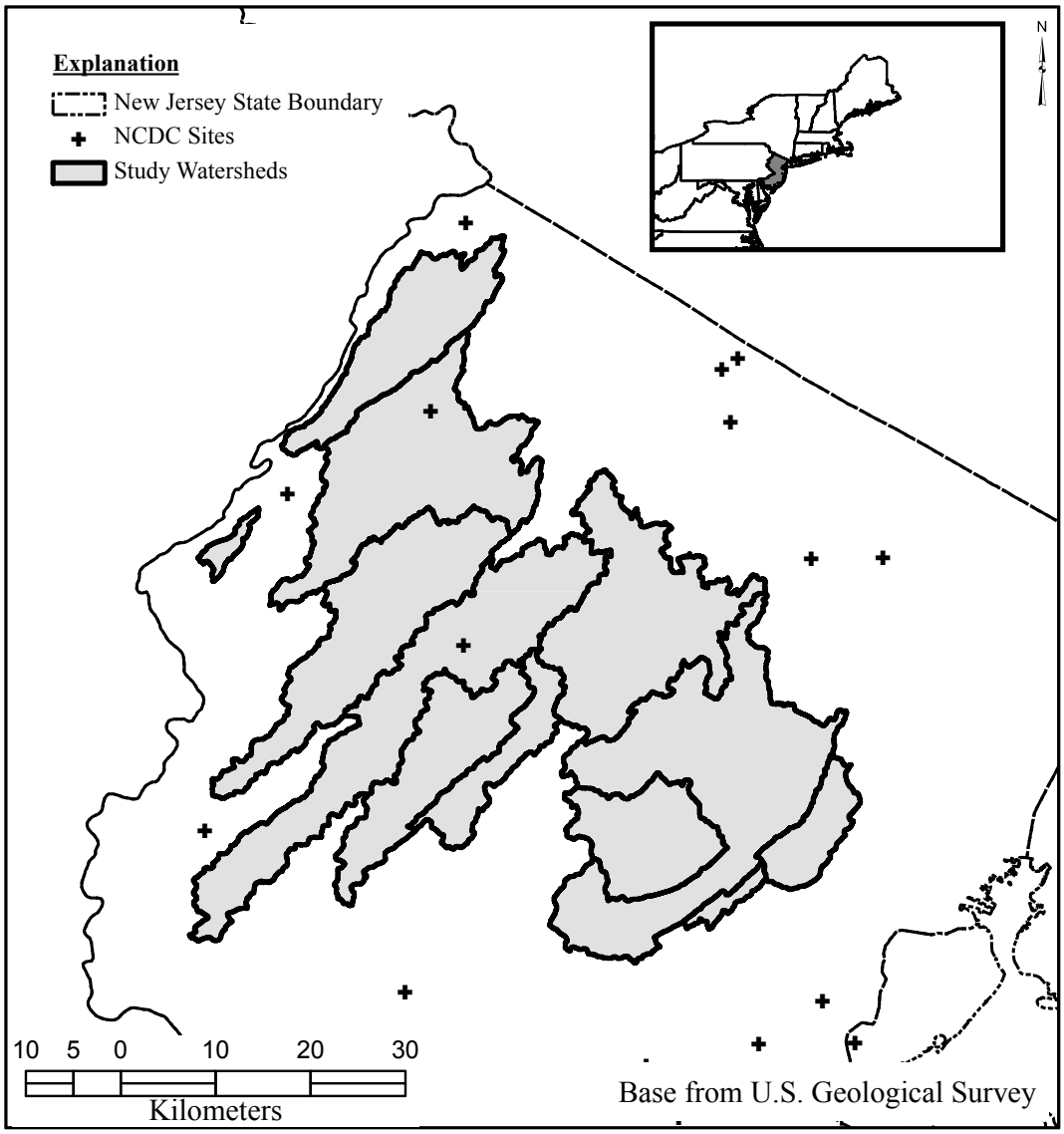

Figure 3-1: Locations of 15 watersheds, National Climatic data sites (NCDC) and Utah Climate Center sites in New Jersey.

Groundwater withdrawals over the period 1990-2007 were obtained from the New Jersey Geological Survey (NJGS, 2011). The withdrawal database contains actual and estimated monthly withdrawals reported by HUC14 regions across the state. Total watershed withdrawals were calculated by aggregating HUC14 withdrawals within delineated watersheds. Total watershed monthly

withdrawals were assumed to be uniformly distributed across the month to obtain daily rates and normalized by contributing watershed area (W[mm d^{-1}]).

4.0 Experimental Design

The four K_b estimators summarized in Table 3-2 are applied at each site i resulting in m_i estimates of the baseflow recession constant, $K_{b_{m_i}}$ where m_i is equal to the number of hydrograph recessions at site i. Ordinary least squares regression approaches to estimate the baseflow recession constant led to serially correlatated model residuals, a phenomenon commonly experienced in hydrologic investigations due to the time dependency of streamflow observations (Vogel and Kroll, 1992; Kirchner, 2009). Johnston and DiNardo (1997) suggest using generalized least squares (GLS) approaches which can account for the serial correlation structures of the residuals, which in the case of experiments performed was relatively well approximated by a lag-one autoregressive process (AR(1)). GLS was used to fit equations for the cases summarized in Table 3-2 within the R-project (R-Development Core Team, 2012) using the "nlme" package (Pineheiro et al., 2012) for each site i at m_i recessions. Vogel and Kroll (1992) document that estimates of K_b at site i tend to be unbiased; larger values of m_i are needed to obtain more precise estimates of the recession constant. Here m_i ranged between 14 and 88.

Table 3-2: Summary of equations used for cases derived**.**

Approach	**Equation**
Case 1: Traditional (W=0)	$\ln(Q_t) = \ln(Q_0) + t \cdot \ln(K_{b1}) + \varepsilon_t$
Case 2: Traditional (W≠0)	$\ln(Q_t) = \ln(-\mathrm{W}) + \ln(Q_0 + W) + t \cdot \ln(K_{b2}) + \varepsilon_t$
Case 3: Recession Envelope (W=0)	$\ln\left(-\frac{dQ_t}{dt}\right) = \ln\left(-ln(K_{b3})\right) + \ln(Q_t) + \varepsilon_t$
Case 4: Recession Envelope (W≠0)	$\ln\left(-\frac{dQ_t}{dt}\right) = \ln\left(-ln(K_{b4})\right) + \ln(Q_t + W) + \varepsilon_t$

Inherent assumptions in GLS approaches include, after removal of autocorrelated structure in the residuals, that model residuals are approximately normally distributed for model inference. This assumption was tested using a Ryan Joiner probability plot correlation coefficients (PPCC) test of normality. Residuals were tested for normality using the PPCC with a 10% significance level.

Seasonal variability in gw-sw behaviors has been noted in previous studies (Szilagyi et al., 2007, for example). Thomas (2012) documented seasonal variability in recession parameters due to the dominant role of season in the hydrologic cycle. To characterize seasonal effects on the estimation of the baseflow recession constant, recession data from each site was separated into 5 categories: winter (Dec-Feb), spring (March-May), summer (Jul-Aug), fall (Sept-Nov) and annual (all available hydrographs) data sets where season was assigned based on the last day of the hydrograph recession.

4.1 Results: K_b Estimation

Estimates of the baseflow recession constant obtained from GLS regression were removed from the analysis if model residuals failed tests for normality using the PPCC test. Out of 2132 estimates of the baseflow recession

constant obtained from available recession hydrographs, 62 of the estimates were obtained from regression models with residuals that were not well approximated by a normal distribution at a significance level of 10%; thus, these estimates were removed from further analysis. An additional 4 estimates of the baseflow recession constant were removed from the analysis as a result of heteroscedastic residuals as determined from the Breusch-Pagan test. A total of 2066 estimates of K_b were therefore analyzed across the 15 sites.

To characterize each site and season with only one estimate of K_b, a recession-length weighted average was employed where

$$K_{b_{i,s}} = \frac{\sum_{j=1}^{m}\left(K_{b_{i,s,j}}\right)w_j}{\sum_{j=1}^{m} w_j} \qquad (19)$$

where w_j is the total number of days of the recession hydrograph period used to estimate the baseflow recession constant, j is the number of recession hydrographs and $K_{b_{i,s,j}}$ is the estimate of K_b from the jth hydrograph recession. Results for the largest watershed (Site 0139700) are illustrated in Figure 3-2. The results are similar to those obtained by Vogel and Kroll (1996) for Case 1 and Case 2 in that a cone-shape can be interpreted with larger variability observed in estimates obtained from shorter recession periods while at longer recession hydrographs, the estimates approach the recession length weighted average calculated by (19). For Case 3 and Case 4, Figure 3-2 illustrates that estimates of K_b do not exhibit a cone shape and do not illustrate improved estimation of K_b given recession length. Thus, we conclude that estimates from Case 1 and Case 2 converge asymptotically to an unknown estimates at long recession records; Case

3 and Case 4 do not exhibit an asymptotic behavior with no improved estimation with longer recession records.

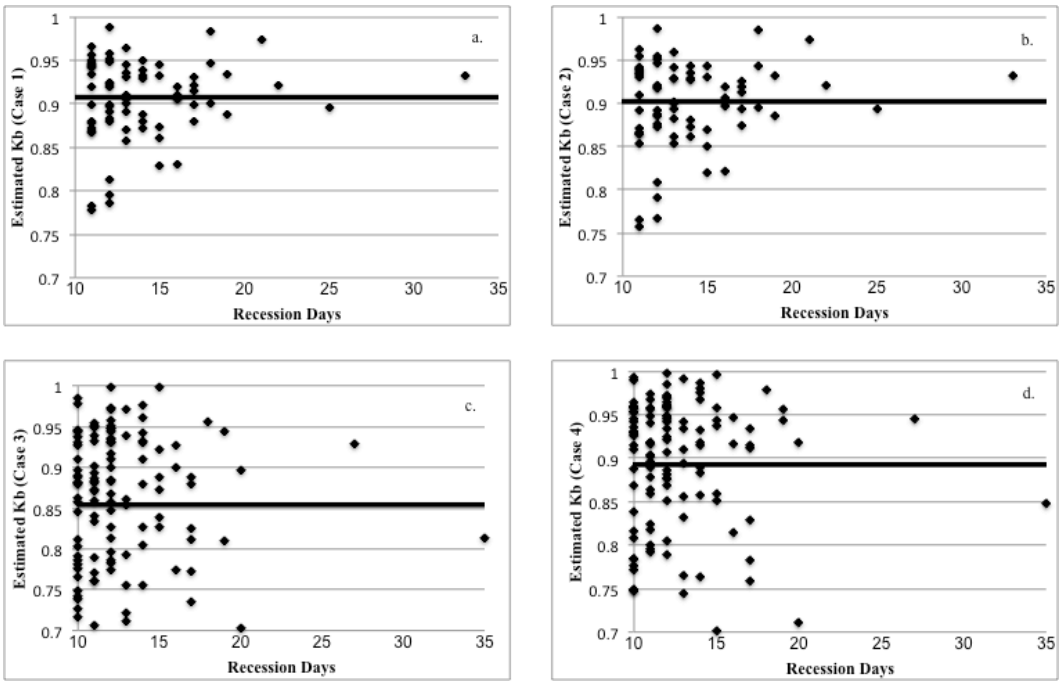

Figure 3-2: Estimates of K_b for individual hydrographs at Site 0139700 using (a) Case 1, (b) Case 2, (c) Case 3 and (d) Case 4 as compared to the horizontal line representing the recession weighted average shown in (19).

Figure 3-3 illustrates recession length weighted averages from (19) for the four cases summarized in Table 3-2. The results in Figure 3-3 indicate that the variability in seasonal estimates of K_b as calculated from (19) tend to be small for Case 1 and Case 2 as compared to results for Case 3 and Case 4. Additionally, annual estimates tend to be located near the median of the four seasonal estimates for Case 1 and Case 2; such a result is not apparent for estimates for Case 3 and Case 4. The seasonal variability of recession weighted averages for all sites is evident in Figure 3-3 in that no seasonal recession estimate tended to be higher or lower for all sites. In general, estimates from summer and spring recessions were

noted to be lower. Such results are not surprising given the unique heterogeneity found in valley aquifer systems found in northern New Jersey (Kummel, 1940). Lins and Slack (2005) report that, for the mid-Atlantic region, low flows tend to occur in September, median flows in January, and high flows in March. Previous studies documented that much of the variability in baseflow recessions between seasons depended on evapotranspiration (Szilygi, 1999; Wittenburg, 2003), which as described previously was ignored for this study. Additional variability in baseflow recession constant estimation may be due to varying hydrogeologic properties of the aquifers within a watershed across different flow regimes. Brutseart and Nieber (1977) and Vogel and Kroll (1992) develop a physical model for the baseflow recession constant which is related to the hydraulic conductivity of the aquifer. In general, groundwater elevations tend to be highest in the spring and lowest in the fall as evidenced in monthly groundwater elevation data obtained from USGS across New Jersey. As described by Van de Griend et al. (2002), physical constraints of aquifer systems such as the decrease in hydraulic conductivity with depth in stratified drift aquifers due to compaction can greatly affect the seasonal storage-discharge behaviors. The variability in climate and hydrologic factors can, therefore, greatly influence seasonal groundwater and surface water behaviors.

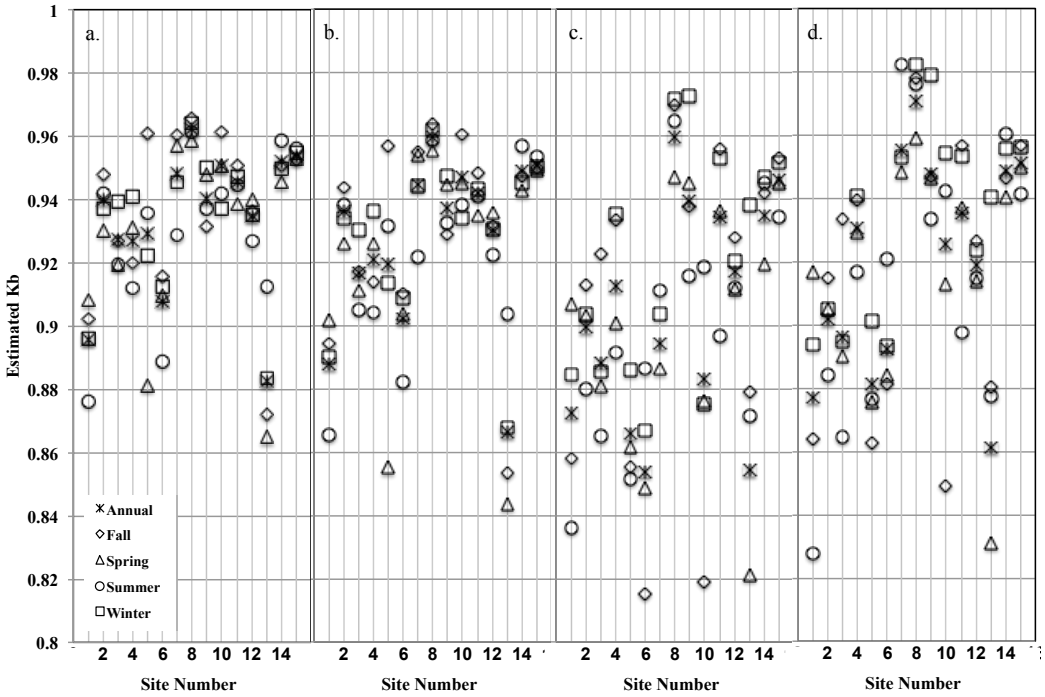

Figure 3-3: Comparison of variability in seasonal recession weighted averages of the baseflow recession constant for Case 1 (a), Case 2 (b), Case 3 (c) and Case 4 (d) summarized in Table 3-2.

Thomas (2012) introduced a dimensionless withdrawal variable to characterize the degree of withdrawal in characterization of gw-sw behaviors. The variable, γ, defines the groundwater withdrawal as a ratio of overall streamflow during the recession

$$\gamma_i = \frac{\sum_{j=1}^{m} \frac{W_j}{Qr_j}}{m_i} \quad (20)$$

where W_j is the daily average groundwater withdrawal for hydrograph recession j, Qr_j represents the average streamflow over the jth hydrograph recession and m_i is the total number of observed hydrograph recessions available at site i.

Figure 3-4(a) illustrates a comparison of estimates of K_b from individual hydrograph recessions obtained from Eqn. 9 (Case 1) and Eqn. 14 (Case 2) for

different ranges of γ. Figure 3-4(a) illustrates that some variability in estimates of K_b can be accounted for due to groundwater withdrawals; this is most clearly illustrated by estimates during which γ is high (points representing $0.5<\gamma<1$ and $\gamma>1$) which show a range in estimated values from 0.80 to 1 obtained for Case 1 with a more limited range from 0.88 to 1 for Case 2. It must be stressed, however, that K_b is an upper bounded parameter ($K_b \leq 1$) and thus an increase in estimates of K_b will naturally result in less variability. Figure 3-4(b) illustrates the comparison in estimates of K_b for Case 3 versus Case 4; the figure does not illustrate a clear pattern as shown in Figure 3-4(a). We conclude from the results in Figure 3-4 that Cases 1 and 2 reflect a systematic impact of human withdrawals on the groundwater response of a watershed, whereas, Cases 3 and 4 do not. Thus there appears to be a greater physical basis for Cases 1 and 2 than for Cases 3 and 4. However all four methods, Figure 3-4 illustrates that incorporation of groundwater withdrawals in baseflow recession constant estimation generally results in an increased value of K_b for all four cases as evidenced by points being to the left of a unity slope relationship.

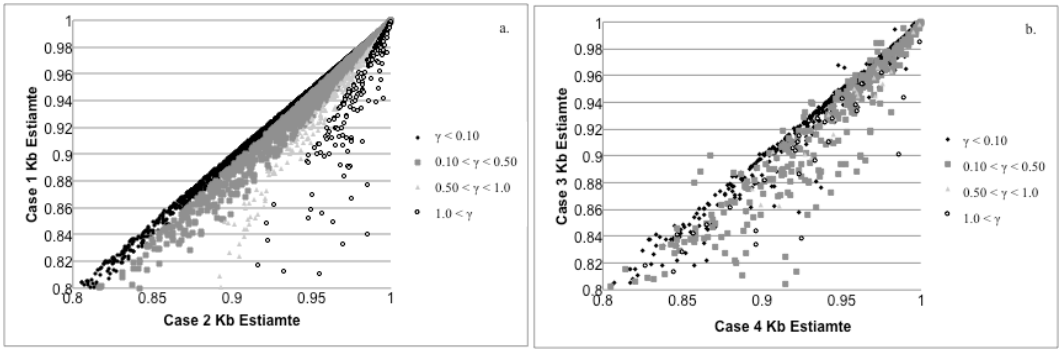

Figure 3-4: Comparison between estimates of K_b obtained from Case 1 and Case 2 (a) and Case 3 and Case 4 (b).

5.0 Multivariate Hypothesis Tests

The baseflow recession constant, K_b, relates observed decreases in streamflow to physical watershed characteristics when observed streamflow is entirely derived from groundwater recharge. Brutseart and Nieber (1977) and Vogel and Kroll (1992) provide a physically-based model to relate K_b to watershed parameters using hydrogeologic assumptions including Dupuit flow. Vogel and Kroll (1992) described a physical model for K_b as

$$K_b = \exp\left[-\frac{\pi^2 k H d_d^2}{\alpha f}\right] \quad (21)$$

where k is the average watershed hydraulic conductivity, H is the basin relief, d_d is the drainage density, α is the fraction of the watershed underlain by aquifers contributing to baseflow and f is the drainable soil porosity..

The physical model presented in (21) relates the baseflow recession constant to physical watershed characteristics; estimates of K_b, however, have been shown to depend on season and groundwater withdrawals. The previous case study of K_b estimators that incorporate groundwater withdrawals resulted in increased estimates which created less variability in estimates obtained from individual recession hydrographs due to the upper bound of K_b. Seasonal variability in K_b illustrated, in general, that higher estimates of K_b were estimated from fall or winter hydrograph recessions while estimates from summer and spring hydrographs tended to be lower. These results suggest that K_b is not a constant related solely to physical characteristics of a watershed and, therefore, may be dependent on temporal variables. To evaluate this hypothesis, we employ multivariate statistical approaches based on spatial and temporal estimates of K_b

and the physical model given in (21), in addition to temporal variables defined below.

Multivariate regression has been used to relate the baseflow recession constant to physical (Brandes et al., 2005b) and climatological (van Dijk, 2010) parameters. For the purpose of this study, our hypothesis is that K_b is a function of anthropogenic and climatic influences and, therefore, is no longer dependent solely on physical characteristics of the watershed. Our process to test this hypothesis is to develop a multivariate statistical approach similar to previous studies of K_b and BFI; our approach accounts for the primary physical determinants related to K_b (Eq. 21) and those due to climatic and anthropogenic influences.

5.1 Multivariate Regression Data

Vogel and Kroll (1992) derived the physical relationships between watershed properties and the baseflow recession constant K_b in (21) for a simplified watershed based on the work of Brutsaert and Nieber (1977). Data necessary for the proposed hypothesis test models include, at a minimum, hydraulic conductivity, basin elevations, porosity, the proportion of the watershed underlain by surficial aquifers and the drainage density. Additional factors including climate indices, seasonality, and the effect of groundwater withdrawals were also included in model testing. Availability of hydrogeologic information, including hydraulic conductivity and porosity, are limited. Limitations of data used in the analysis are included below. A summary of potential explanatory variables is shown in Table 3-3.

Table 3-3: Potential explanatory variables.

Variable Name	Description	Units	Data source
d_d	Drainage density: L/A	1/m	StreamStats
γ	Degree of withdrawal	-	Eqn. (20)
α	Percentage of watershed underlain by aquifer	-	NJGIS
H	Basin relief	m	NJGIS/USGS
f	Porosity	-	NJGIS/Fetter (1998)
k	Hydraulic conductivity	m^2/day	NJGIS
PDSI	Palmer Drought Stress Index	-	NCDC
RR	Runoff Ratio	-	USGS/PRISM
Season	Seasonality	-	Eqn. (22)
W,S,SU,F	Seasonality split into winter (W), spring (S), summer (SU) and fall (F)	-	Takes value of 1 if season and 0 otherwise-
W* γ,S* γ, SU* γ,F* γ	Seasonality interaction terms	-	-

Hydraulic Conductivity. Most watersheds used as part of this study have reported estimates of horizontal hydraulic conductivity derived from groundwater pumping tests (NJGS, DGS02-1). Estimates of hydraulic conductivity are point estimates; therefore, arithmetic averages were used to obtain average watershed hydraulic conductivity. We recognize that such methods do not provide representative estimates of bulk watershed properties; however, for this initial analysis to characterize the effect of withdrawals on gw/sw behaviors, we used available data which included point estimates and aquifer characteristics. Further, such hydraulic conductivity data for multiple watersheds is rare; thus, although the dataset is imperfect, it provides spatially distributed data for the study area to estimate watershed characteristics. For watersheds without estimates of hydraulic conductivity, methods were used to relate watershed properties with hydraulic conductivity estimates to those without documented horizontal conductivity; such

sites are indicated in Table 3-1. The relational properties included GIS documentation of aquifer productivity and aquifer characterization (Herman et al., 1998). In general, aquifers with high aquifer productivity and characterized as being comprised of sand and gravel exhibited high estimates ($k>500$ m/d) of horizontal hydraulic conductivity while lower aquifer productivity and characterization as till or sand/silt exhibited low hydraulic conductivity ($k<300$ m/d). It is important to note that relational comparisons between sites was deemed satisfactory for hypothesis testing using multivariate regression procedures; therefore, although watershed average hydraulic conductivity may not be representative of the spatial heterogeneity of the aquifers in a watershed, the comparative relationship between high conductivity/high yield versus low conductivity/low yield aquifers are preserved.

Alpha (α). The aerial percentage of the watershed underlain by an aquifer was calculated using GIS data available through NJGIS (Herman et al., 1998). Estimates of α represent the ratio of area of aquifer divided by the total contributing watershed area.

Porosity (f). Average watershed porosity was estimated from available GIS coverages (Herman et al., 1998) describing aquifer productivity and aquifer formations and linked to porosity ranges obtained from Fetter (1988). Since actual estimates of aquifer porosity were not available, we selected specific porosity values of 0.1, 0.2 and 0.3 to assign to watersheds based on physical descriptions of aquifer materials. For example, an aquifer characterized as being comprised of silt, sand and clay was assigned a porosity of 0.10 while sand and

gravel aquifers with high yields were assigned porosity values of 0.30. For this study, porosity values preserve the comparative property between watersheds based on reported yields.

Drainage density (d_d). Streamstats for New Jersey (Watson and Schoop, 2009) was used to collect watershed variables to calculate drainage density defined as the ratio of the main stream channel length to drainage area following Vogel and Kroll (1992).

Degree of withdrawal (γ). The variable γ, described by (20), was used in the multivariate approach to characterize the significance of the degree of withdrawal in the estimation of K_b.

Basin relief, H. Vogel and Kroll (1992) evoke the relationship produced by Strahler (1950) relating watershed slope, S, by

$$S \approx 2Hd_d \qquad (22)$$

where H is the basin relief and d_d is the drainage density. Zecharias and Brutsaert (1985) defined H as the difference between the basin summit elevation and basin outlet elevation. For this study, the maximum elevation was determined from New Jersey digital elevation grid data (NJDEP, 2002) while basin outlet elevations were taken as the stream gage elevation reported by the USGS.

Runoff Ratio (RR). The runoff ratio, the ratio of streamflow to precipitation (Q/P), is commonly employed in hydrologic studies to characterize the behavior of watershed response to precipitation. The runoff ratio (RR) is a function of climate and watershed properties as it depends on antecedent moisture conditions and maximum soil water retention. For this study, monthly precipitation data was

obtained from PRISM at the USGS stream gage location for each watershed. PRISM data was selected for this study since the spatial regression procedure to produce the spatial and temporal dataset accounts for topographic impacts on precipitation (Daly et al., 1994). Average monthly streamflow was obtained from USGS stream gages and normalized by contributing watershed area.

Palmer Drought Stress Index (PDSI). PDSI was introduced by Palmer (1965) to evaluate soil moisture deficiency by accounting for the interaction of precipitation and evapotranspiration. Alley (1984) documented deficiencies with PDSI including its inability to characterize temporal estimation of water budget components; despite this criticism, PDSI remains commonly used as a climate index (Huang et al., 2011, for example). Monthly PDSI was obtained for the regions of New Jersey through the National Climatic Data Center (NCDC).

Seasonality. Estimates of K_b were documented to vary depending on season as illustrated in Figure 3-3; to account for the potential relationship between K_b and season, a seasonality term is introduced as

$$Season = \sin(\omega t) \quad (23)$$

where ω is 2π/4 and t is the season numbered from 1 to 4 (winter-fall).

5.2 Model Development

Ordinary least squares (OLS) multivariate regression procedures were used to estimate the model parameters of the hybrid physical/statistical model following Vogel and Kroll (1992) shown in (21). To linearize the model, double-logs were taken to obtain

$$\ln\left(-\ln\left(K_{b_i}\right)\right) = \beta_0 + \beta_1 X_1 + \cdots + \beta_n X_n + \varepsilon_i \quad (24)$$

where $X_i,\ldots,X_n$ are the natural logs of the explanatory variables summarized in Table 3-3, $\beta_o,\ldots,\beta_n$ are model coefficients and ε_i are normally distributed model errors with zero mean and constant variance σ^2. As summarized in Table 3-3, potential explanatory variables include climatic and anthropogenic variables in addition to physical watershed attributes. Various multivariate model selection methods were used including stepwise regression analysis and best subsets regression in addition to the working knowledge of the physical model form for K_b in (21). For this study, we set the significance level to 0.05 to carry out hypothesis testing of the significance of potential explanatory variables to account for the variability in estimates of K_b. In addition, influence and leverage statistics were calculated to isolate observations that exhibited unrealistic influence on the regression model parameter estimates. Assumptions of linear regression were tested including normality of independent, serially uncorrelated residuals. Resulting models for each case are included in Table 3-4; for each case, numerous models are reported as significant variables are introduced.

Table 3-4: Summary of case-specific regression models.

Model	Constant	d_d	γ	α	RR	Season	PDSI	R^2	NSE
Case 1 M1	-2.53 (-45.97)	1.80 (9.68)	0.0815 (3.79)	-	-	-	-	56.6	0.537
Case 1 M2	-2.30 (-24.02)	1.39 (6.27)	0.0546 (2.50)	0.115 (3.35)	-	-	-	74.2	0.631
Case 1 M3	-2.16 (-18.39)	1.47 (6.64)	0.0757 (3.10)	0.110 (3.25)	0.120 (1.93)	-	-	67.8	.632
Case 1 M4	-2.16 (-20.83)	1.45 (7.60)	0.085 (4.07)	0.104 (3.51)	0.188 (2.53)	-0.105 (-2.41)	-	71.3	0.440
Case 2 M1	-2.47 (-34.78)	1.82 (7.62)	0.0639 (2.35)	-	-	-	-	69.4	0.495
Case 2 M2	-2.154 (-21.04)	1.300 (5.51)	0.0616 (2.54)	0.128 (3.42)	-	-	-	74.4	0.612
Case 2 M3	-2.06 (-16.19)	1.52 (6.32)	0.0822 (3.10)	0.108 (2.93)	0.132 (1.98)	-	-	78.5	.617
Case 2 M4	-2.14 (-22.04)	1.49 (8.23)	0.093 (4.66)	0.083 (2.90)	0.156 (2.25)	-0.092 (02.25)	-	72.1	0.685
Case 3 M1	-2.00 (-20.50)	2.24 (6.59)	0.177 (4.710)	-	-	-	-	65.3	0.480
Case 3 M2	-2.13 (-21.69)	2.45 (8.20)	0.190 (5.48)	-	-	-	-0.103 (-2.58)	83.3	.0.400
Case 4 M1	-2.3841 (-23.16)	2.81 8.17)	0.073 (1.95)	-	-	-	-	86.7	0.376
Case 4 M2	-2.44 (-22.28)	2.84 (8.79)	0.137 (3.47)	-	-	-	-0.115 (-2.58)	85.6	0.424

Note: Table 3-4 reports model coefficients (β's in (24)) along with their t-ratios (in parentheses). All coefficients were significant at the 5% level. R^2 calculated from McCuen et al. (1990).

5.3 Goodness of fit

McCuen et al. (1990) and many others have documented regression bias due to retransformation of a model which was fit using a log transformation of model variables, a process used to obtain (24). OLS regression produce unbiased estimates of model coefficients; however, as described by McCuen et al. (1990), correlation coefficient goodness of fit (R^2) in log-space does not accurately reflect model performance. To document the model performance, we applied R^2 as calculated by McCuen et al. (1990) after transformation from log-space and the Nash-Sutcliffe efficiency (NSE). The Nash-Sutcliffe efficiency criterion (Nash and Sutcliffe, 1970) is impacted by bias between observations and predictions and

the variance of the estimator. In general, the closer NSE is to 1, the better the model. Results of R^2 and NSE are included in Table 3-4; the results illustrate that models account for ~70-80% of the observed variability in the estimates of K_b. Figure 3-6 illustrates a comparison between estimated K_b after bias correction using regression equations summarized in Table 3-4 to recession-weighted estimates of K_b. In general, we observe that model results reproduce estimated baseflow recession constants for Cases 1 and 2 with little or no bias after bias correction procedures; results for Case 3 and Case 4 illustrate that large variability remains between estimated and modeled estimates of the baseflow recession constant with little or no bias. Such results support our previous observations of estimator behaviors in that recession envelope estimates (Case 3 and Case 4, Figure 3-4) tend to be less physically consistent estimates of K_b.

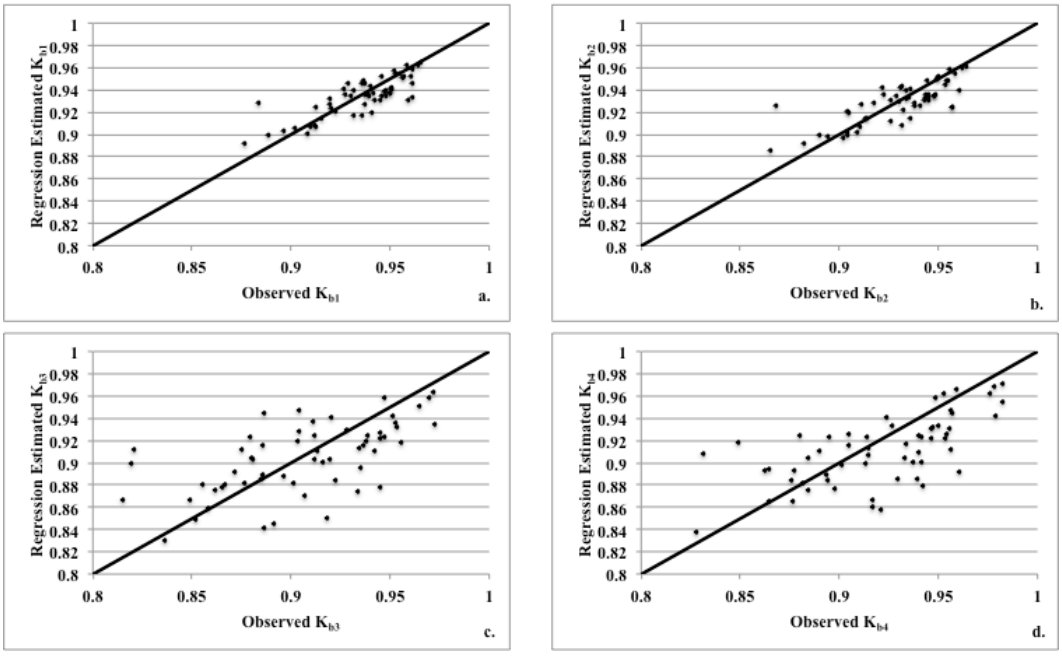

Figure 3-5: Comparison of predicted versus observed baseflow recession constants after bias correction procedures for Case 1 (model 4) (a), Case 2 (model 4) (b), Case 3 (model 2) (c) and Case 4 (model 3) (d).

5.4 Model Validation

Cross validation methods were conducted to evaluate the model coefficients in Table 3-4. Bootstrapping methods were conducted whereby 75% of the datasets were selected to fit the regression model form for each of the cases. The results for Case 2 illustrated in Figure 3-6 show that the variability in coefficients from each model obtained from 10,000 iterations are small and average to those in Table 3-4 and selection of different sites would have estimated similar coefficients for each of the regression models summarized in Table 3-4. Similar figures are included in Appendix 3.A for the other cases. Further support of model coefficients arises from Brandes et al. (2005b) who identified model forms with coefficients of d_d between 1.09 and 1.38, similar to coefficient values obtained for Case 1 and Case 2 (Table 3-4).

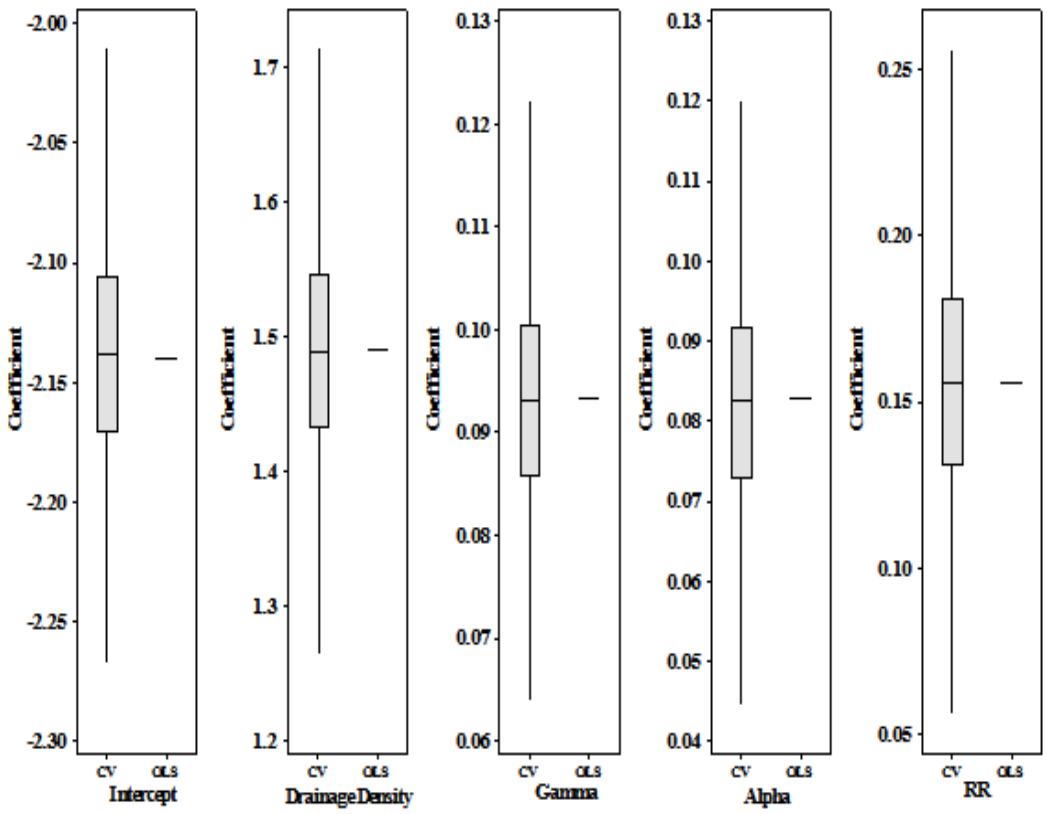

Figure 3-6: Coefficient cross-validation results for Case 2 model summarized in Table 3-4. The results illustrate that selection of watersheds results in median estimates of coefficients similar to those summarized in Table 3-4.

To evaluate the sensitivity of estimates of K_b to changes in the important variables used to explain their variability, we employ the concept of elasticity. Elasticity was introduced to water resources by Schaake (1990) who used elasticity to quantify sensitivity of runoff to changes in climate. Elasticity is used here since it is a dimensionless approach to evaluating sensitivity. Since the units for potential explanatory variables in final model forms (Table 3-4) are not identical, it is difficult to interpret and evaluate the coefficients and their resulting impact on K_b. Elasticity is a dimensionless value defined as

$$\varepsilon_X = \frac{\partial K_b / K_b}{\partial x / x} = \frac{\partial K_b}{\partial x}\frac{x}{K_b} \qquad (25)$$

where x is a significant explanatory variable used to predict K_b as summarized in Table 3-4. Here $\frac{\partial K_b}{\partial x}$ is estimated by employing the regression model from equation (24) developed for each Case. Derivations of $\frac{\partial K_b}{\partial x}$ for each Case and the results from Table 3-4 are included as Appendix 3.B. We define the elasticities as the elasticity of geomorphology (d_d), geology (α), climate (RR) and humans (γ) of K_b. The elasticity of significant variables is illustrated in Figure 3-7. In general, for each case illustrated in Figure 3-7, the geomorphology elasticity of the baseflow recession constant was found to be the most influential factor impacting K_b. This result is consistent with previous research which suggests that drainage density is the main contributor to variance in K_b (Zecharias and Brutsaert, 1998b). The next most influential factor for all cases was the human withdrawal elasticity of K_b. For Case 1 and Case 2, we see that the value of the elasticity of human withdrawals is roughly that of the geomorphology elasticity. Such a result illustrates the important sensitivity of K_b to variations in human groundwater withdrawals.

For Case 1 and 2, the geology elasticity and climate elasticity influence impacting K_b were small. However, it must be stressed that K_b itself is a sensitive parameter; a change in K_b from 0.93 to 0.92, for example, is a large difference and can greatly affect results such as low flow estimation (Kroll et al., 2004) and baseflow separation procedures (Eckhardt, 2011).

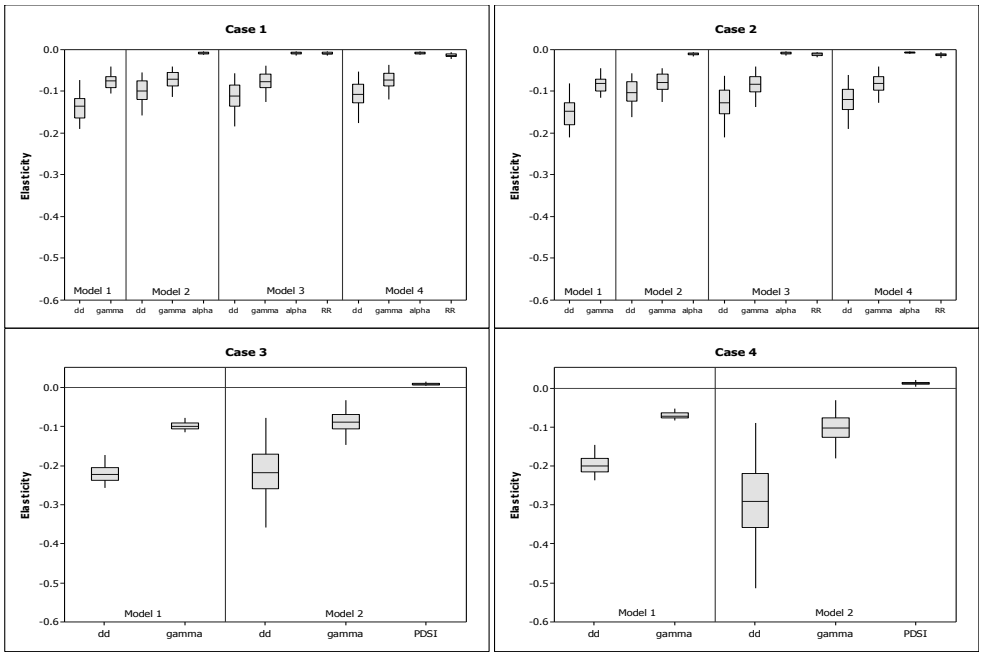

Figure 3-7: Comparison of elasticities obtained from Case 1, Case 2, Case 3 and Case 4 summarized in Table 3-4.

6.0 Conclusions

Results of this analysis illustrate the sensitivity in groundwater/surface water behaviors assuming linear storage interactions. Given the complex human interactions both temporally and spatially, there is a great need to develop methods which can illustrate the effect of anthropogenic interactions which allow for optimal management and prediction of groundwater resources. As increased attention is devoted to groundwater storage to meet water demands, this study illustrates the necessity to incorporate anthropogenic effects, in this case groundwater withdrawals, to characterize groundwater and surface water behaviors.

One of the primary purposes of this study was to develop a new approach for integrating human withdrawals into the estimation of the baseflow recession

constant. Our approach compared traditional semi-log methods and recession envelope methods to new estimators which include human withdrawals. Our findings indicate that traditional approaches which fit a semi-log regression between the log of streamflow and time to obtain the baseflow recession constant yield much more consistent, unbiased and physically realistic estimates of K_b than methods based on the hydrograph recession envelope (Figure 3-5(a)). Furthermore, semi-log methods which include human withdrawals (Case 2) exhibited a smaller variance in estimates suggesting that integration of the impact of groundwater withdrawals into estimation of K_b is paramount. As illustrated in Figure 3-3 and 3-5(b), recession envelope estimators (Case 3 and Case 4) exhibited larger variance in estimates and bias a compared to semi-log approaches. These results illustrate systematic difficulties in the estimation of recession parameters using the recession envelope approach; such results are similar to findings of Thomas (2012) which illustrated the difficulty in the recession envelope approach to characterize groundwater/surface water interaction behaviors.

We also sought to quantify the role of geologic, geomorphic, climatologic, and anthropogenic factors on variations in the value of K_b. For this purpose, the concept of dimensionless elasticity is used. Multivariate regression was conducted using a hybrid physical/statistical approach beginning with (21); such models were found to account for ~80% of the variability in recession-length weighted averages of K_b as summarized in Table 3-4. The poor performance of recession envelope models to reproduce estimates of K_b as shown in Figure 3-5(

c) and 3-5(d) further illustrate our failure to explain variability in estimates obtained from recession envelope approaches as compared to semi-log approaches. Geomorphologic (drainage density) and anthropogenic (human withdrawal) elasticities were found to be the most influential factors impacting the baseflow recession constant, K_b. Previous studies which ignored anthropogenic influences (human withdrawals) either by selecting pristine watersheds or by dismissing groundwater withdrawals isolated geomorphic variables such as drainage density as the most important variable for explaining variations in K_b; our study supports those previous findings but illustrates that groundwater withdrawals also exhibit significant and important influence on observed variations in K_b.

7.0 Acknowledgments

The authors would like to acknowledge partial support through the Summer Institute organized by Charles Vörösmarty at The City College of New York as part of the NSF-funded Hydrologic Synthesis project "Humans Transforming the Hydrologic Cycle (NSF Grant 0854957, C. Vörösmarty, PI). Additional project support was provided by a fellowship awarded to the first author by the Tufts Institute for the Environment (TIE).

Bibliography

Chapter 1 References

Adamowski, K., Dalezios, N. R., and Gingras, G. (1986). "A comparison of parameter estimation procedures in groundwater level modeling." Conjunctive water use: Understanding and managing surface water groundwater interactions, IAHS publication No. 156, S. M. Gorelick, ed., International Association of Hydrological Sciences, Wallingford, UK.

Aldrich, H. P., and Lambrechts, J. R. (1986). "Back Bay Boston, part II: Groundwater levels." Civ. Eng. Pract., 1(2), 1–63.

Allen, R. G. (1993). "Evaluation of a temperature difference method for computing grass reference evapotranspiration." Rep. to Water Resources Development and Management Service Land and Water Development Division, FAO, Rome.

Azmon, B. (1989). "Pumpage, water levels and rainfall in three wellfields in Western Galilee, Israel." J. Hydrol. (Amsterdam), 110(3–4), 369–372.

Bear, J. (1972). Dynamics of fluids in porous media, Dover Publications, New York.

Carnerio, J., and Carvalho, J. M. (2010). "Groundwater modeling as an urban planning tool: Issues raised by a small-scale model." Q. J. Geol. Hydrogeol., 43(2), 157–170.

Endreny, T., and Collins, V. (2009). "Implications of bioretention basin spatial arrangements on stormwater recharge and groundwater mounding." Ecol. Eng., 35(5), 670–677.

Fennessey, N. M., and Vogel, R. M. (1996). "Regional models of potential

evaporation and reference evapotranspiration for the northeast USA." J. Hydrol. (Amsterdam), 184(3–4), 337–354.

Foster, S. S. D., Morris, B. L., and Chilton, P. J. (1999). "Groundwater in urban development-a review of linkages and concerns." Impacts of urban growth on surface water and groundwater quality, IAHS publication No. 259, J. B. Ellis, ed., International Association of Hydrological Sciences, Wallingford, UK.

Freeze, R. A., and Witherspoon, P. A. (1967). "Theoretical analysis of regional groundwater flow II: Effect of water table configuration and subsurface permeability variations." Water Resour. Res., 3(2), 623–634.

Gilroy, K. L., and McCuen, R. H. (2009). "Spatio-temporal effects of low impact development practices." J. Hydrol. (Amsterdam), 367(3–4), 228–236.

GÖbel, P., et al. (2004). "Near-natural stormwater management and its effects on the water budget and groundwater surface in urban areas taking account of the hydrogeologic conditions." J. Hydrol. (Amsterdam), 299(3–4), 267–283.

Helsel, D. R., and Hirsch, R. M. (2002). "Statistical methods in water resources." Chapter A3, Book 4, Hydrologic Analysis and Interpretation, Techniques of water-resources investigations of the United States Geological Survey, U.S. Geological Survey, Denver, CO.

Hodgson, F. D. I. (1978). "The use of multiple linear regression in simulating ground-water level responses." Ground Water, 16(4), 249–253.

Holman-Dodds, J. K., Bradley, A. A., and Potter, K.W. (2003). "Evaluation of

hydrologic benefits of infiltration based urban storm water management." J. Am. Water Resour. Assoc., 39(1), 205–215.

Horner, R. R., Skupien, J. J., Livingston, E. H., and Shaver, H. E. (1994). Fundamentals of urban-runoff management-technical and institutional issues, Terrene Institute, Washington, DC.

Jensen, M. E., Burman, R. D., and Allen, R. G. eds. (1990). Evapotranspiration and irrigation water requirements (manual of practice No. 70), ASCE, New York.

Lemonsu, A., Masson, V., and Berthier, E. (2007). "Improvement of the hydrological component of an urban soil-vegetation-atmospheretransfer model." Hydrol. Processes, 21(16), 2100–2111.

Lerner, D. N. (1990). "Groundwater recharge in urban areas." Atmos. Environ. Part B, 24(1), 29–33.

Lerner, D. N. (2002). "Identifying and quantifying urban recharge: A review." Hydrogeol. J., 10(1), 143–152.

Li, S. G., McLaughlin, D., and Liao, H. S. (2003). "A computationally practical method for stochastic groundwater modeling." Adv. Water Resour., 26(11), 1137–1148.

Machusick, M., Welker, A., and Traver, R. (2011). "Groundwater mounding at a storm-water infiltration BMP." J. Irrig. Drain. Eng., 137(3), 154–160.

Minitab 15 [Computer software]. Minitab, State College, PA.

Nash, J. E., and Sutcliffe, J. V. (1970). "River flow forecasting through conceptual models part I-A discussion of principles." J. Hydrol.

(Amsterdam), 10(3), 282–290.

Newman,W. A., and Holton,W. E. (2006). Boston's Back Bay, the story of America's greatest nineteenth-century landfill project, Northeastern University Press, Boston.

Otto, B., Ransel, K., Todd, J., Lovaas, D., Stutzman, H., and Bailey, J. (2002). Paving our way to water shortages: How sprawl aggravates the effects of drought, American Rivers, Natural Resources Defense Council, and Smart Growth America, Washington, DC.

Perez-Pedini, C., Limbrunner, J., and Vogel, R. M. (2005). "The optimal location of infiltration-based BMP's for stormwater management." J. Water Resour. Plann. Manage., 131(6), 441–448.

Prince George's County. (1999). Low-impact design strategies: An integrated design approach, Maryland Dept. of Environmental Resource Programs and Planning Division, Largo, MD.

Scanlon, B. R., Healy, R. W., and Cook, P. G. (2002). "Choosing appropriate techniques for quantifying groundwater recharge." Hydrogeol. J., 10(1), 18–39.

Seasholes, N. S. (2003). Gaining ground: A history of landmaking in Boston, MIT Press, Cambridge, MA.

Shuttleworth, W. J. (1993). "Evaporation." Handbook of hydrology, D. R. Maidment, ed., McGraw-Hi1l, New York, 4.18.

Strack, O. D. L. (1989). Groundwater mechanics, National Water Well Association, Dublin, OH.

U.S. Environmental Protection Agency(USEPA). (2002). Considerations in the design of treatment best management practices (BMPs) to improve water quality, EPA/600/R-03/103, Cincinnati, OH.

Yao, L., Pengpeng, H., and Shikun, S. (2010). **"**A perturbation stochastic finite-element method for groundwater flow models based on undetermined-coefficients approach.**"** Hydrogeol. J., 18(7), 1603–1609.

Yi, M. J., and Lee, K. K. (2004). **"**Transfer function-noise modeling of irregularly observed groundwater heads using precipitation data.**"** J. Hydrol. (Amsterdam), 288(3–4), 272–287.

Chapter 2 References

Ahlfeld, D.P. (2004), Nonlinear response of streamflow to groundwater pumping for a hydrologic streamflow model*, Advances in Water Resources*, 27, 349-360.

Alley, W. M., R. W. Healy, J. W. LaBaugh, and T. E. Reilly (2002), Flow and storage in groundwater systems, Science, 296, 1985–1990, doi:10.1126/science.1067123.

Amit, H., V. Lyakhovsky, A. Katz, A. Starinsky and A. Burg (2002), Interpretation of spring recession curves*, Ground Water*, 40. 543–551, doi: 10.1111/j.1745-6584.2002.tb02539.x

Bear, J. (1972) *Dynamics of fluids in porous media*, American Elsevier Publishing Company, New York, NY.

Birk, S. and S. Hergarten (2010) Early recession behavior of spring hydrographs, *Journal of Hydrology*, 387(1-2), 24-32, doi:10.1016/j.jhydrol.2010.03.026.

Boussinesq, J. (1877), Essai sur la theorie des eaux courantes: Du mouvemont non permanent des eaux souterraines, Acad. Sci. Inst. Fr., 23, 252-260.

Bozzini, M. and M. Rossini (2003), Numerical differentiation of 2D functions from noisy data, *Computers and Mathematics with Applications*, 45, 309-327.

Brutsaert, W., and J.L. Nieber (1977), Regionalized drought flow hydrographs from a mature glaciated plateau, *Water Resources Research*, 13(3), 637-643.

Brutsaert, W. (2008), Long-term groundwater storage trends estimated from streamflow records: Climatic perspective, *Water Resour. Res.*, 44, W02409, doi:10.1029/2007WR006518

Chapra, S. and R. Canale (2005), *Numerical methods for engineers*, McGraw Hill, New York, NY.

Clark, M., H. McMillan, D. Collins, D. Kavetski, and R. Woods (2011) Hydrological field data from a modeller's perspective: Part 2: process-based evaluation of model hypotheses, Hydrological Processes, 523–543.

Craven P. and G. Wahba (1979), Smoothing noisy data with spline functions, *Numerical Mathematics*, 31, 377-403

D'Amigo, M. and G. Ferrigno (1992), Comparison between the more recent techniques for smoothing and derivative assessment in biomechanics, *Medical & Biological Engineering & Computing*, 30, 193-204.

Devito, K.J., A.R. Hill and N. Roulet (1996), Groundwater-surface water interactions in headwater forested wetlands of the Canadian Shield, Journal of Hydrology, 181, 127-147.

Domenico, P.A. and F.W. Schwartz (1998), *Physical and chemical hydrogeology*, John Wiley and Sons, New York, NY.

Dooge, J.C.I. (1973), Linear theory of hydrologic systems, Technical Bulletin, U.S. Department of Agriculture, 1468, 327 pp.

Dow, C. L. (1999), Detecting base flow impacts in coastal plain streams, JAWRA Journal of the American Water Resources Association, 35, 349–362, doi: 10.1111/j.1752-1688.1999.tb03595.x

Dow, C.L. (2007), Assessing regional land-use/cover influences on New Jersey Pinelands streamflow through hydrograph analysis, *Hydrological Processes*, 21, 185-197.

Dupuit, J. (1863). Estudes Thèoriques et Pratiques sur le mouvement des Eaux dans les canaux dècouverts et à travers les terrains permèables.

Eng, K., and P. C. D. Milly (2007), Relating low-flow characteristics to the base flow recession time constant at partial record stream gauges, *Water Resour. Res*., 43, W01201, doi:10.1029/2006WR005293.

Federer, C.A. (1973), Forest transpiration greatly speeds streamflow recession, *Water Resources Research*, 9(6), 1599-1604.

Fetter, C.W. (1998), *Applied Hydrogeology*, Prentice Hall, New York, NY.

Francke, T., J. López-Tarazón, and B. Schröder (2008), Estimation of suspended sediment concentration and yield using linear models, random forests and

quantile regression forests. *Hydrological Processes,* 22, 4892–4904, doi: 10.1002/hyp.7110.

Hall, F.R. (1968), Base flow recessions: a review, *Water Resources Research*, 4(5), 973-983.

Hao, L. and D.Q. Naiman (2007), Quantile Regression, Sage University Papers Series on Quantitative Applications in the Social Sciences, 07-149, Thousand Oaks, CA.

Harman, C., and M. Sivapalan (2009), Effects of hydraulic conductivity variability on hillslope-scale shallow subsurface flow response and storage-discharge relations, *Water Resour. Res*., 45, W01421, doi:10.1029/2008WR007228.

James, A.T. and R.A.J. Conyers (1985), Estimation of a derivative by a difference quotient: it's application to hepatocyte lactate metabolism, *Biometrics*, 41(2), 467-476.

Johnston, J. and J. DiNardo (1997), *Econometric Methods*, McGraw-Hill Companies, New York, NY.

Kirchner, J.W. (2009), Catchments as simple dynamical systems: Catchment characterization, rainfall-runoff modeling, and doing hydrology backwards, Water Resour. Res., 45, W02429, doi:10.1029/2008WR006912.

Knisel, W.G. (1963), Baseflow recession analysis for comparison of drainage basins and geology, *Journal of Geophysical Research*, 68(12), 3679-3653.

Koenker R. and G. Bassett (1978), Regression Quantiles, *Econometrica*, 46, 33-50.

Koenker R. (2005), *Quantile Regression*, Cambridge University Press, New York, NY.

Koenker, R. (2012) quanreg: Quantile Regression, R package version 4.71.

Lins, H.F. and J.R. Slack (2005), Seasonal and regional characteristics of U.S. streamflow trends in the United States from 1940 to 1999*, Physical Geography*, 26(6),489-501, doi:10.274/0272-3646.26.6.489.

Liu, J., T. Dietz, S.R. Carpenter, M. Alberti, C. Folke, E. Moran, A.N. Pell, P. Deadman, T. Kratz, J. Lubchenco, E. Ostrom, Z. Ouyang, W. Provencher, C.L. Redmen, S.H. Schneider, and W.W. Taylor (2007), Complexity of coupled human and natural systems, *Nature*, 317, 1513-1516.

Lo, M.-H., J.S. Famiglietti, P.J.-F. Yeh, and T.H. Syed (2010), Improving parameter estimation and water table depth simulation in a land surface model using GRACE water storage and estimated baseflow data, Water Resour. Res., 46, W05517, doi:10.1029/2009WR007855/

Maechler, M. (2012), sfsmisc: Utilities from seminar fuer statistic ETH Zurich, R package version 1.0-16.

Maillet, E. (1905) Essais d'Hydraulique Souterraine et Fluviale. Herman, Paris, France.

Pulido-Velazquez, M.A., A. Sahuquillo-Herraiz, J. Camilo Ochoa-Rivera, and D. Pulido-Velazquez, (2005) Modeling of stream–aquifer interaction: the

embedded multireservoir model, *Journal of Hydrology*, Volume 313(3-4),166-181, doi:10.1016/j.jhydrol.2005.02.026.

Mendoza,G.F., T.S. Steenhuis, M.T. Walter, J.-Y. Parlange (2003) Estimating basin-wide hydraulic parameters of a semi-arid mountainous watershed by recession-flow analysis, *Journal of Hydrology*, 279(1-4), 57-69, doi:10.1016/S0022-1694(03)00174-4.

New Jersey Geological and Water Survey (2011), DGS 10-3, New Jersey water transfer model withdrawal, use, and return data.

Poff, N. L., and J. D. Allan (1995), Functional organization of stream fish assemblages in relation to hydrological variability, *Ecology*, 76, 606–627, doi:http://dx.doi.org/10.2307/1941217.

R Development Core Team (2012). R: A language and environment for statistical computing. R Foundation for Statistical Computing, Vienna, Austria.

Ragozin, D.L. (1983), Error bounds for derivative estimates based on spline smoothing of exact or noisy data, *Journal of Approximation Theory*, 37, 335-355.

Ripley, B. (2012), pspline: Penalized smoothing splines, R package version 1.0-14.

Ritter, K. (1996), Almost optimal differentiation using noisy data, *Journal of Approximation Theory*, 86, 293-309.

Robinson, C.T., G.W. Minshall and T.V. Royer (2000), Inter-annual patterns in macroinvertebrate communities of wilderness streams in Idaho, U.S.A., *Hydrobiologia*, 421(1), 187-198, doi:10.1023/A:1003956114073.

Schilling, K. E. and R.D. Libra (2003), Increased baseflow in Iowa over the second half of the 20th century, *JAWRA Journal of the American Water Resources Association*, 39, 851–860. doi: 10.1111/j.1752-1688.2003.tb04410.x

Shepherd, K.A., P.A. Ellis, and M.O. Rivett (2006) Integrated understanding of urban land, groundwater baseflow and surface-water quality-The City of Birmingham, UK, *Science of the Total Environment*, 360, 180-195.

Singh, K. P. (1968), Some factors affecting baseflow, *Water Resour. Res.*, 4(5), 985–999, doi:10.1029/WR004i005p00985.

Szilagyi, J. and M.B. Parlange (1988), Baseflow separation based on analytical solutions of the Boussinesq equation, *Journal of Hydrology*, 204, 251-260.

Szilagyi, J., Z. Bribovszki, and P. Kalicz (2007), Estimation of catchment-scale evapotranspiration from baseflow recession data: Numerical model and practical application results, *Journal of Hydrology*, 336, 206-217.

Tague, C. and G. E. Grant (2004), A geological framework for interpreting the low-flow regimes of Cascade streams, Willamette River Basin, Oregon, *Water Resour. Res*., 40, W04303, doi:10.1029/2003WR002629.

Tallaksen, L.M. (1995), A review of baseflow recession analysis, *Journal of Hydrology*, 165, 345-370.

Troch, P. A., F. P. De Troch and W. Brutsaert (1993), Effective water table depth to describe initial conditions prior to storm rainfall in humid regions, *Water Resour. Res*., 29, 427–434, doi:10.1029/92WR02087.

Van de Griend, A.A., J.J. De Vries and E. Seyhan (2002) Groundwater discharge from areas with a variable specific drainage resistance. Journal of Hydrology, 259, 203-220.

Vogel, R.M. and C.N. Kroll (1992), Regional geohydrologic-geomorphic relationships for the estimation of low-flow statistics, *Water Resour. Res*., 38(9), 2451-2458.

Vogel, R.M. and C.N. Kroll (1996), Estimation of baseflow recession constants, *Water Resources Management*, 10, 303-320.

Wahba, G. (1973), Smoothing noisy data with spline functions, *Numerical Mathematics*, 24, 383-393.

Wang, D. (2011), On the base flow recession at the Panola Mountain Research Watershed, Georgia, United State, *Water Resources Research*, 47, W03527.

Wang, D. and X. Cai (2009), Detecting human interferences to low flows through base flow recession analysis, *Water Resour. Res*., 45, W07426, doi:10.1029/2009WR007819.

Wang, D., and X. Cai (2010), Recession slope curve analysis under human interferences, *Advances in Water Resources*, 33, 1053-1063.

Watson, K.M., and Schopp, R.D. (2009), Methodology for estimation of flood magnitude and frequency for New Jersey streams: U.S. Geological Survey Scientific Investigations Report 2009-5167.

Weerts, A.H. (2011), Estimation of predictive hydrologic uncertainty using quantile regression: examples from the National Flood Forecasting System

(England and Wales), *Hydrology and Earth System Sciences,* 15(1), 255-265.

Wayland, K.G., D.T. Long, D.W. Hyndman, B.C. Pijanowski, S.M. Woodhams, and S.K. Haack (2003), Identifying relationships between baseflow geochemistry and land use with synoptic sampling and R-mode factor analysis, *J. Environ. Qual*., 32, 180-190.

Wittenberg, H. (1994), Nonlinear analysis of flow recession curves, IAHS Publ., 221, 61-67.

Wittenberg, H. (1999), Baseflow recession and recharge as nonlinear storage processes, *Hydrol. Processes*, 13, 715– 726, doi:10.1002/(SICI) 1099-1085(19990415)13:5<715::AID-HYP775>3.0.CO;2-N.

Wittenberg, H. and M. Sivapalan (1999), Watershed groundwater balance estimation using streamflow recession analysis and baseflow separation, *Journal of Hydrology*, 219, 20-33.

Chapter 3 References

Alley, W.M. (1984) The Palmer drought severity index: limitations and assumptions. *Journal of Climate and Applied Meteorology*, 23, 1100-1109.

Barber, N.L. (2009) Summary of estimated water use in the United States in 2005: U.S. Geological Survey Fact Sheet 2009-3098.

Barnes, B.S. (1939) The structure of discharge-recession curves, Trans. Am. Geophysi. Union, 20(4), 721-725.

Bear, J. (1972) *Dynamics of fluids in porous media*, American Elsevier Publishing Company, New York, NY.

Beven, K.J., R. Lamb, P. Quinn, R. Romanowicz nad J. Freer (1995) TOPMODEL, in Singh, V.P. (ed), Computer Models of Watershed Hydrology, Water Resource Publications, Colorado, 627-668.

Biswal, B. and M. Marani (2010). Geomorphological origin of recession curves, Geophsycial Research Letters, 37, L24403, doi:10.1029/2010GL045415.

Blom, G. (1953) Statistical estimates and transformed beta variables, John Wiley, New York.

Bloomfield, J.P., D.J. Allen, and K.J. Griffiths (2009). Examining geological controls on baseflow index (BFI) using regression analysis: An illustration from the Thames Basin, UK, J. of Hydrol., 373 164-176.

Boussinesq, J. (1877), Essai sur la theorie des eaux courantes: Du mouvemont non permanent des eaux souterraines, Acad. Sci. Inst. Fr., 23, 252-260.

Brandes, D., G.J. Cavallo and M.L. Nilson (2005a), Baseflow trends in urbanizing watersheds of the Delaware river basin, Journal of the American Water Resources Association, 41(6), 1377-1391.

Brandes, D., J.G. Hoffman, and J.T. Mangarillo (2005b), Base flow recession rates, low flows, and hydrologic features of small watersheds in Pennsylvania, USA. Journal of the American Water Resources Association, 41(5), 1177-1186.

Breusch, T.S. and A.R. Pagan (1979). A simple test for heteroscedasticity and random coefficient variation. Econometrica, 47(5), 1287-1294.

Brutsaert, W. (2008), Long-term groundwater storage trends estimated from streamflow records: Climatic perspective, Water Resour. Res., 44, W02409, doi:10.1029/2007WR006518.

Brutsaert, W., and J.L. Nieber (1977), Regionalized drought flow hydrographs from a mature glaciated plateau, *Water Resources Research*, 13(3), 637-643.

Carlston, C.W. (1965). The relation of free meander geometry to stream discharge and its geomorphic implications, Am. Journ. Sci. 263, 864-885.

Craven P. and G. Wahba (1979), Smoothing noisy data with spline functions, *Numerical Mathematics*, 31, 377-403.

Daly, C., R.P. Neilson, and D.L. Phillips (1994). A Statistical-Topographic Model for Mapping Climatological Precipitation over Mountanious Terrain. J. Appl. Meteor., 33, 140-158.

Dingman, S.L. (2002) Physical hydrology, Prentice-Hall, Upper Saddle River, New Jersey.

Dooge, J.C.I. (1973), Linear theory of hydrologic systems, Technical Bulletin, U.S. Department of Agriculture, 1468, 327 pp.

Domenico, P.A. and F.W. Schwartz (1998), Physical and chemical hydrogeology, John Wiley and Sons, New York, NY.

Dupuit, J. (1863). Estudes Thèoriques et Pratiques sur le mouvement des Eaux dans les canaux dècouverts et à travers les terrains permèables.

Eckhardt, K. (2008). A comparison of baseflow indices, which were calculated with seven different baseflow separation methods, J. of Hydro., 352, 168-173.

Eckhardt, K. (2011). Technical note: analytical sensitivity analysis of a two parameter recursive digital baseflow separation filter, Hydrol. Earth Syst. Sci. Discuss., 8, 9469-9480.

Eng, K., and P. C. D. Milly (2007), Relating low-flow characteristics to the base flow recession time constant at partial record stream gauges, *Water Resour. Res*., 43, W01201, doi:10.1029/2006WR005293.

Farvolden, R.N. (1963). Geologic controls on ground-water storage and base flow, J. of Hydrol., 1, 219-249.

Ferguson, R.I. (1986) River loads underestimated by rating curves, Water Resources Research 22(1), 74-76.

Ferket, B., V.R.N. Pauwels, B. Samain, and W. Defloor (2010) Internal validation of conceptual rainfall-runoff models using baseflow separation, J. of Hydro., 381(1-2), 158-173.

Fetter, C.W. (1988). Applied hydrogeology. Macmillian College Publishing Company, New York, NY.

Filliben, J.J. (1975), The probability plot correlation coefficient test for normality, Technometrics, 17(1), 111-117.

Hall, F.R. (1968), Base flow recessions: a review, *Water Resources Research*, 4(5), 973-983.

Herman, G.C., R. Canace, M.A. French, J.L. Hoffman, W.J. Mennel, R.S. Pristas, P.J. Sugarman, and S.D. Stanford (1998). Aquifers of New Jersey. N.J. Geological Survey Open File Map OFM-24, 1:100,000 map.

Hothorn, T. and A. Zeileis (2012), Diagnostic checking in regression relationships, R News 2(3), 7-10.

Huang, S., D. Dahal, C. Young, G. Chander, and S. Liu, (2011) Integration of Palmer Drought Severity Index and remote sensing data to simulate wetland water surface from 1910 to 2009 in Cottonwood Lake area, North Dakota. *Remote Sensing of Environment*, 115, 3377-3389.

Institute of Hydrology. (1980). Low-flow studies, Rep. No 1, Wallingford, Oxon, U.K.

Johnston, J. and J. DiNardo (1997), *Econometric Methods*, McGraw-Hill Companies, New York, NY.

Kirchner, J.W. (2009), Catchments as simple dynamical systems: Catchment characterization, rainfall-runoff modeling, and doing hydrology backwards, Water Resour. Res., 45, W02429, doi:10.1029/2008WR006912.

Kroll, C., J. Luz, B. Allen and R.M. Vogel (2004) Developing a watershed characteristics database to improve low streamflow prediction, Journal of Hydrologic Engineering, 9(2), 116-125.

Kummel, H.B. (1940), The Geology of New Jersey, Bulletin 50, Department of Conservation and Development, State of New Jersey.

Lacey, G.C. and R.B. Grayson (1998). Relating baseflow to catchment properties in south-eastern Australia, Journal of Hydrology, 204(1-4), 231-250.

Lins, H.F. and J.R. Slack (2005), Seasonal and regional characteristics of U.S. streamflow trends in the United States from 1940 to 1999*, Physical Geography*, 26(6),489-501, doi:10.274/0272-3646.26.6.489.

Lo, M.-H., J.S. Famiglietti, P.J.-F. Yeh, and T.H. Syed (2010), Improving parameter estimation and water table depth simulation in a land surface model using GRACE water storage and estimated baseflow data, Water Resour. Res., 46, W05517, doi:10.1029/2009WR007855/

Longobardi, A. and P. Villani (2008). Baseflow index regionalization analysis in a mediterranean area and data scarcity context: Role of the catchment permeability index, J. of Hydrol., 355 63-75.

Maechler, M. (2012), sfsmisc: Utilities from seminar fuer statistic ETH Zurich, R package version 1.0-16.

Maillet, E. (1905) Essais d'Hydraulique Souterraine et Fluviale. Herman, Paris, France.

McCuen, R.H., R.B. Leahy, and P.A. Johnson (1990). Problems with logarithmic transformations in regression, J. of Hydraulic Engineering, 116(3), 414-428.

Mendoza,G.F., T.S. Steenhuis, M.T. Walter, J.-Y. Parlange (2003) Estimating basin-wide hydraulic parameters of a semi-arid mountainous watershed by recession-flow analysis, *Journal of Hydrology*, 279(1-4), 57-69, doi:10.1016/S0022-1694(03)00174-4.

Mwakalila, S., J. Feyen, G. Wyseure (2002). The influence of physical catchment properties on baseflow in semi-arid environments, Journal of Arid Environments, 52, 245-258.

Nash, J.E. and J.V. Sutcliffe (1970), River flow forecasting through conceptual models part I-A discussion of principles, Journal of Hydrology, 10(3), 282-290.

New Jersey Department of Environmental Protection (2012), New Jersey Geolgoical Survey Hydro Database, New Jersey Geological Survey, Trenton, NJ.

New Jersey Geological Survey (1999), Digital elevation grids for New Jersey (1:100,000 scale) compiled by G.C. Herman, N.J. Geological Survey Digital Geodata Series DGS99-4.

New Jersey Geological and Water Survey (2011), DGS 10-3, New Jersey water transfer model withdrawal, use, and return data.

Nie, W.M., Y.P. Yuan, W. Kepner, M.S. Nash, M. Jackson, and C. Erickson, (2011). Assessing impacts of landuse and landcover changes on hydrology for the upper San Pedro watershed, J. of Hydol., 407(1-4), 105-114.

Palmer, W.C. (1965) Meteorological Drought, Research Paper 45. Washington DC, U.S. Department of Commerce Weather Bureau.

Pinheiro, J., D. Bates, S. DebRoy, D. Sarkar and the R Development Core Team. (2012) nlme: linear and nonlinear mixed effect models. R package version 3.1-103.

R Development Core Team (2012). R: A language and environment for statistical computing. R Foundation for Statistical Computing, Vienna, Austria.

Ripley, B. (2012), pspline: Penalized smoothing splines, R package version 1.0-14.

Schaake, J.C. (1990), From climate to flow, in Climate Change and U.S. Water Resources, edited by P. E. Waggoner, chap. 8, pp. 177-206, John Wiley, New York.

Schilling, K.E. (2005). Relation of baseflow to row crop intensity in Iowa, Agriculture, Ecosystem & Environment, 105(1-2), 433-438.

Schilling, K.E. and R.D. Libra (2003), Increased baseflow in Iowa over the second half of the 20th century, Journal of the American Water Resources Association, 39(4), 851-860.

Schilling, K.E. and Y.K. Zhang (2006), Increasing streamflow and baseflow in Mississippi River since the 1940s: effect of land use change, Journal of Hydrology, 324, 412-422.

Smakhtin, V. U. (2001). Low-flow hydrology: A review. J. Hydrol., 240(3-4), 147–186.

Strahler, A.N. (1950). Equilibrium theory of erosional slopes approached by frequency distribution analysis, I., Am. J. Sci, 248, 673-696.

Szilagyi, J., 1999. On the use of semi-logarithmic plots for baseflow separation, Ground Water, 37(5): 660-662.

Szilagyi, J., Z. Bribovszki, and P. Kalicz (2007), Estimation of catchment-scale evapotranspiration from baseflow recession data: Numerical model and practical application results, *Journal of Hydrology*, 336, 206-217.

Tallaksen, L.M. (1995), A review of baseflow recession analysis, *Journal of Hydrology*, 165, 345-370.

Theis, C.V. (1940), The source of water derived from wells: essential factors controlling the response of an aquifer to development, Civil Engineer, 10, 277-280.

Van de Griend, A.A., J.J. De Vries and E. Seyhan (2002) Groundwater discharge from areas with a variable specific drainage resistance. Journal of Hydrology, 259, 203-220.

van Dijk, A.I.J.M. (2010) Streamflow response and recession in Australian catchments. Hydrol. Earth Syst. Sci., 14, 159-169.

Vogel, R.M. and C.N. Kroll (1992), Regional geohydrologic-geomorphic relationships for the estimation of low-flow statistics, *Water Resour. Res*., 38(9), 2451-2458.

Vogel, R.M. and C.N. Kroll (1996), Estimation of baseflow recession constants, *Water Resources Management*, 10, 303-320.

Vorosmarty, C.J., P. Green, J. Salisbury and R.B. Lammers (2000), Global water resources: vulnerability from climate change and population growth. Science, 289(5477), 284-288.

Vorosmarty, C.J., P.B. McIntyre, M.O. Gessner, D. Dudgeon, A. Prusevich, P. Green, S. Glidden, S.E. Bunn, C.A. Sullivan, C. Reidy Libermann and

P.M. Davies (2010), Global threats to human water security and river biodiversity, Nature, 467, 555-561.

Wagener, T., M. Sivapalan, P. A. Troch, B. L. McGlynn, C. J. Harman, H. V. Gupta, P. Kumar, P. S. C. Rao, N. B. Basu, and J. S. Wilson (2010), The future of hydrology: An evolving science for a changing world, Water Resour. Res., 46, W05301, doi:10.1029/2009WR008906.

Wang, D. and X. Cai (2009), Detecting human interferences to low flows through base flow recession analysis, *Water Resour. Res*., 45, W07426, doi:10.1029/2009WR007819.

Wang, D., and X. Cai (2010), Recession slope curve analysis under human interferences, *Advances in Water Resources*, 33, 1053-1063.

Watson, K.M., and Schopp, R.D. (2009), Methodology for estimation of flood magnitude and frequency for New Jersey streams: U.S. Geological Survey Scientific Investigations Report 2009-5167.

Wittenberg, H. and M. Sivapalan (1999), Watershed groundwater balance estimation using streamflow recession analysis and baseflow separation, *Journal of Hydrology*, 219, 20-33.

Wittenberg, H. (2003), Effects of season and man-made changes on baseflow and flow recession: Case studies, *Hydrol. Processes*, 17, 2113–2123, doi:10.1002/hyp.1324.

Zecharias, Y.B., and W. Brutsaert (1985). Ground surface slope as a basin scale parameter, Water Resources Research, 21(12), 1895-1902.

Zecharias, Y.B., and W. Brutsaert (1988a), The influence of basin morphology on groundwater outflow, Water Resour. Res., 24(10),1645-1650.

Zecharias, Y.B. and W. Brutsaert (1988b), Recession characteristics of groundwater outflow and base flow from mountainous watersheds, *Water Resour. Res*., 24(10),1651-1658.

Appendix 2.A

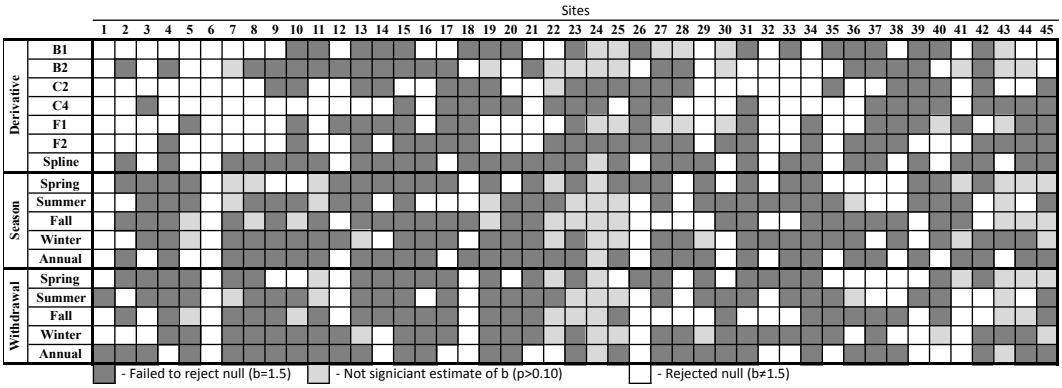

Hypothesis test results for H_o: b=1.5

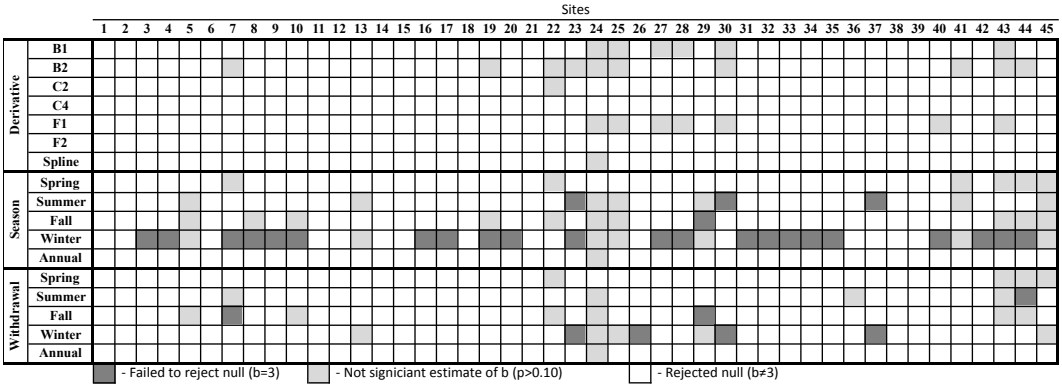

Hypothesis test results for H_o: b=3.0

Appendix 3.A

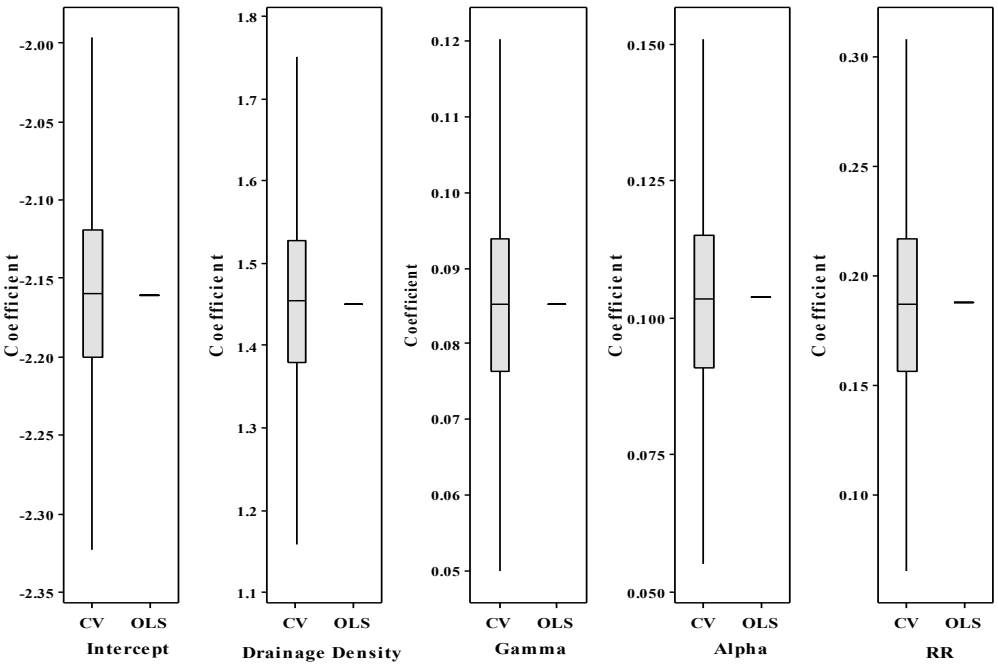

Case 1

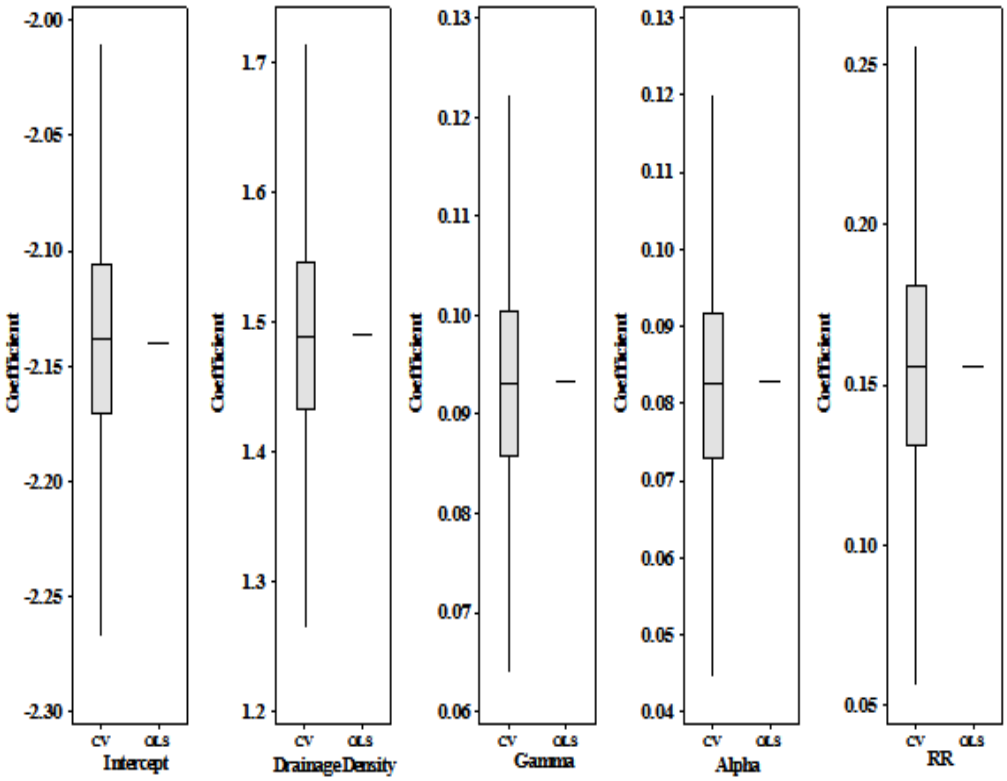

Case 2

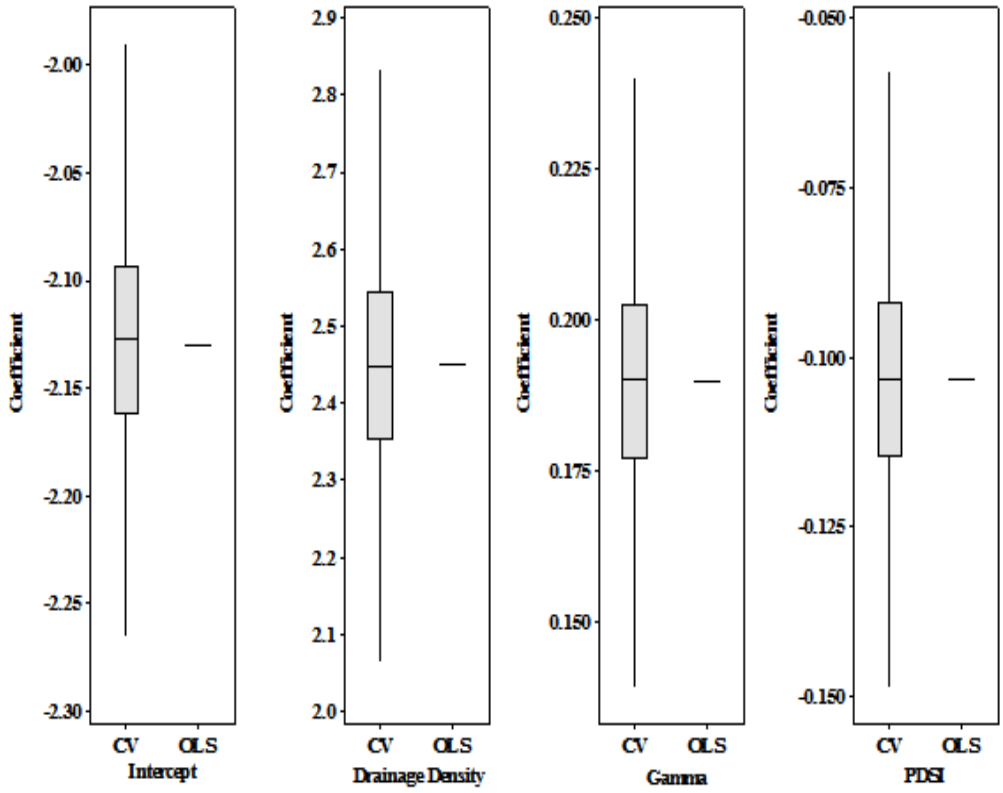
Coefficient
-2.00
-2.05
-2.10
-2.15
-2.20
-2.25
-2.30
CV
OLS
Intercept
2.9
2.8
2.7
2.6
2.5
2.4
2.3
2.2
2.1
2.0
Drainage Density
0.250
0.225
0.200
0.175
0.150
Gamma
-0.050
-0.075
-0.100
-0.125
-0.150
PDSI

Case 3

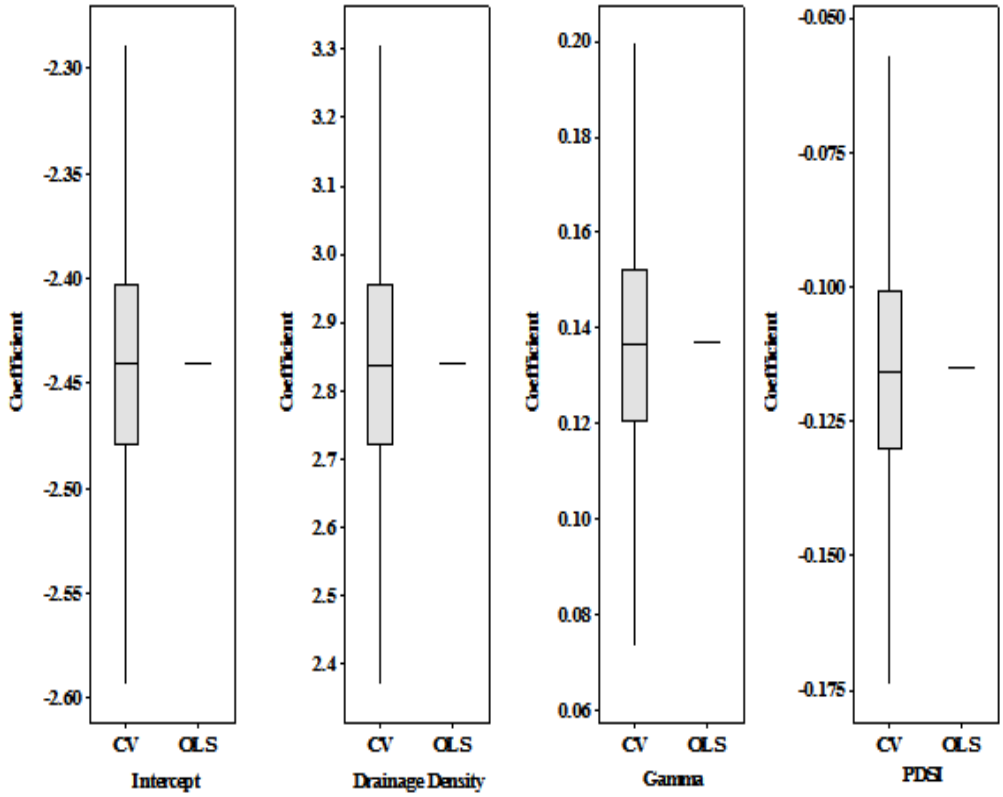
Coefficient
-2.30
-2.35
-2.40
-2.45
-2.50
-2.55
-2.60
CV
OLS
Intercept
3.3
3.2
3.1
3.0
2.9
2.8
2.7
2.6
2.5
2.4
Drainage Density
0.20
0.18
0.16
0.14
0.12
0.10
0.08
0.06
Gamma
-0.050
-0.075
-0.100
-0.125
-0.150
-0.175
PDSI

Case 4

Appendix 3.B

Case 1-Model 4:

From Table 3-4, $K_{b1} = e^{\left(-e^{-2.16}{d_d}^{1.45}\gamma^{0.0853}\alpha^{0.104}RR^{0.188}Season^{-0.105}\right)}$

Elasticity of Geomorphology (ε_{d_d})

$$\varepsilon_{d_d} = \frac{dK_{b1}}{dd_d}\frac{d_d}{K_{b1}} = \frac{-1.384e^{-2.16}RR^{0.188}\alpha^{0.104}d_d^{1.45}}{Season^{0.105}}$$

Let $\theta_1 = \frac{e^{-2.16}RR^{0.188}\alpha^{0.104}d_d^{1.45}}{Season^{0.105}}$, so $\varepsilon_{d_d} = -1.384\theta_1$

Elasticity of Humans (ε_γ)

$$\varepsilon_\gamma = \frac{dK_{b1}}{d\gamma}\frac{\gamma}{K_{b1}} = \frac{-0.954e^{-2.16}RR^{0.188}\alpha^{0.104}d_d^{1.45}}{Season^{0.105}} = -0.945\theta_1$$

Elasticity of Geology (ε_α)

$$\varepsilon_\alpha = \frac{dK_{b1}}{d\alpha}\frac{\alpha}{K_{b1}} = \frac{-0.099e^{-2.16}RR^{0.188}\alpha^{0.104}d_d^{1.45}}{Season^{0.105}} = -0.099\theta_1$$

Elasticity of Climate (ε_{RR})

$$\varepsilon_{RR} = \frac{dK_{b1}}{dRR}\frac{RR}{K_{b1}} = \frac{-0.179e^{-2.16}RR^{0.188}\alpha^{0.104}d_d^{1.45}}{Season^{0.105}} = -0.179\theta_1$$

Case 2-Model 4:

From Table 3-4, $K_{b2} = e^{(-e^{-2.14}{d_d}^{1.49}\gamma^{0.0829}\alpha^{0.0829}RR^{0.156}Season^{-0.0925})}$

Elasticity of Geomorphology (ε_{d_d})

$$\varepsilon_{d_d} = \frac{dK_{b2}}{dd_d}\frac{d_d}{K_{b2}} = \frac{-1.415e^{-2.14}RR^{0.156}\alpha^{0.0829}d_d^{1.49}}{Season^{0.0925}}$$

Let $\theta_2 = \frac{e^{-2.14}RR^{0.156}\alpha^{0.0829}d_d^{1.49}}{Season^{0.0925}}$, so $\varepsilon_{d_d} = -1.415\theta_2$.

Elasticity of Humans (ε_γ)

$$\varepsilon_\gamma = \frac{dK_{b2}}{d\gamma}\frac{\gamma}{K_{b2}} = \frac{-0.950e^{-2.14}RR^{0.156}\alpha^{0.0829}d_d^{1.49}}{Season^{0.0925}} = -0.950\theta_2$$

Elasticity of Geology (ε_α)

$$\varepsilon_\alpha = \frac{dK_{b2}}{d\alpha}\frac{\alpha}{K_{b2}} = \frac{-0.079e^{-2.14}RR^{0.156}\alpha^{0.0829}d_d^{1.49}}{Season^{0.0925}} = -0.079\theta_2$$

Elasticity of Climate (ε_{RR})

$$\varepsilon_{RR} = \frac{dK_{b2}}{dRR}\frac{RR}{K_{b2}} = \frac{-0.148e^{-2.14}RR^{0.156}\alpha^{0.0829}d_d^{1.49}}{Season^{0.0925}} = -0.148\theta_2$$

Case 3-Model 2:

From Table 3-4, $K_{b3} = e^{\left(-e^{-2.31} {d_d}^{2.45} \gamma^{0.1901} PDSI^{-0.103}\right)}$

Elasticity of Geomorphology (ε_{d_d})

$$\varepsilon_{d_d} = \frac{dK_{b3}}{dd_d}\frac{d_d}{K_{b3}} = \frac{-1.769e^{-2.31}d_d^{2.45}}{PDSI^{0.103}}$$

Let $\theta_3 = \frac{e^{-2.31}d_d^{2.45}}{PDSI^{0.103}}$, so $\varepsilon_{d_d} = -1.769\theta_3$

Elasticity of Humans (ε_γ)

$$\varepsilon_\gamma = \frac{dK_{b3}}{d\gamma}\frac{\gamma}{K_{b3}} = \frac{-0.722e^{-2.31}d_d^{2.45}}{PDSI^{0.103}} = -0.722\theta_3$$

Elasticity of Climate (ε_{PDSI})

$$\varepsilon_{PDSI} = \frac{dK_{b3}}{dPDSI}\frac{PDSI}{K_{b3}} = \frac{0.074e^{-2.31}d_d^{2.45}}{PDSI^{0.103}} = 0.074\theta_3$$

Case 4-Model 2:

From Table 3-4, $K_{b4} = e^{(-e^{-2.44}{d_d}^{2.84}\gamma^{0.3711}PDSI^{-0.115})}$

Elasticity of Geomorphology (ε_{d_d})

$$\varepsilon_{d_d} = \frac{dK_{b4}}{dd_d}\frac{d_d}{K_{b4}} = \frac{-1.769e^{-2.44}d_d^{2.84}}{PDSI^{0.115}}$$

Let $\theta_4 = \frac{e^{-2.44}d_d^{2.84}}{PDSI^{0.115}}$, so $\varepsilon_{d_d} = -2.634\theta_4$

Elasticity of Humans (ε_γ)

$$\varepsilon_\gamma = \frac{dK_{b4}}{d\gamma}\frac{\gamma}{K_{b4}} = \frac{-0.927e^{-2.44}d_d^{2.84}}{PDSI^{0.115}} = -0.927\theta_4$$

Elasticity of Climate (ε_{PDSI})

$$\varepsilon_{PDSI} = \frac{dK_{b4}}{dPDSI}\frac{PDSI}{K_{b4}} = \frac{0.107e^{-2.44}d_d^{2.84}}{PDSI^{0.115}} = 0.107\theta_4$$